



**NTNU – Trondheim**  
Norwegian University of  
Science and Technology

# Wet Gas Compressor Transients

**Bjørn Berge Owren**

Master of Science in Mechanical Engineering

Submission date: June 2014

Supervisor: Lars Eirik Bakken, EPT

Co-supervisor: Håvard Nordhus, Statoil  
Tor Bjørge, Statoil

Norwegian University of Science and Technology  
Department of Energy and Process Engineering





Norwegian University  
of Science and Technology

Department of Energy  
and Process Engineering

EPT-M-2014-84

## MASTER THESIS

for

Student Bjørn B Owren

Spring 2014

Wet Gas Compressor Transients

*Våtgasskompressor - transienter*

### Background and objective

Major challenges are related to efficient utilization of existing infrastructure and exploration of new fields in the North Sea. Increased production of gas demands new field development based on sub-sea production, including bulk separation and wet gas compression. The wet gas compression represents an energy-intensive production segment in which limited research has been invested. Specifically this relates to the wet gas compression operation scenarios.

In order to reveal the wet gas compressor behaviour it is of vital importance to develop models and validate experimental test data from the NTNU test rig. The compressor and system behaviour under different operating conditions have to be explored and representative analytical models verified.

### The following tasks are to be considered:

Based on literature review and experimental work at the NTNU wet gas compressor rig it is of importance to analyse and document the test rig and compressor behaviour under different transient operating conditions.

1. Establish a dynamic simulation model for the compressor test facility. Model functionality and shortcomings to be documented.
2. Validate model against dry and wet trip scenarios. Challenges related to accurate transient rig measurements to be included.
3. Establish a representative transient operating scenario and predict deviation between dry and wet compressor behavior.

-- " --

Within 14 days of receiving the written text on the master thesis, the candidate shall submit a research plan for his project to the department.

When the thesis is evaluated, emphasis is put on processing of the results, and that they are presented in tabular and/or graphic form in a clear manner, and that they are analyzed carefully.

The thesis should be formulated as a research report with summary both in English and Norwegian, conclusion, literature references, table of contents etc. During the preparation of the text, the candidate should make an effort to produce a well-structured and easily readable report. In order to ease the evaluation of the thesis, it is important that the cross-references are correct. In the making of the report, strong emphasis should be placed on both a thorough discussion of the results and an orderly presentation.

The candidate is requested to initiate and keep close contact with his/her academic supervisor(s) throughout the working period. The candidate must follow the rules and regulations of NTNU as well as passive directions given by the Department of Energy and Process Engineering.

Risk assessment of the candidate's work shall be carried out according to the department's procedures. The risk assessment must be documented and included as part of the final report. Events related to the candidate's work adversely affecting the health, safety or security, must be documented and included as part of the final report. If the documentation on risk assessment represents a large number of pages, the full version is to be submitted electronically to the supervisor and an excerpt is included in the report.

Pursuant to "Regulations concerning the supplementary provisions to the technology study program/Master of Science" at NTNU §20, the Department reserves the permission to utilize all the results and data for teaching and research purposes as well as in future publications.


The final report is to be submitted digitally in DAIM. An executive summary of the thesis including title, student's name, supervisor's name, year, department name, and NTNU's logo and name, shall be submitted to the department as a separate pdf file. Based on an agreement with the supervisor, the final report and other material and documents may be given to the supervisor in digital format.

- Work to be done in lab (Water power lab, Fluids engineering lab, Thermal engineering lab)  
 Field work

*(Guided work only)*

Department of Energy and Process Engineering. 14. January 2014

  
\_\_\_\_\_  
Olav Bolland  
Department Head

  
\_\_\_\_\_  
Lars E Bakken  
Academic Supervisor

Research Advisor:  
H. Nordhus, Statoil  
T. Bjørge, Statoil





## **Preface**

I would like to thank my supervisor L.E. Bakken and my co-supervisors T. Bjørge and H. Nordhus for their support and help through the work of this master thesis.

I would also like to thank Statoil and General Electric for their generous contribution to the field trip in April 2014. Without their donation the excursion to General Electric's facilities in Florence would not have been possible.





## Sammendrag

Denne masteroppgaven tar for seg tre deloppgaver i forbindelse med ikke-stasjonær drift av våtgasskompressorer.

Den første oppgaven etablerer en dynamisk simuleringsmodell for våtgass-kompressorriggen på NTNU. Modellen er utviklet i programvaren «HYSYS Dynamics» og er designet for å kunne simulere tørr- og våtgass kompressorrespons ved tripp av driver. Det er foretatt en validering av modellytelsen under stasjonære forhold. Med unntak av ett testpunkt avviker modellen mindre enn 1% for målt polytropisk løftehøyde og volumstrøm på innsugsiden.

Den andre deloppgaven validerer modellytelse ved tripp av driver for både tørr- og våtgass. Avvik mellom simuleringsmodell og testing i rigg blir evaluert i forhold til rotasjonshastighet, polytropisk løftehøyde og volumstrøm på innsugssiden. Det er svært lite avvik mellom simulert rotasjonshastighet og målt rotasjonshastighet.

På det meste avviker den simulerte polytropiske løftehøyden med 7.21% i forhold til løftehøyden utregnet fra testresultater. Imidlertid skyldes mye av avvikene en systematisk forskyvning av kurvene. Det forventes derfor at avviket kan reduseres ved kurvetilpasning.

Den simulerte volumstrømmen på innsugssiden avviker til dels kraftig fra utregnet volumstrøm basert på testresultater. Dette gjelder også de første sekundene etter tripp, noe som er uheldig med tanke på modellens evne til å forutsi surge ved lave strømningsrater. Maksimalt avvik er 8.68%.

Den siste deloppgaven tar for seg avvik mellom tørr og våt gass ved et valgfritt men representativt ikke-stasjonært driftsscenario. Det ble valgt å undersøke kompressorrespons ved hastighetsopptrapping fra 9 000 rpm til 11 000 rpm for både tørr og våt gass. Scenarioene ble også testet i kompressorriggen.

Simuleringen indikerer en mer langsom økning av rotasjonshastighet ved våtgass sammenliknet med tørrgass. Testresultater tilbakeviser dette, da målt rotasjonshastighet øker helt likt for tørr- og våtgass. Forøvrig avslører testresultatene at den dynamiske modellen ikke gjengir den transiente responsen til kompressorriggen på en nøyaktig måte ved hastighetsopptrapping.



## Abstract

This master thesis considers three subtasks related to transient operation of wet gas compressors.

HYSYS Dynamics is used to establish a dynamic simulation model in the first subtask. The model is designed to predict transient behavior of the compressor test facility at NTNU during dry and wet gas trip scenarios. Its steady state performance has been validated against test data. The deviation of polytropic head and suction volume flow is less than 1% for all test points but one.

Dry and wet gas model performance during trip is validated in the second subtask. The deviation is evaluated in terms of rotational speed, polytropic head and suction volume flow. Minimal deviation is observed for rotational speed.

The polytropic head prediction deviates up to 7.21% compared to values calculated from test data. The deviation is partly due to consistent offset between the predicted and calculated curves. Curve fitting is expected to significantly reduce the polytropic head deviation.

The predicted suction volume flow deviates severely from the values based on test data. This is also evident during the first seconds of trip, which is unfortunate in terms of surge behavior prediction. The maximum deviation is 8.68%

The last subtask considers deviation between dry and wet compressor behavior during a representative transient operating scenario. It was decided to investigate compressor response during speed ramp-up from 9 000 rpm to 11 000 rpm for dry and wet gas. The scenarios are also performed in the lab facility.

The simulations suggest a slower increase in rotational speed for wet gas compared to dry gas. This is not confirmed by test results which indicate no difference between wet and dry gas. The dynamic model is not able to accurately predict the transient behavior of the compressor test facility during speed ramp-up.

## Content

Preface.....	V
Sammendrag .....	VII
Abstract .....	IX
Content.....	X
List of tables .....	XII
List of figures .....	XIII
Nomenclature.....	XV
1. Introduction.....	1
1.1. Motivation .....	1
1.2. Structure and layout of the report .....	3
2. Theory.....	7
2.1. Introduction.....	7
2.2. Compression fundamentals.....	8
2.3. Wet gas impact.....	14
2.4. Compressor trip.....	17
2.5. Orifice plate .....	21
2.6. Energy balance for rotating parts.....	23
2.7. HYSYS Dynamics .....	24
3. NTNU wet gas test facility .....	31
3.1. Introduction.....	31
3.2. Main layout.....	31
3.3. Sensors .....	34
4. HYSYS and HYSYS Dynamics .....	39
4.1. Introduction.....	39
4.2. HYSYS Steady state model.....	40
4.3. HYSYS Dynamics model .....	46
4.4. Compressor characteristics .....	54
4.5. Tuning of orifice non-recoverable pressure loss.....	56
4.6. Instability challenges in HYSYS Dynamics.....	58
4.7. Shortcomings of HYSYS Dynamics model.....	61
5. Results and discussion.....	65
5.1. Introduction.....	65
5.2. Validation of steady state performance of dynamic model.....	66

5.3.	Trip test scenarios .....	72
5.4.	Trip test results.....	73
5.5.	Challenges related to accurate transient measurements .....	87
5.6.	Discussion of trip scenarios .....	89
5.7.	Speed ramp-up scenarios.....	92
5.8.	Speed ramp-up results .....	94
5.9.	Discussion of speed ramp-up results.....	99
6.	Conclusion .....	103
7.	Further work.....	105
	References.....	106
	Appendices .....	i
A.	Steady state model layout.....	ii
B.	Test data for development of compressor curves .....	iii
C.	Steady state validation of dynamic model .....	v

## List of tables

Table 2-1 - Tables for Kårstø wet gas performance testing .....	14
Table 3-1 - List of sensors used for evaluation of experimental compressor rig .....	34
Table 4-1 - Input parameters for the dynamic model .....	48
Table 4-2 - Boundary conditions and dynamic specifications for the dynamic model .....	49
Table 4-3 - Deviation of curve fit at 1.12m <sup>3</sup> /s and GMF0.8.....	55
Table 4-4 - Test points for development of non-recoverable pressure loss in orifice plate .....	56
Table 5-1 - List of test points for steady state validation of dynamic model .....	66
Table 5-2 - Steady state validation of dry gas low volume flow.....	66
Table 5-3 - Steady state validation of dry gas BEP .....	67
Table 5-4 - Steady state validation of dry gas high volume flow.....	67
Table 5-5 - Steady state validation of wet gas low volume flow.....	68
Table 5-6 - Steady state validation of wet gas BEP .....	68
Table 5-7 - Steady state validation of wet gas high volume flow.....	68
Table 5-8 - Maximum deviation of dynamic model .....	71
Table 5-9 - Test points for trip scenarios.....	72
Table 5-10 - Maximum deviation of dynamic trip simulation .....	86
Table 5-11 - Test points for speed ramp-up test.....	93
Table 5-12 - Time to reach 95% and 99% of steady state speed for ramp-up simulation .....	94
Table 5-13 - Time to reach 95% and 99% of steady state polytropic head for ramp-up simulation ....	95
Table 5-14 - Time to reach 95% and 99% of steady state suction volume flow for ramp-up simulation .....	96
Table 5-15 - Time to reach 95% and 99% of steady state speed for ramp-up test.....	96
Table 5-16 - Time to reach 95% and 99% of steady state polytropic head for ramp-up test .....	97
Table 5-17 - Time to reach 95% and 99% of steady state suction volume flow for ramp-up test.....	98

## List of figures

Figure 1-1 - Historical production of oil and gas, and prognosis for production in coming years (Ministry of Petroleum and Energy 2014) .....	1
Figure 2-1 - Siemens Demag Delaval ECOII centrifugal compressor with integrated motor (Brenne, Bjørge et al. 2008) .....	8
Figure 2-2 – Polytropic head for a centrifugal compressor.....	9
Figure 2-3 – Polytropic efficiency for a centrifugal compressor .....	10
Figure 2-4 - Isentropic and polytropic compression process .....	11
Figure 2-5 - Specific polytropic head versus suction volumetric flow (Hundseid, Bakken et al. 2008)	15
Figure 2-6 - Specific polytropic head versus suction volumetric flow (Hundseid, Bakken et al. 2008)	15
Figure 2-7 - Polytropic efficiency versus suction volumetric flow (Hundseid, Bakken et al. 2008) .....	16
Figure 2-8 - Run down characteristics of different polar inertia (Tveit, Bakken et al. 2004) .....	17
Figure 2-9 - Run down characteristics of different power decay rate (Tveit, Bakken et al. 2004).....	18
Figure 2-10 - Run down characteristics of different drives (Tveit, Bakken et al. 2004) .....	18
Figure 2-11 - Impact of suction and discharge volume on run down characteristics (Tveit, Bjørge et al. 2005).....	19
Figure 2-12 - Orifice plate (Crane Co. 2011).....	21
Figure 2-13 - Polytropic method selection in HYSYS .....	26
Figure 2-14 - Curve Input Option in HYSYS.....	27
Figure 3-1 - The air intake section .....	31
Figure 3-2 - Orifice plate and injection module .....	32
Figure 3-3 - The manually operated discharge valve .....	33
Figure 3-4 - Process flow diagram of the compressor test facility .....	36
Figure 4-1 - Inlet section of the steady state model .....	40
Figure 4-2 - Input spreadsheet operator .....	41
Figure 4-3 - Orifice section of the steady state model .....	42
Figure 4-4 - Orifice spreadsheet operator of the steady state model .....	42
Figure 4-5 - Injection module and compressor section of the steady state model .....	43
Figure 4-6 - GMF spreadsheet operator of the steady state model .....	44
Figure 4-7 - Calculations spreadsheet operator of the steady state model.....	45
Figure 4-8 - Layout of HYSYS Dynamic model .....	47
Figure 4-9 - Process flow diagram showing differences in mass flow and pressure drop calculation..	50
Figure 4-10- Motor spreadsheet of the dynamic model .....	51
Figure 4-11 - Compressor operator rating tab of the dynamic model .....	52
Figure 4-12 - Process flow diagram showing mass flow and pressure drop calculation of the dynamic model.....	52
Figure 4-13 - Polytropic head of test points and fitted curve .....	54
Figure 4-14 - Polytropic efficiency of test points and fitted curve .....	55
Figure 4-15 - Non-recoverable pressure drop versus orifice differential pressure for a selection of test points.....	57
Figure 4-16 - Instable behavior of HYSYS Dynamics during early stage model development .....	59
Figure 4-17 - Instability in HYSYS Dynamic during mixing of non-saturated air and water .....	60
Figure 5-1 - Deviation in polytropic head due to curve fit and linear interpolation .....	69
Figure 5-2 - Compressor speed versus time for dry gas BEP trip .....	74
Figure 5-3 - Polytropic head versus time for dry gas BEP trip.....	74

Figure 5-4 - Suction volume flow versus time for dry gas BEP trip .....	75
Figure 5-5 - Polytropic head versus suction volume flow for dry gas BEP trip.....	75
Figure 5-6 - Compressor speed versus time for wet gas BEP trip .....	76
Figure 5-7 - Polytropic head versus time for wet gas BEP trip .....	76
Figure 5-8 - Suction volume flow versus time for wet gas BEP trip .....	77
Figure 5-9 - Polytropic head versus suction volume flow for wet gas BEP trip.....	77
Figure 5-10 - Compressor speed versus time for dry gas surge trip .....	78
Figure 5-11 - Polytropic head versus time for dry gas surge trip .....	78
Figure 5-12 - Suction volumetric flow versus time for dry gas surge trip .....	79
Figure 5-13 - Polytropic head versus suction volume flow for dry gas surge trip.....	79
Figure 5-14 - Compressor speed versus time for wet gas surge trip .....	80
Figure 5-15 - Polytropic head versus time for wet gas surge trip .....	80
Figure 5-16 - Suction volume flow versus time for wet gas surge trip.....	81
Figure 5-17 - Polytropic head versus suction volume flow for wet gas surge trip .....	81
Figure 5-18 - Compressor speed versus time for dry gas open valve trip.....	82
Figure 5-19 - Polytropic head versus time for dry gas open valve trip .....	82
Figure 5-20 - Suction volume flow versus time for dry gas open valve trip.....	83
Figure 5-21 - Polytropic head versus suction volume flow for dry gas open valve trip .....	83
Figure 5-22 - Compressor speed versus time for wet gas open valve trip.....	84
Figure 5-23 - Polytropic head versus time for wet gas open valve trip.....	84
Figure 5-24 - Suction volume flow versus time for wet gas open valve trip test.....	85
Figure 5-25 - Polytropic head versus suction volume flow for wet gas open valve trip .....	85
Figure 5-26 - Travel time for different suction volume flow .....	88
Figure 5-27 - Compressor speed versus time for dry and wet ramp-up simulation .....	94
Figure 5-28 - Polytropic head versus speed for dry and wet gas ramp-up simulation .....	95
Figure 5-29 - Suction volume flow versus time for dry and wet ramp-up simulation .....	95
Figure 5-30 - Compressor speed versus time for dry and wet gas ramp-up test.....	96
Figure 5-31 - Polytropic head versus time for dry and wet gar ramp-up test.....	97
Figure 5-32 - Suction volume flow versus time for dry and wet ramp-up test .....	97
Figure 5-33 - Test and simulation results in a polytropic head versus suction volume flow diagram..	98



## Nomenclature

### List of symbols

Symbol	Description	Unit
H	Head	[m]
Q	Volume flow	[m <sup>3</sup> /s]
$\eta$	Efficiency	[-]
h	Enthalpy	[kJ/kg]
s	Entropy	[kJ/kg*K]
p	Pressure	[bar]
v	Specific volume	[m <sup>3</sup> /kg]
k	Isentropic exponent	[-]
$c_p$	Isobaric specific heat capacity	[kJ/(kmol*K)]
$c_v$	Isochronic specific heat capacity	[kJ/(kmol*K)]
T	Temperature	[K]
n	Polytropic exponent	[-]
m	Mass flow	[kg/s]
N	Rotational speed	[rpm]
P	Power	[kW]
c	Flow coefficient	[-]
Y	Expansion factor	[-]
$\rho$	Density	[kg/m <sup>3</sup> ]
d	Diameter	[m]
$\beta$	Orifice diameter ratio	[-]
I	Moment of inertia	[kg*m <sup>2</sup> ]
$\omega$	Angular velocity	[rad/s]
$\Delta t$	Time step	[s]
f	Polytropic head factor	[-]
$R_0$	Universal gas constant	[kJ/kmol*K]
Z	Compressibility factor	[-]
MW	Molecular weight	[kg/kmol]
$h_{fg}$	Heat of vaporization	[kJ/kg]

### List of subscripts

<b>Symbol</b>	<b>Description</b>
p	Polytropic
s	Isentropic
1	Start
2	End
g	Gas
l	Liquid
orifice	Orifice
pipe	Pipe
non-recoverable	Non-recoverable
driver	Driver
fluid	Fluid
n	Current time step
n+1	Next time step
tp	Two-phase
phase exchange	Phase exchange
experimental	Experimental

### List of abbreviations

<b>Abbreviation</b>	<b>Description</b>
rpm	Rotations per minute
GVF	Gas volume fraction
GMF	Gas mass fraction
IGV	Inlet guide vanes
MW	Molecular weight
BEP	Best efficiency point





# 1. Introduction

## 1.1. Motivation

Natural gas accounts for more than 20% of the global energy demand. Current trends along with future prospects suggest natural gas to become even more important as an energy source in years to come.

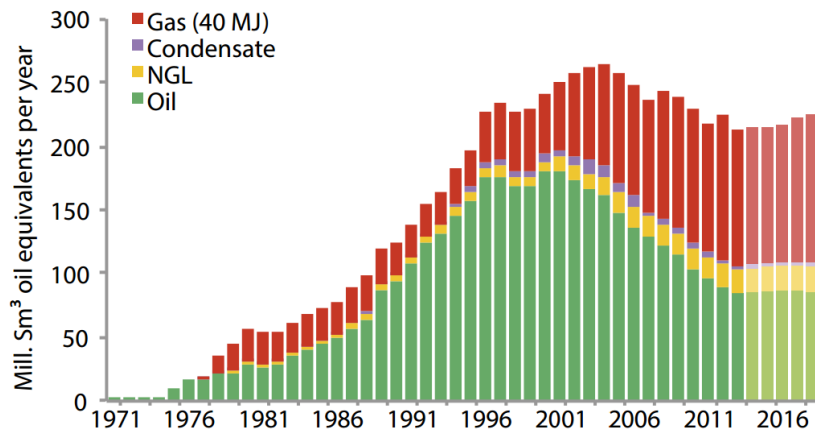


Figure 1-1 - Historical production of oil and gas, and prognosis for production in coming years (Ministry of Petroleum and Energy 2014)

Since oil production started on the Norwegian shelf in 1971, the majority of the large oil fields in the North Sea have been developed. To obtain production, attention has been shifted to gas/condensate fields, as well as smaller and more remote areas. These areas require new and cost effective technology to achieve profitability.

Subsea gas compression is considered a key element in future development of new gas/condensate fields. Utilization of such new technology allows for:

- Increased recovery at tail end production in depleted fields
- Reduced investment and operational cost of production facilities
- Development of more remote areas
- Reduced impact on environment

Dynamic simulations can be a powerful tool in the process of designing subsea compressor systems. Design and verification of control systems is a central area for such simulations. Control of multiple compressors in series or parallel is another. Other applications where transient behavior is important include (Patel, Feng et al. 2007):

- Compressor startup, shutdown and turndown
- Equipment failure
- Anti-surge protection
- Driver size selection

Typical use of dynamic simulations through a project development can be (Patel, Feng et al. 2007):

- Driver size selection in early phase of project
- Sizing of recirculation valves and coolers, startup power requirements and robustness of control system in the engineering phase
- Evaluation of possible system modifications during operation phase

This work will investigate the ability to predict dry and wet gas compressor behavior

## 1.2. Structure and layout of the report

### Background

This work is the result of a Master thesis in thermal energy at Department of Energy and Process Engineering from January to June 2014. The title of the assignment is «Wet Gas Compressor Transients». L.E. Bakken is the supervisor of the work. The co-supervisors are H. Nordhus and T. Bjørge.

The objective of this master thesis is divided into three subtasks: The first objective is to establish a dynamic simulation model for the compressor test facility at NTNU. Model shortcomings and functionality are included. The simulation tool HYSYS Dynamics by AspenTech is used to develop the model. HYSYS is a well-tested and reliable process simulation software used extensively in the industry. HYSYS Dynamics is an operation mode which allows steady state models to easily be converted into dynamic scenarios. Both development of actual compressor characteristic and validation of steady state performance are considered part of the model establishment.

The second objective is to validate the dynamic model against dry and wet gas trip scenarios. Attention is given to its ability to correctly predict rotational speed, polytropic head and suction volume flow during driver trip. Challenges related to accurate transient rig measurements are also evaluated.

The third objective is to establish a representative transient operating scenario and predict deviation between dry and wet gas compressor behavior. The author has taken initiative to run the operation scenario in the compressor lab in order to validate the dynamic model prediction. For this reason the choice of representative transient operating scenario was somewhat limited by the current compressor lab facility.

### Layout and structure of report

The report is structured into seven chapters. The first chapter is an introduction to the report which presents the main objectives and guides the reader through the chapters to follow.

The second chapter presents the fundamental theory forming the basis of the assignment.

The NTNU wet gas test facility is documented in the third chapter. Both main layout and all relevant sensors are described in detail. The chapter includes a process flow diagram of the compressor rig.

The fourth chapter presents the work related to development of simulation models. Both a steady state model used for test data analysis and a dynamic model used for transient performance prediction are thoroughly described. The chapter also includes compressor characteristic development and tuning of orifice pressure drop prediction. Instability challenges related to HYSYS Dynamics and the shortcomings of the dynamic model is presented in Section 4.7.

Chapter five presents the results of three different test activities:

- Steady state performance of dynamic model
- Dry and wet gas trip scenarios
- Speed ramp-up testing

Each testing activity consists of both predicted performance from the dynamic model and actual test data from the compressor test facility. The chapter also includes discussions and conclusions based on the results.

Chapter six contains the conclusion of the work. The three subtasks from the assignment text are addressed in this chapter.

The last chapter is suggestions to further work. A reference list is provided at the end.

### Challenges and limitations

The most severe challenge through the work of this Master thesis has been the functionality of HYSYS Dynamics. The current software is based on a user friendly drag-and-drop interface which enables models to be developed in an intuitive and graphical manner. Experience from the simulation tool has however revealed major instability problems related to compressor systems. It has not succeeded to identify the triggering factors for the instability, but the challenges seem related to low pressure ratio compression of wet gas.

The instability problems of HYSYS Dynamics are the main reason why piping in the test rig is not represented with any physical volume in the dynamic model. It also resulted in the model development being very time consuming.

The last subtask of the assignment text encourages the student to seek a representative transient operating scenario to identify deviation between dry and wet gas compressor behavior. In order to support any findings, it was determined that it should be possible to run the scenario in the current compressor test facility.

The compressor rig is open-looped and has manually operated valves for water flow rate and discharge air. This significantly limits the opportunities to perform repeatable experiments in the lab. It was chosen to perform compressor speed ramp-up testing which can completely be executed via the compressor control system. The test results did however reveal minimal deviation between dry and wet gas.







## 2. Theory

### 2.1. Introduction

This chapter presents some important theory which forms the basis for the assignment. The chapter consists of six sections plus the introduction. Some text is extracted from (Owren 2013).

The first section presents the most fundamental theory related to centrifugal compressors and compression theory.

The next section briefly documents the wet gas impact of compression processes.

Section 2.4 describes compressor trip and related challenges mainly based on experience from Troll-Kollsnes.

Orifice plates including relevant equations are presented in Section 2.5. This section contains fundamental relations used for design of both the steady state and dynamic HYSYS models.

Section 2.6 presents energy balances for rotating parts. The derived relations are used in the motor spreadsheet of the dynamic model in order to calculate transient response of the compressor.

The last section documents the system functionality of HYSYS Dynamics in order to model wet gas compression.

## 2.2.Compression fundamentals

### Centrifugal compressor

The centrifugal compressor has traditionally been dominant in oil and gas applications due to its robustness and capability to handle relatively large volume flows (Brenne, Bjørge et al. 2008) Prospects for future technology needs combined with promising test results have led to considerable interest in the centrifugal compressors capability to handle wet gas.

The centrifugal compressor consists essentially of a rotating impeller and a stationary diffuser. The impeller accelerates the incoming fluid to high velocity as well as increasing the pressure. The diffuser consists of diverging passages through which the fluid is decelerated, providing the final pressure increase. A common design criterion is that half of the pressure increase is done in the impeller, while the rest is provided by the diffuser. Because the diffuser is stationary, all the work is done on the fluid passing through the impeller. A centrifugal compressor with integrated motor is shown in Figure 2-1.

In HYSYS the user can chose between a reciprocating or centrifugal compressor. The latter enables compressor characteristics to be used as a specification in the model.

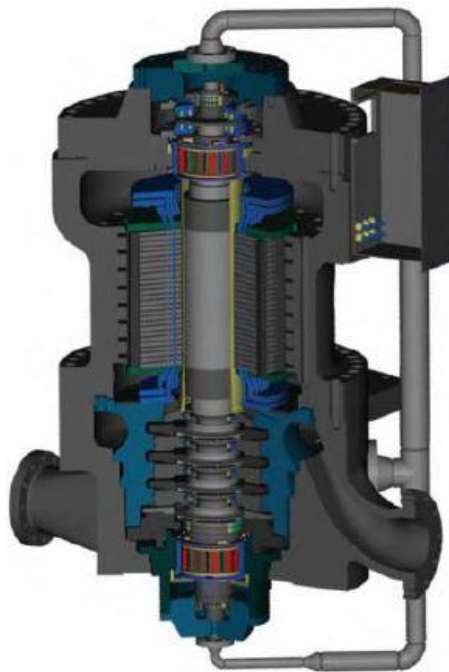


Figure 2-1 - Siemens Demag Delaval ECOII centrifugal compressor with integrated motor (Brenne, Bjørge et al. 2008)

### Compressor characteristics

A compressor curve is a plot showing compressor performance versus flow for different rotational speeds. It is usually assumed that the compressor performance is completely described by plotting two set of compressor curves. It is convenient to plot polytropic head as an equivalent to pressure rise, and polytropic efficiency as an equivalent to temperature rise.

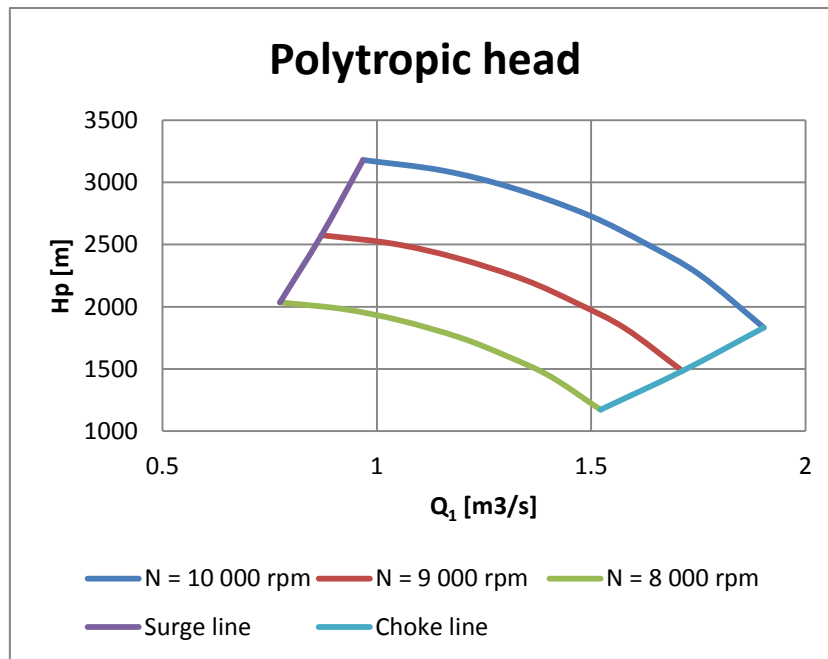


Figure 2-2 – Polytypic head for a centrifugal compressor

Figure 2-2 shows the polytypic head for a centrifugal compressor for three different speeds. The surge line is indicated left in the diagram. In this area the speed curves are at their maximum value for polytypic head. Any further reduction in volume flow will induce a phenomenon known as surging. Low gas velocities cause flow separation in the compressor. Increased losses make the compressor unable to generate the head required by the system. Surging is associated with rapid drop in delivered pressure and can create damaging pressure pulsations in the machine. High temperatures due to declining efficiency may damage internal or surrounding equipment. Control mechanisms to avoid operation in the surge area are a key element for viable compressor operation.

Rotating stall is another cause of instability and reduced compressor performance. Local unstable flow may be deflected in such a way that it induces flow breakdown in neighboring channels. Rotating instability along the compressor circumference causing damaging vibrations and poor performance may be observed. Rotating stall can contribute to surge, but may even appear in the nominally stable operating range (Saravanamutto, Rogers et al. 2009).

The choke line is indicated to the right. Beyond this line the head decreases rapidly with little or no change in volume flow. Increased losses are due to compressibility effects as the fluid approaches sonic velocity. At some point the flow cannot be increased any further for the given rotational speed, in which the compressor is choked.

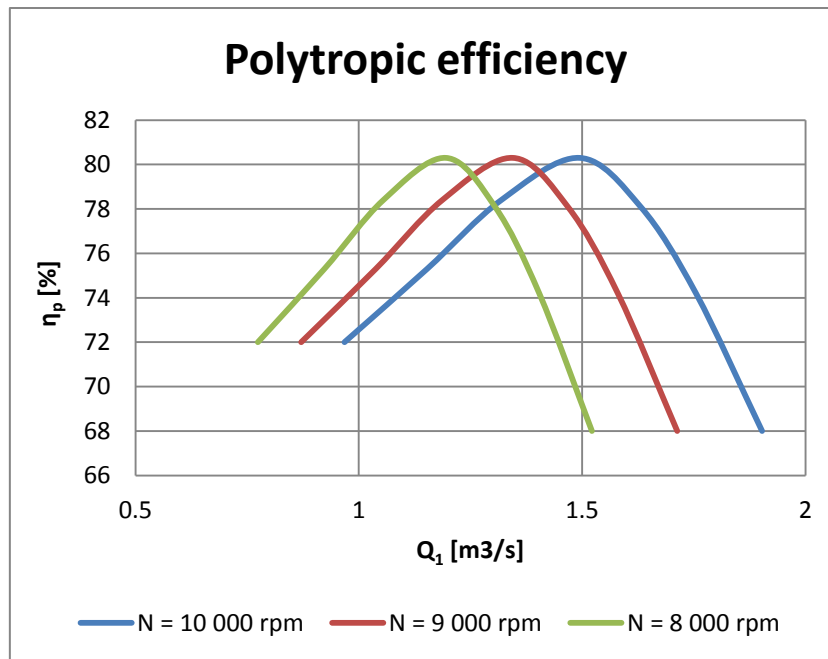


Figure 2-3 – Polytropic efficiency for a centrifugal compressor

Figure 2-3 shows the polytropic efficiency for a centrifugal compressor for three different rotational speeds. The efficiency varies with flow rate similar to the polytropic head. The point of maximum polytropic efficiency is however fairly constant for the curves. If the compressor can be controlled in terms of rotational speed, it is possible to operate close to the maximum obtainable efficiency for a wide range of flow rates.

Compressor characteristics have been used as input specification for the compressor operator in the dynamic model through this work. The characteristics presented in Section 4.4 are developed from actual compressor performance in the lab facility.

#### Compression process

Compressor performance can be calculated with either isentropic or polytropic analysis. This section will briefly explain the very fundamentals. Figure 2-4 shows a compression process in an enthalpy – entropy diagram with isobars indicated.

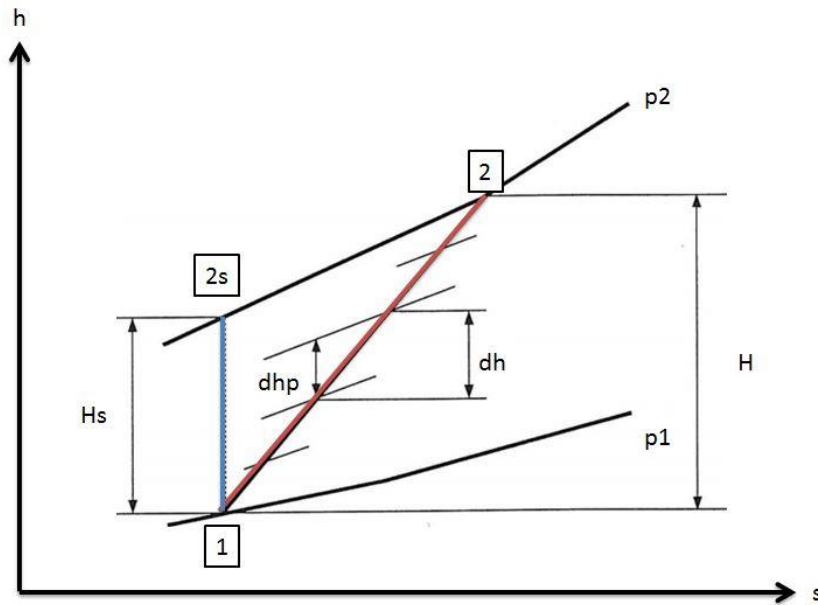


Figure 2-4 - Isentropic and polytropic compression process

The isentropic process is an ideal compression at constant entropy. HYSYS Dynamics uses the term «adiabatic» for isentropic processes. No heat exchange is taking place. An isentropic process is indicated with a blue line in Figure 2-4 and is defined:

$$pv^k = \text{constant} \quad (2-1)$$

For basic isentropic analysis, the isentropic exponent  $k$  is defined by the ratio of specific heats:

$$k = \frac{c_p}{c_v} \quad (2-2)$$

Because the isobars in Figure 2-4 are diverging  $[(dh/ds)_p = T]$ , two identical compressors operating under different suction pressure will give different isentropic head and efficiency (Hundseid, Bakken et al. 2008). By assuming a polytropic process, this effect is taken into account.

A polytropic process is defined:

$$pv^n = \text{constant} \quad (2-3)$$

It relates to many infinite small isentropic compression processes along the actual path of compression, indicated with a red line in Figure 2-4.

For ideal gases, the polytropic exponent  $n$  is related to the isentropic exponent  $k$  through the following expression:

$$\frac{n-1}{n} = \frac{k-1}{k \eta_p} \quad (2-4)$$

The isentropic efficiency is given by:

$$\eta_s = \frac{H_s}{H} \quad (2-5)$$

The polytropic efficiency is given by (2-6), where  $H_p$  is the polytropic head (not indicated in Figure 2-4)

$$\eta_p = \frac{dh_p}{dh} = \frac{\sum dh_p}{H} = \frac{H_p}{H} \quad (2-6)$$

Because the polytropic process follows the actual path of compression, the polytropic efficiency will be higher than the isentropic efficiency for a given path of compression.

Section 2.7 documents the equations HYSYS use for polytropic calculations.

### Wet gas

Gas containing liquid up to 5% on a volume basis is defined as wet gas (Hundseid and Bakken 2006, Brenne, Bjørge et al. 2008, Hundseid, Bakken et al. 2008). Two important parameters are gas volume fraction (GVF) and gas mass fraction (GMF):

$$GVF = \frac{Q_g}{Q_g + Q_l} \quad (2-7)$$

$$GMF = \frac{m_g}{m_g + m_l} \quad (2-8)$$

Due to significant differences in phase densities, a small content of liquid on a volume basis may consist of large quantities of liquid in terms of mass.

HYSYS assumes homogenous flow for two-phase applications. A single fluid model is used for wet gas calculations, documented in Section 2.7.

### Affinity laws

Affinity laws can be used to express the relationship between volume flow, head and power for different rotational speeds or diameters of turbo machines. For a centrifugal compressor of constant diameter  $D$ , the volume flow capacity  $Q$  can be expressed as in terms of rotational speed  $N$ :

$$\frac{Q_1}{Q_2} = \frac{N_1}{N_2} \quad (2-9)$$

The polytropic head  $H$  is proportional to the square of the rotational speed:

$$\frac{H_1}{H_2} = \left(\frac{N_1}{N_2}\right)^2 \quad (2-10)$$



The consumed power  $P$  is proportional to the cube of the rotational speed:

$$\frac{P_1}{P_2} = \left(\frac{N_1}{N_2}\right)^3 \quad (2-11)$$

These relations assume constant polytropic efficiency  $\eta$ :

$$\eta_{p,1} = \eta_{p,2} \quad (2-12)$$

Affinity laws are sometimes referred to as fan laws. The wet gas validity of affinity laws is discussed in Section 4.4.

### 2.3. Wet gas impact

The presence of a liquid phase in gas compressing significantly affects the performance. This section will briefly present the wet gas impact based on available literature.

Wet gas performance testing was performed at Kårstø north of Stavanger in 2003 and 2004. Two papers have been published presenting the test results: (Brenne, Bjørge et al. 2005) and (Hundseid, Bakken et al. 2008)

The test variables are summarized in Table 2-1.

Variable	Range	Unit
Gas volume fraction (GVF)	0.97 – 1.00	[-]
Gas volumetric flow rate	1600 – 2400	[m <sup>3</sup> /h]
Compressor speed	9651, 10723	[rpm]
Suction pressure	30, 50, 70	[bar]
Pressure ratio	~ 1.12 – 1.19	[-]
Test gas	Natural gas	[-]
Test liquid	Stabilized condensate, Water	[-]

Table 2-1 - Tables for Kårstø wet gas performance testing

The tested compressor was a single stage centrifugal compressor dated 1986. It was built to handle dry hydrocarbon gas, which suggests the design may not be optimal for wet gas service.

The purpose of the testing was to establish and verify wet gas correction methods (Hundseid, Bakken et al. 2008), and to initially verify boosting capabilities of a centrifugal compressor and provide data to compare the performance with other available wet gas concepts (Brenne, Bjørge et al. 2005). The low pressure ratios and the rather stable sales gas / condensate mixture utilized in the test may not reveal the true extent of multiphase behavior for subsea compressors.

Figure 2-5 and Figure 2-6 are taken from (Hundseid, Bakken et al. 2008) and shows how specific head varies with GVF, inlet pressure and liquid composition for a compressor operating under wet gas conditions. The figures have actual volumetric flow at compressor inlet plotted along the abscissa. The y-axis represents the specific polytropic head, which is the produced work per mass unit of flow through the compressor.

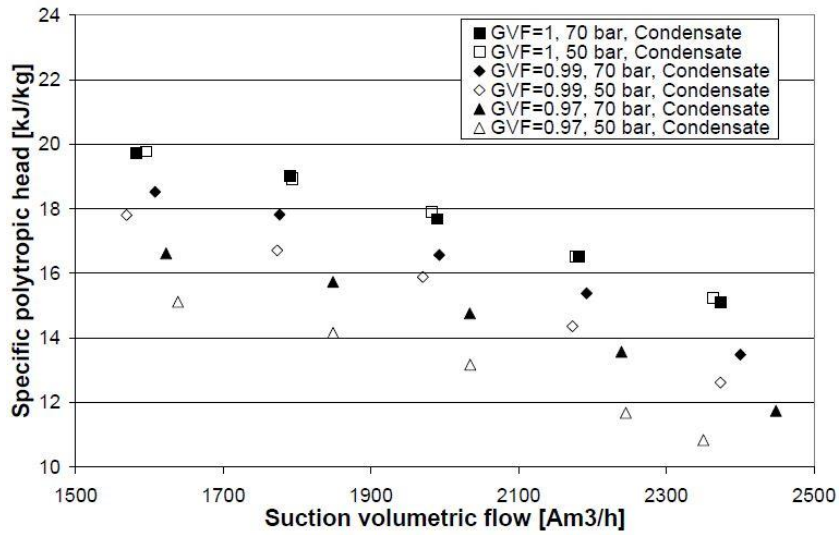


Figure 2-5 - Specific polytropic head versus suction volumetric flow (Hundseid, Bakken et al. 2008)

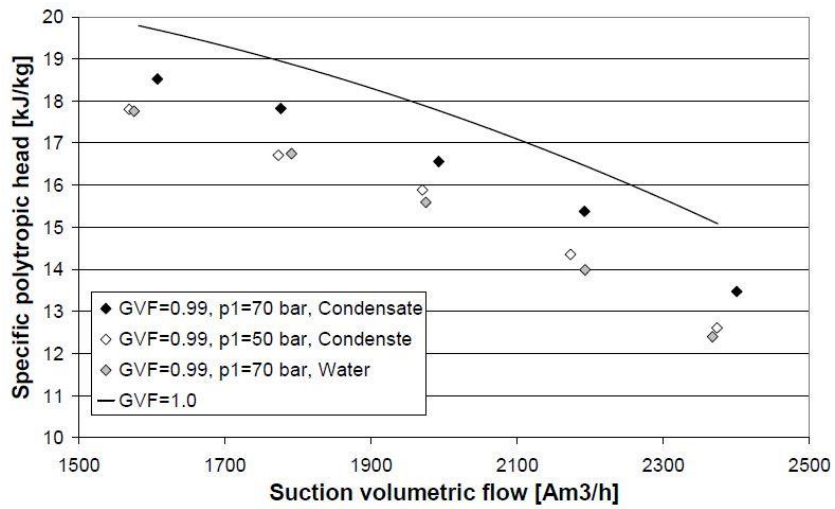


Figure 2-6 - Specific polytropic head versus suction volumetric flow (Hundseid, Bakken et al. 2008)

Figure 2-7 shows how polytropic efficiency varies with GVF, inlet pressure and liquid composition for a compressor operating under wet gas conditions (Hundseid, Bakken et al. 2008).

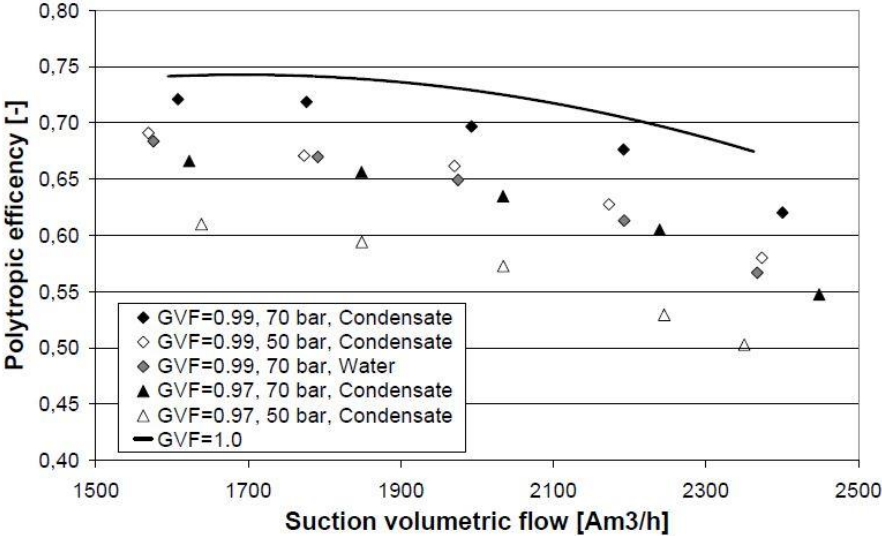


Figure 2-7 - Polytropic efficiency versus suction volumetric flow (Hundseid, Bakken et al. 2008)

It is obvious that GVF, inlet pressure and liquid properties have a significant influence on compressor performance. The reduction in head and efficiency is explained by an increase in mass flow due to the high density of the liquid phase. Low inlet pressures imply a high density ratio between gas and liquid due to the incompressibility of the latter. Correspondingly, water has high density compared to condensate, which gives the same effect (Hundseid, Bakken et al. 2008).

The test results reveal that wet gas compressor performance cannot easily be represented as single lines of constant speed in compressor characteristic diagrams, as of the procedure for dry gas applications. Compressor performance calculations need to compensate for wet gas effects.

Three different speed curves are used to specify the compressor unit in the dynamic model in this work. The curves are based on experimental data at 11 000 rpm and GMF-values of 1.00, 0.80 and 0.70.

## 2.4. Compressor trip

Dry and wet gas compressor trip testing has been performed in the compressor facility at NTNU during this work. This section presents results from former dry gas trip testing at Troll-Kollsnes. Experience from these tests formed the basis for both execution and discussion of the current trip testing and simulation.

Electrical drivers provide a promising alternative for future subsea compressor power supply. Electrical motors connected to an external power grid may trip if the voltage supply decreases below 80% of design value (Bakken, Bjørge et al. 2002, Tveit, Bakken et al. 2004, Tveit, Bjørge et al. 2005). Experience from Troll-Kollsnes has shown that during driver trips, the compressor may be forced into the surge and rotating stall area. Heavy vibrations and internal damage may occur, impairing the compressor seals.

Trip scenarios are divided into process trips and driver trips. Severe process system upsets can cause shut down, but in such events the driver shutdown can be delayed until the compressor protection systems are activated. For trips caused by the driver itself, no protective actions can be initiated prior the trip. This makes driver trips the most severe of all trip incidents (Tveit, Bakken et al. 2004).

### Polar inertia and power decay rate

The tendency for a system to enter surge during trip is affected by driver inertia and the driver power decay. Low polar inertia entails fast compressor speed deceleration and forces the operating point into the surge area. An electric drive typically has high polar inertia compared to gas turbine drivers of similar application, for which reason electrical drivers require less stringent compressor protection systems. Figure 2-8 shows the rundown characteristics of a compressor trip for three different polar inertias. The two systems with lower inertia clearly enter an operating region beyond the surge line. The high inertia line is inside the normal operating area during trip.

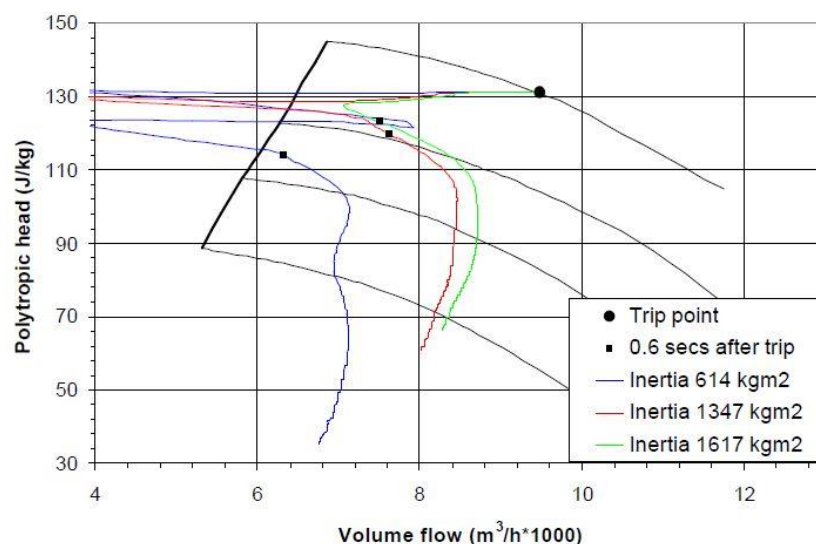


Figure 2-8 - Run down characteristics of different polar inertia (Tveit, Bakken et al. 2004)

The power decay rate has major impact on compressor rundown characteristics. While the electric motor power decay is instantaneous, the gas turbine decay is slower due to fuel valve shut-in time of approximately 100 ms (Tveit, Bakken et al. 2004). Slow power decay reduces the speed reduction

and stabilizes the compressor run down. Figure 2-9 shows the rundown characteristics of four different power decay rates. Even small changes in decay rate clearly show a large impact on the tendency to enter surge.

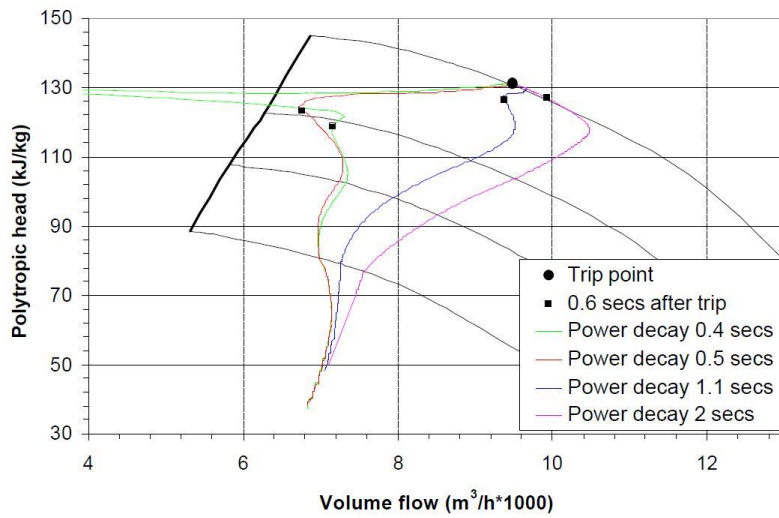


Figure 2-9 - Run down characteristics of different power decay rate (Tveit, Bakken et al. 2004)

An electric driver is favorable in terms of polar inertia, while the gas turbine driver has the advantage of slower power decay. For the Troll-Kollsnes case presented in (Tveit, Bakken et al. 2004), the two tendencies are equally effective, and the rundown characteristics of an electrical or gas turbine driven compressor are quite similar as shown in Figure 2-10. For subsea applications, electrical drivers are currently being used for power supply.

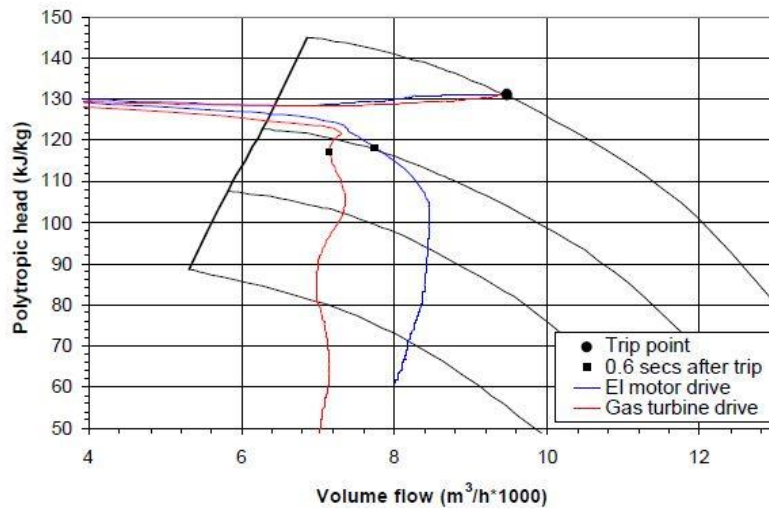


Figure 2-10 - Run down characteristics of different drives (Tveit, Bakken et al. 2004)

### Pipe volumes and protection valves

Gas compression systems usually include an anti-surge system. Such systems recycle the flow from the high pressure side to the suction side of the compressor to increase the volume flow and reduce head requirement. For high volume flow applications, an anti-surge capacity has to be increased beyond normal limits to protect the compressor from surge during trip (Tveit, Bjørge et al. 2005). To improve the run down characteristics a hot or cold bypass valve may be introduced parallel to the anti-surge. The bypass valve is only activated during trip. A fast response of the bypass valve is critical. At Troll-Kollsnes a time delay from 150 to 300 ms makes the bypass system unable to protect the compressor from entering the surge area.

Piping layout affects transient compressor performance. A large compressor discharge volume will give a slow pressure ratio reduction during trip. The operating point will be forced into the surge area. Figure 2-11 shows how the run down characteristics change when the discharge volume is increased (case 2.2) from the base case at Troll-Kollsnes. A slow discharge pressure reduction will increase the tendency of surge.

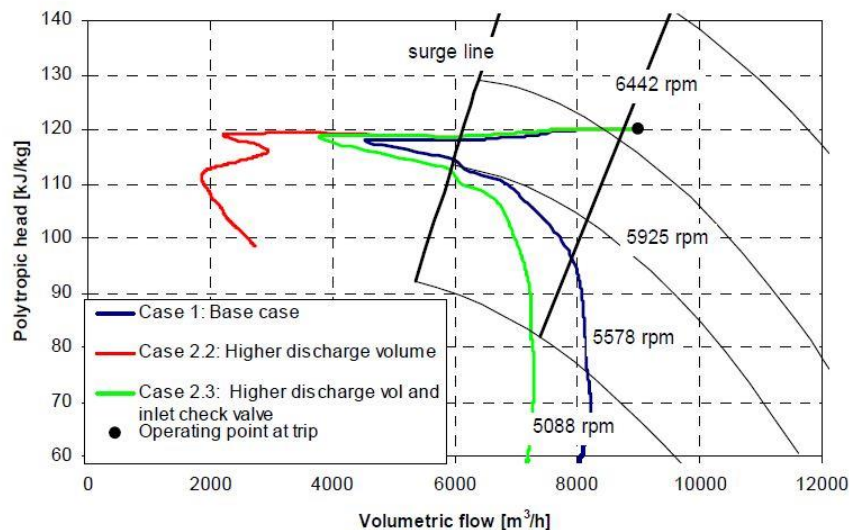


Figure 2-11 - Impact of suction and discharge volume on run down characteristics (Tveit, Bjørge et al. 2005)

In case 2.3 a check valve is installed which makes the cold gas bypass system increase the suction pressure more rapidly. The resulting run down characteristic becomes more favorable.

In order to reduce challenges related to surge during trip the discharge volume should be kept minimal. Anti-surge protective systems are more efficient if the suction volume is small.

### Trip testing at NTNU compressor rig

Note that the above presented figures and results are based on the Troll-Kollsnes pipeline compressors. The equipment is located onshore, compressing treated natural gas at high volume flow and pressure ratio. The actual behavior of a given plant may vary considerably, especially for wet gas applications. Subsea applications may involve very different system layout. Still the data from Troll-Kollsnes provides general expected behavior in terms of polar inertia, piping volumes and surge protection systems.

The NTNU wet gas compressor rig operates with air and water at low pressure ratio. The facility does not include an anti-surge protective system. During this work, both dry and wet gas trip test has been performed from an operating point close to the surge line. The purpose was to investigate the tendency for the compressor to enter the surge area during wet gas operation.



## 2.5.Orifice plate

Calculation of flow rate by measuring the differential pressure across a restriction is the most commonly used measurement technique in industrial applications (Crane Co. 2011). The calculations are based on Bernoulli's principles, and their accuracy has been extensively documented over the years.

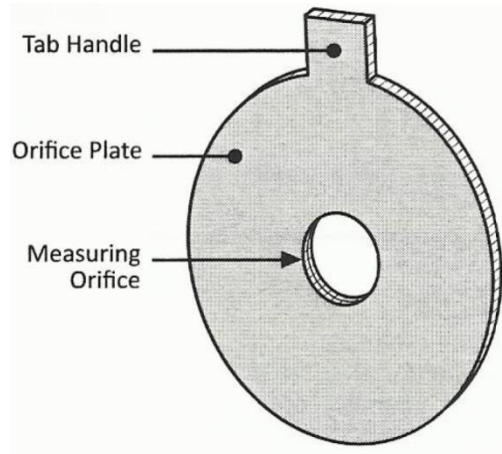


Figure 2-12 - Orifice plate (Crane Co. 2011)

The orifice plate consists of a thin plate with a concentric hole in the middle. The mass flow through the plate is given by (2-13)

$$\dot{m} = c * Y * \rho * \left(\frac{\pi}{4}\right) * d_{orifice}^2 * \sqrt{\frac{2 * \Delta p_{orifice}}{\rho * (1 - \beta^4)}} \quad (2-13)$$

The flow coefficient  $c$  is given by (2-14)

$$c = 0.5959 + 0.0312 * \beta^{2.1} - 0.184 * \beta^8 \quad (2-14)$$

$Y$  is the expansion factor given by (2-15)

$$Y = 1 - \frac{\Delta p_{orifice}}{P_1 * k} (0.41 + 0.35 * \beta^4) \quad (2-15)$$

The parameter  $\rho$  is the fluid density at the orifice inlet.  $d_{orifice}$  is the diameter of the orifice inner hole.  $\Delta p_{orifice}$  is the differential pressure across the orifice plate and should not be confused with the non-recoverable pressure loss. Sometimes referred to as constant pressure loss, it is the difference in static pressure before the impact of the pipe restriction and the section downstream the pipe where the static pressure recovery can be considered completed.

The isentropic exponent  $k$  is defined in (2-2). The beta ratio  $\beta$  is defined as

$$\beta = \frac{d_{orifice}}{d_{pipe}} \quad (2-16)$$

$d_{\text{pipe}}$  is the pipe flow diameter at orifice location. A relation for the non-recoverable pressure loss ( $\Delta p_{\text{non-recoverable}}$ ) is necessary to model the orifice plate in the dynamic model. Such a relation is provided in (Urner 1997):

$$\Delta p_{\text{non-recoverable}} = \frac{\sqrt{1 - \beta^4} - c\beta^2}{\sqrt{1 - \beta^4} + c\beta^2} \Delta p_{\text{orifice}} \quad (2-17)$$

More comprehensive relations exist to determine the mass flow rate through orifice plates based on differential pressure and inlet thermal properties. Many of these involve iterative algorithms. The accuracy of the above presented equations is considered to satisfy the exactness requirements for the current dynamic simulation application.

## 2.6. Energy balance for rotating parts

The kinetic energy of rotating parts in a compressor and driver system is given by (2-18).

$$Kinetic\ Energy = \frac{1}{2}I\omega^2 \quad (2-18)$$

I is the total inertia of compressor, coupling and driver.  $\omega$  is the angular velocity.

The compressor and driver are assumed directly coupled without gearing. The energy balance becomes

$$\frac{d}{dt}Kinetic\ energy = \frac{d}{dt}\left(\frac{1}{2}I\omega^2\right) = P_{driver} - P_{fluid} \quad (2-19)$$

$$\frac{1}{2}I * 2 * \omega \frac{d}{dt}\omega = P_{driver} - P_{fluid} \quad (2-20)$$

$$\frac{d}{dt}\omega = \frac{P_{driver} - P_{fluid}}{I * \omega} \quad (2-21)$$

$P_{driver}$  is the power delivered to the system.  $P_{fluid}$  is the power absorbed by the fluid. The rotational speed is given by (2-22)

$$N = \frac{60 * \omega}{2\pi} \quad (2-22)$$

The change in rotational speed is given by (2-23)

$$\dot{N} = \frac{(P_{driver} - P_{fluid})}{I * N} * \left(\frac{60}{2 * \pi}\right)^2 \quad (2-23)$$

(2-24) gives the rotational speed of the compressor and driver system. This numerical relation has proven to be quite accurate for the compressor rig despite its simple nature.

$$N_{n+1} = N_n + (\dot{N} * \Delta t) \quad (2-24)$$

$\Delta t$  is the calculation time step.

The above presented procedure forms the basis for determining the rotational speed in HYSYS Dynamics. The relations are included in the compressor unit operator, and HYSYS will automatically calculate the unknown parameters depending on the input specifications.

Through this work the compressor energy and speed calculations is performed externally in a spreadsheet in the dynamic model. This is done to ensure easy monitoring and access to all the variables during simulation. This will be documented in Section 4.3.

## 2.7.HYSYS Dynamics

This section will present fundamental theory regarding HYSYS Dynamics general ability to perform wet gas compression calculations. The functionality of the specific model developed through this work is documented in Chapter 4. The following section should be considered introductory. For further reference consult (Owren 2013).

HYSYS is a process simulation software made by Aspentech. HYSYS Dynamics is an operating mode integrated in the simulation tool. As HYSYS is used for stationary simulation cases, the dynamic mode allows non-steady state simulations.

HYSYS Dynamics has been chosen as the dynamic simulation software for three main reasons:

- HYSYS Dynamics system functionality was investigated in the project thesis, so its main principles of operation are known.
- HYSYS Dynamics is intuitive and easy to use.
- HYSYS is currently used extensively in the industry. The idea of easily converting existing steady state models into dynamic cases appears promising

### Conservation relationships

The conservation relationships in HYSYS Dynamics are similar to steady state balances, except for an accumulation term. This term allows output to vary over time. Mass balance is given by the following relation:

$$\begin{aligned} & \text{Rate of accumulation of mass} && (2-25) \\ & = \text{Mass flow into system} \\ & - \text{Mass flow out of system} \end{aligned}$$

Similar for component balance, except that components can also be formed by reaction:

$$\begin{aligned} & \text{Rate of accumulation of component } j && (2-26) \\ & = \text{Flow of component } j \text{ into the system} \\ & - \text{Flow of component } j \text{ out of the system} \\ & + \text{Rate of formation of component } j \text{ by reaction} \end{aligned}$$

For the energy balance, additional two terms are added:

$$\begin{aligned} & \text{Rate of accumulation of total energy} && (2-27) \\ & = \text{Flow of total energy into the system} \\ & - \text{Flow of total energy out of the system} \\ & \quad + \text{Heat generated by reaction} \\ & + \text{Heat added to system across its boundary} \\ & - \text{Work done by system on surroundings} \end{aligned}$$

### Solution method

HYSYS uses Implicit Euler Method to solve ordinary differential equations. Volume (pressure-flow), Energy and Composition relations are solved at different frequencies in order to save calculation

time. By default in HYSYS, the relations are solved every first, second and tenth time step respectively. The procedure can be altered by the user.

### Pressure Flow relations

Pressure and flow in the flow sheet is mainly based on two basic equations:

- Volume balance equations
- Resistance equations

For volume balance equations, the underlying principle is that the physical volume of the units does not change in time. The balance can be expressed as follows:

$$\begin{aligned} & \text{Volume change due to pressure} \\ & + \text{Volume change due to flows} \\ & + \text{Volume change due to temperature} \\ & + \text{Volume change due to other factors} \\ & = 0 \end{aligned} \tag{2-28}$$

Resistance equations calculate flow rates based on pressure differences of the surrounding units. For a valve the resistance term can be based on flow coefficients. For a compressor the heat flow and work define the pressure flow relation.

### Lumped model

Most unit operators in HYSYS use a lumped model. That is, the thermal and component concentration gradient in space is ignored. This enables use of ordinary differential equations to describe the process, saving calculation time compared to a distributed model. Columns and pipes are examples of unit operations in HYSYS which can include gradients in performance calculations. The compressor operator is lumped however.

The lack of gradients in space implies that some physical phenomena cannot be modeled. Two areas of particular interest are:

- Thermal non-equilibrium
- Flow regimes

Consequently, their influence on compressor performance will be neglected. This includes liquid film formation, droplet deposition and heat transfer. Compressor inlet flow regime is another variable which HYSYS does not include in its model.

Compressor test results suggest that the inlet flow regime is not of vital importance for a wet gas compressor. The compressor inlet acts as mixer making internal flow of the compressor independent of inlet flow regime (Brenne, Bjørge et al. 2005)

### Polytropic calculations

In HYSYS the compressor operation uses work to increase pressure of an inlet gas stream. Steady state calculations on design point are based on either adiabatic (isentropic) or polytropic approach.

The system needs to be fully specified, but the user is free to choose input parameters. HYSYS will calculate the unknown values.

In the user manuals AspenTech states that the general calculation procedure for polytropic head is based on ASME methods given by (Schultz 1962). Three different polytropic calculation methods for compressor head are available in HYSYS, see Figure 2-13

- Schultz
- Huntington
- Reference

However, the polytropic method selection is not covered in the user manuals, and it is not obvious how the Huntington and Reference method are implemented. The only information from AspenTech regarding the two polytropic methods is given in (Aspen Engineering 2009). In this text, the reader is referred to (Huntington 1985) for approaches of the polytropic head calculations. It is stated that the Huntington method and Reference method is only supported in steady state mode, and for the latter, a constant value for the polytropic efficiency has to be provided.

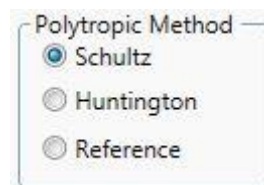


Figure 2-13 - Polytropic method selection in HYSYS

Nøvik evaluated the Reference method in his master thesis (Nøvik 2013). Due to the lack of insight in HYSYS calculation procedures he was not able to conclude how HYSYS had implemented the method in the software. A comparison between Schultz (HYSYS), Reference (HYSYS) and his self-developed direct integration model, strongly suggested that HYSYS has not implemented the method according to referred literature. Uncertainty about calculation procedures is a major drawback when using a simulation tool. Very small deviations in discharge temperature may provide large impact on calculated efficiencies.

For wet gas compression a calculation procedure utilizing a «direct integration» method is clearly favorable (Hundseid, Bakken et al. 2006). Unlike Schultz procedure, the Reference method allows thermodynamic and fluid properties to be updated along the compression path. In this way, heat and mass transfer effects can be included in compressor performance analysis.

However, in dynamic mode only Schultz procedure can be chosen, and the reliability of the Reference method has been questioned. It is not known whether these problems are solved in HYSYS Dynamics version 8.

### Compressor performance

For off design calculations, performance of the compressor cannot be set to a constant value. Instead speed curves should be used. With speed curves specified, the adiabatic or polytropic head and efficiency are fixed for a given rotational speed and volume flow. HYSYS can interpolate and

extrapolate the values of the compressor characteristics if the operating point does not match the provided curves.

Compressor internal geometry is not a part of HYSYS Dynamics functionality. The consequence is that HYSYS Dynamics has no means to evaluate change in compressor map due to change in operating conditions. However, in the option «curve input parameter» the user can choose between different methods to specify variation in compressor characteristics.

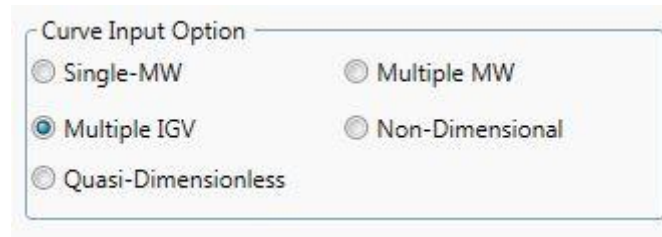


Figure 2-14 - Curve Input Option in HYSYS

The multiple IGV option allows the user to enter different collection of compressor curves for various IGV positions. Although designed for a variable inlet guide vane (IGV) feature, this option gives the user freedom to control the curve selection according to own preferences. The curve selection is based on a current IGV-position which is specified by the user. If the user has information about compressor performance which is not covered by HYSYS Dynamics calculation procedure, the multiple IGV option allows implementation of such effects in the compressor curves.

The multiple IGV feature is of special interest as it can be used to correct for wet gas performance effects. By inserting a curve collection for different GMF labeled to different IGV-positions, a controller can be used to choose the appropriate set of curves. However, this solution is based on the assumption that wet gas impact on compressor characteristics is solely a function of GMF. Challenges arise due to the fact that wet gas compressor performance also depends on suction pressure and fluid characteristics as discussed by (Brenne, Bjørge et al. 2005, Brenne, Bjørge et al. 2008, Hundseid, Bakken et al. 2008)

An alternative strategy for compressor curve implementation in HYSYS is to import compressor curves from a spreadsheet operator. This feature provides large flexibility in terms of customizing the curves to the respective operating conditions. While the multiple IGV option allows the user to insert known compressor characteristics corresponding to any given scenario, the use of spreadsheet allows continuous modification of the compressor curves. By the use of correction methods, wet gas compressor maps for any given conditions may automatically be generated from dry gas curves.

The use of compressor curves in dynamic mode is made difficult by a restriction in HYSYS Dynamic mode: The program does not allow changes to be made in the compressor curves while the simulator is running. In other words, the compressor map cannot continuously be changed to match variation in operating conditions. In his master thesis, Aguilera solved this problem by using excel and a Visual Basics Application code to automatize the procedure of correcting and activating the compressor curves. For further reading, consult (Aguilera 2013).

### Single fluid model

The compressor operation in HYSYS uses a single fluid model to model compressor performance. The model calculates polytropic head and exponent based on averaged specific volumes:

$$H_p = f * \frac{n_{TP}}{n_{TP} - 1} (p_2 * v_{TP2} - p_1 * v_{TP1}) \quad (2-29)$$

$$n_{TP} = \frac{\ln\left(\frac{p_2}{p_1}\right)}{\ln\left(\frac{v_{TP1}}{v_{TP2}}\right)} \quad (2-30)$$

The specific volume is based on homogeneous flow:

$$v_{TP} = \frac{1}{GVF * \rho_g + (1 - GVF) * \rho_l} \quad (2-31)$$

f is the polytropic head factor. It ensures that the calculated polytropic head is identical to the enthalpy difference for an isentropic compression:

$$f = \frac{h_{2s} - h_1}{\left(\frac{k}{k-1}\right) * [p_2 v_{2,s} - p_1 v_1]} \quad (2-32)$$

The single fluid model assumes multiphase flow to behave as a single phase. An alternative polytropic performance model is the two phase model, which calculates the contribution to the polytropic head separately for the two phases. This model is not included in the compressor operation in HYSYS.

$$H_p = GMF_1 \frac{n}{n-1} \frac{R_0}{MW_{g,1}} Z_1 T_1 \left[ \left(\frac{p_2}{p_1}\right)^{\frac{n-1}{n}} - 1 \right] + (1 - GMF_1) v_{l,1} (p_2 - p_1) \quad (2-33)$$

Where fluid quality and polytropic exponent is defined as follows:

$$GMF = \frac{\dot{m}_g}{\dot{m}_g - \dot{m}_l} \quad (2-34)$$

$$n = \frac{\ln\left(\frac{p_2}{p_1}\right)}{\ln\left(\frac{v_{g,1}}{v_{g,2}}\right)} \quad (2-35)$$

For a typical compression path, phase change is partly taken into account by the reduction in discharge temperature due to the liquid phase. A reduced temperature implies a lower specific



volume, which affects the polytropic exponent. However, in the two phase model it is possible to include phase exchange as a separate term:

$$H_{phase\ exchange} = (GMF_2 - GMF_1)h_{fg} \quad (2-36)$$

Test results from K-lab suggest that the calculated difference between the single fluid model and two phase model is insignificant (Brenne, Bjørge et al. 2005, Hundseid, Bakken et al. 2008). These tests were performed at low pressure ratios, with a two phase fluid consisting of sales gas and stabilized condensate. The content of propane and butane was low compared to unprocessed hydrocarbons. Due to the low pressure rise and fluid composition, any impact from phase exchange was neglected for both tests.

A subsea compressor will typically be required to operate with wet gas at higher pressure ratios, quite different from conditions tested on K-lab. For such applications, contribution from phase transition cannot be neglected, and the single phase model may not be a good approximation. For correct prediction of compressor performance, a model which explicitly includes phase exchange will most likely be necessary.

All testing through this work is performed with very low pressure ratios. The single fluid model is considered to satisfy the accuracy requirements.



### 3. NTNU wet gas test facility

#### 3.1.Introduction

This chapter presents the wet gas compressor test facility at NTNU. The first section describes the main layout and dimensions of the system. The next section presents the sensors which are used for performance documentation through this work. A process flow diagram with all sensors indicated is provided at the end.

#### 3.2.Main layout

The NTNU wet gas compressor test facility is located in the basement floor of Varmeteknisk laboratory in Trondheim. The rig consists of a single stage centrifugal compressor, working with atmospheric air and water in an open-loop layout.

Air at atmospheric conditions is sucked into a steel pipe of 250 mm inner diameter. Temperature, pressure and relative humidity is measured in close proximity to the inlet. A bell mouth of 500 mm diameter is mounted at the pipe entrance to obtain stable flow. Figure 3-1 shows the air intake section with the bell mouth and the ambient pressure, temperature and relative humidity sensors hanging to the left.

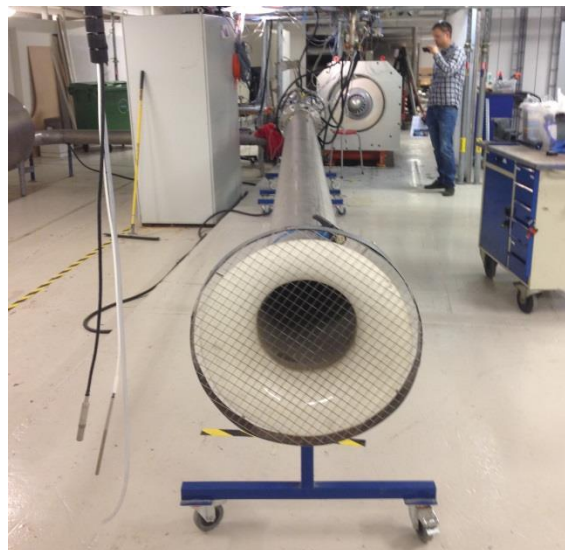


Figure 3-1 - The air intake section

The volumetric flow rate is measured with an orifice plate 5000 mm downstream the air intake. The beta value of the plate is 0.64. A differential pressure meter is installed over the orifice plate, which also supplies the static pressure at the orifice inlet. A temperature sensor is installed 690 mm upstream the orifice.

The water injection module is positioned 1150 mm downstream the orifice section. The injection module consists of 16 circularly mounted nozzles. Each nozzle has a manually operated valve. The water is fed from a large tank with a variable speed water pump. A volumetric flow meter and a manually operated valve are mounted on the water pipe. Figure 3-2 shows the orifice plate to the left and the injection module with the nozzles to the right. The water is entering the system via the water flow meter at the top.

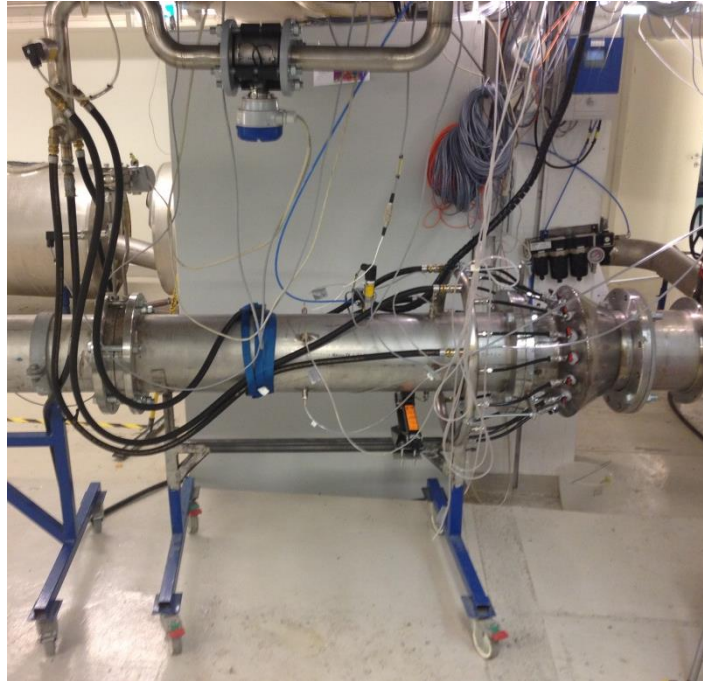
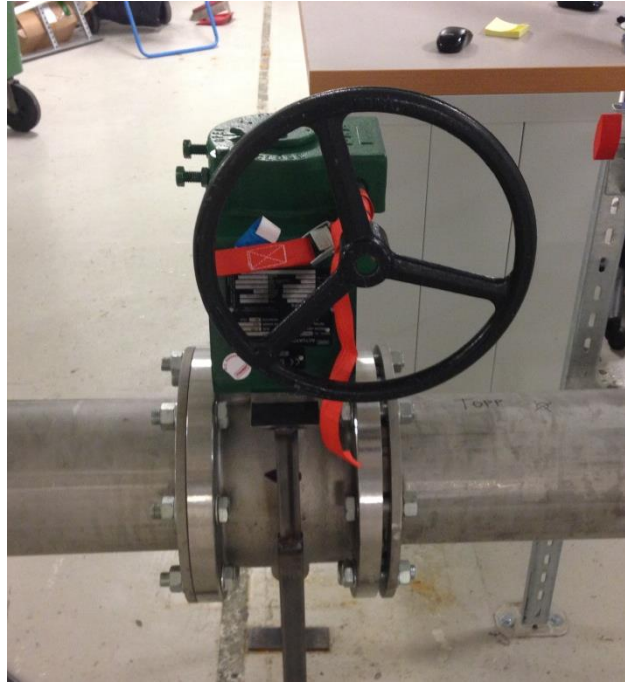


Figure 3-2 - Orifice plate and injection module

A rigid frame holds the compressor block, coupling and electric motor. Power is supplied from a variable speed drive, and is capable of delivering 450 kW at 11 000 rpm. A torque transducer is mounted on the coupling to the compressor block. The test facility is designed to handle different impeller geometries and diffuser widths.

The impeller has a direct axial inlet. No instrumentation is installed between the injection module and the compressor inlet. Plexiglas configuration at the compressor inlet and on sections on the compressor block itself enables visual inspection of flow pattern at inlet and through the impeller. A detailed picture of the multiphase flow can be obtained by the use of stroboscopic lamps during wet gas testing.



**Figure 3-3 - The manually operated discharge valve**

A 200 mm inner diameter steel pipe is connected to the radial compressor discharge. Pressure and temperature sensors are mounted on the pipe. The flow rate is controlled by a manually operated discharge valve 2270 mm downstream the compressor, shown in Figure 3-3. Water can be injected to the flow after the valve to reduce the exit temperature and hence limit the rise in room temperature during dry gas testing. The flow terminates in two atmospheric tanks where the liquid water is drained and the air re-enters the ambient.

### 3.3.Sensors

#### Existing sensors of the lab facility

The logging system of the compressor test facility is set up with 47 different channels. 19 of these sensors are being used through this work, presented in Table 3-1. All other sensors mounted on the test rig will not be further described.

Sensor label	Sensor name	Unit	Sensor description
ST-1.1	Compressor speed	rpm	
PT-3.1	dP Orifice	mbar	The differential pressure over the orifice plate
PT-1.1	IM Pressure	mbar	Pressure at injection module inlet.
TT-5.1	Orifice inlet temperature	C	Temperature at orifice inlet
PT-3.3	Orifice inlet pressure	mbar	Pressure at orifice inlet
PT-3.5	Discharge pressure	mbar	Pressure at compressor discharge
FT-1.5	Water flow rate	l/s	
XT-3.1P	Ambient pressure	Pa	Measured at bell mouth
XT-3.1T	Ambient temperature	C	Measured at bell mouth
XT-3.1R	Relative humidity	%	Measured at bell mouth
TT-500.16 to 19	Inlet temperature	C	Temperature at injection module inlet
TT-500.20 to 23	Discharge temperature	C	Temperature at discharge pipe
TT-500.24	Water temperature	C	Temperature at upstream injection module

Table 3-1 - List of sensors used for evaluation of experimental compressor rig

Note that the inlet temperature and discharge temperature are average readings from four different inlet temperature sensors and four different discharge temperature sensors.

A process flow diagram with the sensors and main equipment indicated is provided in Figure 3-4.

Sensor measurements are stored as TDMS-files in the lab control system. The files can be opened in MS Excel. The sampling time interval can be set by the user. During steady state testing for development of compressor curves the logging frequency was set to 2 Hz. During transient operation, the logging interval was set to 1000 Hz.

#### Sensor functionality for dynamic analysis

Strict sensor requirements are necessary in order to perform accurate dynamic analysis. Fast sensor response is the key feature of dynamic measuring equipment. The current temperature sensors of the lab are able to perform very accurate readings, but the response time is very slow. This makes the discharge temperature sensors unable to represent the compressor behavior during trip. The inlet temperature does not change dramatically, for which reason the readings are still considered acceptable. The discharge pressure sensors are satisfying in terms of response time.

Challenges related to accurate measurements for the specific trip tests results are documented in Section 5.5.

#### Lab facility control system

It should be noted that the calculation procedures of the compressor facility control system in some instances differs from relations used in this work. This is most evident for compressor rotational speed and GMF-values during wet gas testing. When the compressor speed is set to 11 000 rpm in

the control system, the real speed is typically between 10 840 rpm and 10 900 rpm. Similarly for GMF the calculation procedures used in the HYSYS models will predict a GMF value slightly lower compared to the value entered into the control system. This is due to the evaporation of liquid water into the non-saturated air which is taken into account in the model but not in the lab control system.

All results, calculations and discussions through this work are based on the actual sensor readings processed by the steady state HYSYS model of the compressor rig. The control system of the lab facility is only used for control purposes.

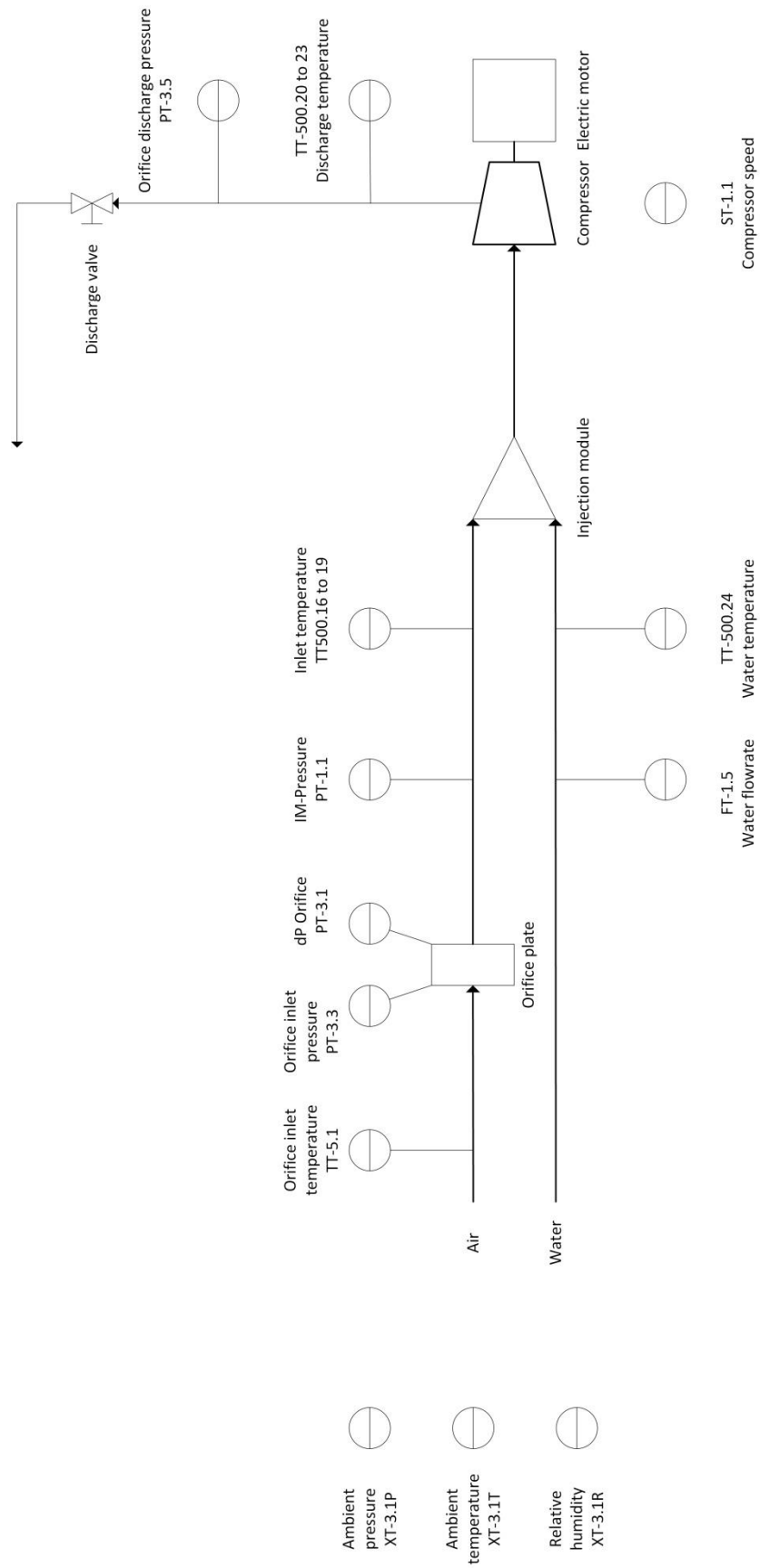


Figure 3-4 - Process flow diagram of the compressor test facility







## 4. HYSYS and HYSYS Dynamics

### 4.1. Introduction

The simulation software HYSYS including the dynamic simulation package HYSYS Dynamics has been the key tool for evaluation and prediction of both steady state and dynamic compressor behavior through this work. Two models have been developed to represent the wet gas test facility at NTNU:

- Steady state model for evaluation of test data
- Dynamic model for prediction of transient behavior

Even though the respective flow sheet of each model appears quite similar, the two models are based on very different approaches to determine the physical properties. Great care should be taken to understand how the two models calculate pressure, flow and temperatures for the unit operators.

The next two sections describe the steady state model and the dynamic model respectively.

Section 4.4 presents the compressor characteristics developed from steady state testing in the compressor lab facility.

It was necessary to tune the dynamic model in order to accurately predict the pressure loss over the orifice plate. The calculations and modified orifice relations are presented in Section 4.5.

Section 4.6 documents challenges related to stability of the HYSYS Dynamics simulation tool. Problems related to software functionality during of wet gas compression simulations have been a major challenge through this work.

The last section of the chapter documents the shortcomings of the dynamic model.

## 4.2.HYSYS Steady state model

### Introduction

Test data from the compressor lab at NTNU are mainly extracted as pressure and temperature readings from the instrumentation sensors presented in Table 3-1. In order to evaluate the results in terms of polytropic head, suction flow rate and polytropic efficiency, the data must be analyzed according to compression theory. The HYSYS steady state model is used for this purpose.

Through this work, the model was first used to develop compressor characteristics which were then used as specifications for the compressor unit in the dynamic model. Later the steady state model was used to evaluate data from the transient tests performed in the lab.

### Model layout

Appendix A shows the layout of the steady state model. It consists of three main parts from left to right:

- Inlet section
- Orifice section
- Injection module and compressor section

The following text describes each section in detail.

### Inlet section

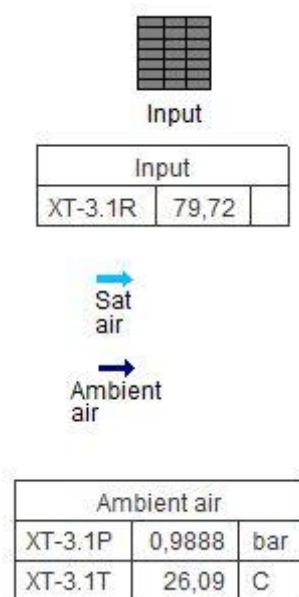


Figure 4-1 - Inlet section of the steady state model

The inlet section (Figure 4-1) consists of three units:

- Input spreadsheet operator
- Ambient air stream
- Sat air stream

All input parameters to the model are specified in the input spreadsheet operator. The values inserted in the cells are the only parameters that change during testing in the lab. All other parameters used in the model are related to facility geometries or fixed relations that do not change with operating conditions.

	A	B	C
2			
3	ST-1.1	Compressor speed	1.084e+004
4	PT-3.1	dP Orifice	100.2
5	PT-1.1	IM pressure	916.7
6	TT-5.1	Orifice Inlet temperat	25.94
7	PT-3.3	Orifice inlet pressure	987.6
8	PT-3.5	Discharge pressure	1203
9	FT-1.5	Water flow rate	0.5024
10	XT-3.1P	Ambient pressure	9.888e+004
11	XT-3.1T	Ambient temperature	26.09
12	XT-3.1R	Relative humidity	79.72
13	TT-500.16-19	IM temperature	25.58
14	TT-500.20-23	Discharge temperatur	31.09
15	TT-500.24	Water temperature	14.61
16			

Figure 4-2 - Input spreadsheet operator

Figure 4-2 shows the input spreadsheet operator. The input variables are specified in column C in the same order as they appear in the TDMS-test results file. Each value in column C is exported to one or multiple unit operators or streams in the flow sheet. By inserting values in the 13 cells in column C, an operating point is fully specified.

The stream Ambient air represents the intake air to the compressor rig. The pressure and temperature is defined by XT-3.1P (ambient pressure) and XT-3.1T (ambient temperature)

Relative humidity for air is not a specification which directly can be used as an input parameter in HYSYS. The unit «saturate with water» in the custom ribbon can be used for this purpose. It is however chosen to explicitly perform the relative humidity calculations in the input spreadsheet in order to obtain a simple and transparent model. An imaginary stream called Sat air is established as an aid to determine the relative humidity of the Ambient air. The pressure and temperature of the Sat air stream is defined by XT-3.1T (ambient temperature) and XT-3.1P (ambient pressure). The composition is set to 50% mole fraction water and 50% mole fraction air. This is done to ensure that the vapor phase of the Sat air stream will be saturated with water. The water mole fraction of the vapor phase is multiplied with the relative humidity from XT-3.1R (Relative humidity) and exported to the stream Ambient air. The corresponding mole fraction of air is set to unity minus the mole fraction of water. The composition of Ambient air is now specified.

## Orifice section

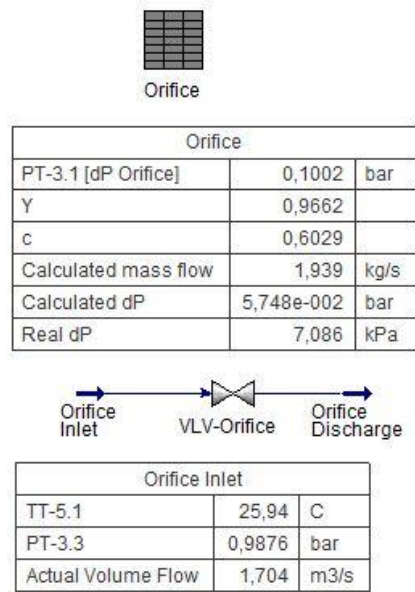


Figure 4-3 - Orifice section of the steady state model

The orifice section (Figure 4-3) consists of four units:

- Orifice spreadsheet operator
- Orifice inlet stream
- Orifice valve operator
- Orifice discharge stream

The Orifice inlet stream composition is identical to the one of Ambient air. The pressure and temperature are defined by PT-3.3 (Orifice inlet pressure) and TT-5.1 (Orifice inlet temperature)

	A	B
1		
2	Beta	0.6401
3	Pressure	0.9876 bar
4	k	1.405
5	dP_orifice	0.1002 bar
6	Density	1.138 kg/m3
7	diameter	0.1600
8	Y	0.9662
9	c	0.6029
10	m	1.939 kg/s
11		

Figure 4-4 - Orifice spreadsheet operator of the steady state model

The main objective of the orifice spreadsheet operator (Figure 4-4) is to calculate the mass flow of air. The calculations are based on the differential pressure of the orifice plate (PT-3.1) and thermodynamic properties of the orifice inlet stream according to equation (2-13) to (2-16).

It should be noted that the mass flow of air is based on experimental readings of the PT-3.1 (dP Orifice) and that the valve pressure drop is specified by the upstream and downstream pressure readings of sensor PT-3.3 (Orifice inlet) and PT-1.1 (IM-inlet) The relations for orifice recovery pressure drop as of (2-17) along with built-in relations for temperature change through the valve provides no impact on steady state model performance.

Injection module and compressor section

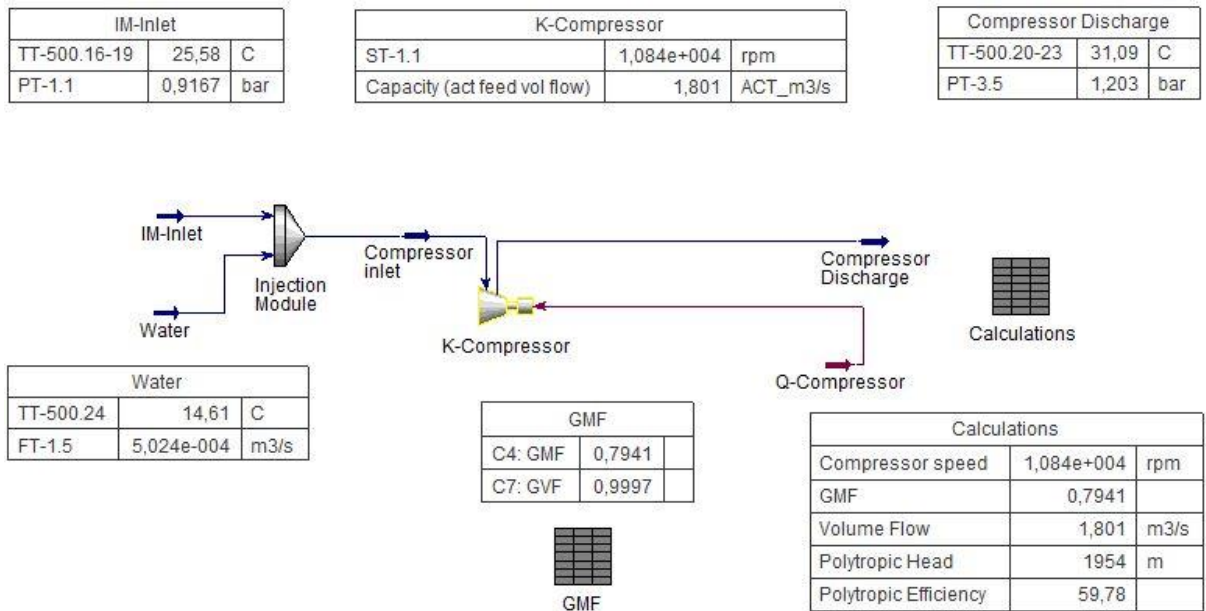


Figure 4-5 - Injection module and compressor section of the steady state model

The injection module and compressor section (Figure 4-5) calculates the main performance parameters in the steady state model. It consists of the following streams and operators:

- IM-inlet stream
- Water stream
- Injection module mixer
- Compressor inlet stream
- K-Compressor operator
- Compressor discharge stream
- Q-Compressor energy stream
- GMF spreadsheet
- Calculations spreadsheet

The pressure and temperature of the IM-inlet stream are defined by PT-1.1 (IM pressure) and TT-500.16-19 (Inlet temperature). The molar composition is imported from the Ambient air stream. The mass flow is imported from the Orifice inlet stream.

The temperature and flow rate of the Water stream are defined from TT-500.24 (Water temperature) and FT-1.5 (Water flow rate). At the test facility, the water is injected into the air through nozzles in the injection module. This is modeled by setting the water pressure equal to the IM-inlet pressure (PT-1.1) at all times, disregarding the velocity of the water flow.

The IM-inlet and Water streams are mixed in the Injection module mixer unit, which outlet is the Compressor inlet stream. Due to the lack of sensors between the Injection module and impeller inlet in the lab, the module is assumed to be without pressure loss or heat loss. The pressure of the Compressor inlet stream is hence equal to the IM-inlet stream. The temperature is calculated by HYSYS as an energy balance in the mixer, assuming equilibrium at the outlet.

The assumption of equilibrium at the outlet is mandatory when simulating in HYSYS as most of the units, including compressor operator, is not designed to handle non-equilibrium flow. It is outside the scope of this Master thesis to determine the accuracy of this assumption. It should be observed however that the predicted inlet temperature is dramatically changed through mixing of non-saturated air and water. This is also true for the values of relative humidity, temperatures and flow rates experienced in the lab facility. It is further assumed thermal equilibrium at compressor discharge, a statement which experience from literature suggests being incorrect (Hundseid and Bakken 2006).

	B	C	D
1			
2	total mass flow	2.441 kg/s	
3	vapor mass flow	1.938 kg/s	
4	GMF	0.7941	
5	total volume flow	1.801 m3/s	
6	vapor volume flow	1.801 m3/s	
7	GVF	0.9997	
8			

Figure 4-6 - GMF spreadsheet operator of the steady state model

The GMF spreadsheet operator (Figure 4-6) calculates the actual GMF and GVF of the compressor inlet stream. Due to evaporation of liquid water to the non-saturated ambient air in the mixer, the GMF and GVF have to be calculated based on stream properties downstream the injection module.

The GMF and GVF are explicitly included as a stream property in HYSYS under the name Phase Fraction [Mass Basis] and Phase Fraction [Act. Vol. Basis] respectively. Calculation of GMF and GVF in the spreadsheet operator is thus redundant in the steady state model. However, in the dynamic model the GMF is exported to the compressor control system as an input parameter, for which a spreadsheet operator is necessary.

The pressure and temperature of the compressor discharge stream is defined by PT-3.5 (Discharge pressure) and TT.500.20-23 (Discharge temperature). The mass flow rate and composition is equal to the compressor inlet which is defined by the injection module mixer operator.

Because pressure and temperature is specified both upstream and downstream the compressor operator, its only purpose is to calculate polytropic head and efficiency. The reader should take great care to understand that the compressor calculates polytropic head and efficiency based on surrounding stream conditions as opposed to the dynamic model where downstream properties are determined based on compressor characteristics.



	B	C	D
1			
2	Compressor speed	1.084e+004 rpm	
3	GMF	0.7941	
4	Volume flow	1.801 m3/s	
5	Polytropic head	1954 m	
6	Polytropic efficiency	60	
7			
8			

Figure 4-7 - Calculations spreadsheet operator of the steady state model

The Calculations spreadsheet operator (Figure 4-7) includes all the output parameters. The volume flow, polytropic head and polytropic efficiency are imported from the compressor unit operator. The GMF is imported from the GMF spreadsheet operator, while the compressor speed is imported directly from the input compressor spreadsheet. The calculations spreadsheet operator thus contains all the variables necessary to construct compressor characteristics in terms of compressor speed and GMF.

#### Simulation workbook

The steady state model was used to analyze data from trip scenarios performed in the test facility. In order to obtain detailed knowledge of the transient behavior of the system, it is necessary to perform polytropic calculations for thousands of time steps during the run down of the impeller. It would not be possible to manually insert the sensor readings into the input spreadsheet operator, activate the software, and export the polytropic calculations for each operational point of the transient scenario. During this work, Aspen Simulation Workbook was used to obtain an automatic analysis of test data from the lab facility.

Aspen Simulation Workbook is a tool which connects a HYSYS model to a Microsoft Excel spreadsheet. It exports values from an excel spreadsheet to stream or unit properties in the HYSYS flow sheet, runs the simulation, and exports the output variables back to the spreadsheet. Once initiated, it allows large amount of operational points to be calculated without the user interfering with the HYSYS interface at all.

In this work, the polytropic head and efficiency, volume flow and GMF was automatically calculated directly from the data files of sensor readings exported from the lab facility.

### 4.3.HYSYS Dynamics model

#### Introduction

This section describes the dynamic model developed in HYSYS Dynamics. The description loosely follows the flow sheet along the path of flow from left to right. The model is however rather complicated in terms of control, and multiple cross references are required to understand the architecture. This is especially true for mass flow calculation and orifice pressure drop.

#### Model background

In order to predict transient compressor behavior, a dynamic model was developed in HYSYS Dynamics. The model is based on the steady state model described in Section 4.2. The user interfaces of the models are similar, but it should be emphasized that the calculation procedures for which the thermal properties are determined differs significantly.

Figure 4-8 shows the layout of the dynamic model. It consists of two main parts from left to right:

- Inlet section
- Main section

#### Inlet section

The inlet section of the dynamic model is similar to the steady state model. Its purpose is to import values to define the system, and to calculate the composition of the inlet air in terms of relative humidity. It consists of three units:

- Input spreadsheet operator
- Sat air stream
- Ambient inlet air stream

The input spreadsheet operator includes all sensor readings presented in Table 3-1 in the same order as for the steady state model. This is convenient as it enables the same set of readings to be used in both models. Table 4-1 presents the application for each variable in the dynamic model. Four of the variables are not utilized. This is related to the architecture of the model which does not define stream properties beyond the boundary conditions. The pressure and flow of the internal streams are defined by unit operators in the flow sheet.

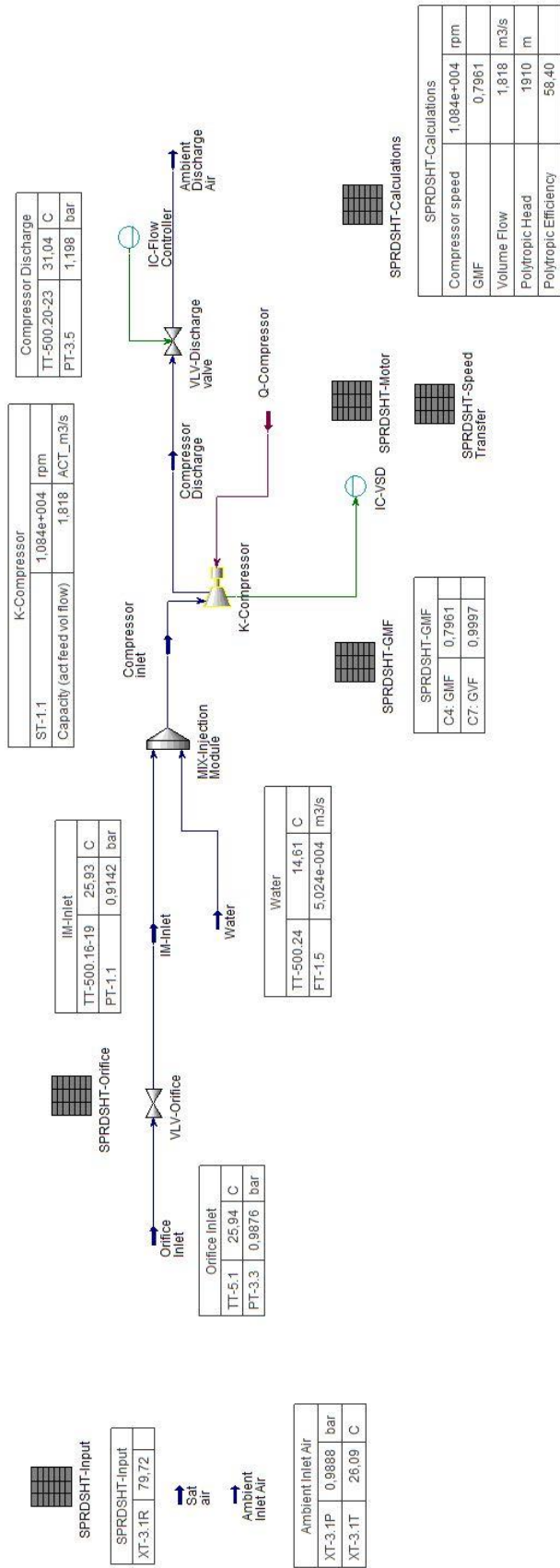


Figure 4-8 - Layout of HYSYS Dynamic model

Sensor ID	Sensor name	Used for
ST-1.1	Compressor speed	Control of IC-VSD
PT-3.1	dP Orifice	Control of IC-Flow controller
PT-1.1	IM pressure	Not used
TT-5.1	Orifice inlet temperature	<b>Boundary condition</b>
PT-3.3	Orifice inlet pressure	<b>Boundary condition</b>
PT-3.5	Discharge pressure	Not used
FT-1.5	Water flow rate	<b>Boundary condition</b>
XT-3.1P	Ambient pressure	<b>Boundary condition</b> Composition of orifice inlet stream
XT-3.1T	Ambient temperature	<b>Boundary condition</b> Composition of orifice inlet stream
XT-3.1R	Relative humidity	<b>Boundary condition</b> Composition of orifice inlet stream
TT-500.16-19	Inlet temperature	Not used
TT-500.20-23	Discharge temperature	Not used
TT-500.24	Water temperature	<b>Boundary condition</b>

Table 4-1 - Input parameters for the dynamic model

An Ambient air stream and a Sat air stream are included in order to determine the inlet air composition based on reading for relative humidity. The set-up is identical to the steady state model, and the reader is referred to Section 4.2 for further information.

#### Dynamic specifications and boundary conditions

A list of the dynamic specification and boundary conditions for the main section is given in Table 4-2. Pressure is used as the dynamic specification for the inlet and discharge air. The work done by the compressor provides the flow, which is limited by the resistance in the orifice plate and discharge valve. The water stream is specified in terms of mass flow rate in the dynamic model, defined by the sensor reading of FT-5.1 (Water flow rate). In reality the water flow rate is controlled by the water pump speed and nozzle position of the injection module in the lab.

The general strategy for the model development was to build the model as simple as possible. For this reason the system boundary of the inlet air is set to the orifice inlet. This is done to eliminate the potential source of error by modelling the initial pipe section. Experience has shown non-consistency between the ambient and orifice inlet pressure and temperature readings.

Name	Type	Dynamic specification	Other specifications	Comment
<b>Orifice inlet</b>	Stream	Pressure	Temperature Composition	-
<b>VLV-orifice</b>	Valve	Delta P	-	Pressure loss calculated in SPRDSHT-Orifice
<b>Water</b>	Stream	Mass flow	Temperature Composition	Temperature and composition specified as input parameters
<b>MIX-Injection module</b>	Mixer	Equalize pressure	-	-
<b>K-compressor</b>	Compressor	Speed	Compressor characteristics	Speed calculated in SPRDSHT-Motor
<b>VLV-Discharge valve</b>	Valve	Pressure flow relation	-	Valve opening controlled by IC-flow controller
<b>Ambient discharge air</b>	Stream	Pressure	-	The air flow downstream the discharge valve. Pressure set equal to ambient (XT.3.1P)

Table 4-2 - Boundary conditions and dynamic specifications for the dynamic model

### Orifice plate

A spreadsheet operator and a valve unit are used to predict the pressure drop over the orifice plate in the dynamic model.

The orifice inlet pressure and temperature are defined by sensor PT-3.3 (Orifice inlet pressure) and TT-5.1 (Orifice inlet temperature). The composition of the stream is set identical to the Ambient air stream similar to the steady state model. Note that the Orifice inlet stream is the system boundary of the main section.

The SPRDSHT-Orifice operator calculates the differential pressure across the orifice valve based on the mass flow according to equation (2-13). The recovery pressure drop is calculated according to (2-17) but the relation is modified to match experimental data as will be shown in Section 4.5. The pressure drop is exported to the VLV-orifice valve as a pressure drop specification. Note that the pressure and temperature of the IM-inlet stream is defined by the pressure and temperature change in the valve, not readings from sensor PT.1.1 (IM pressure) and TT-500.16-19 (Inlet temperature) as for the steady state model. Also note that the differential pressure readings across the orifice plate (PT-3.1) is not used for the orifice calculations. Unlike the steady state model, the differential pressure is calculated based on mass flow through the orifice. The differential pressure reading is however used as a set point for the flow controller as will be shown later.

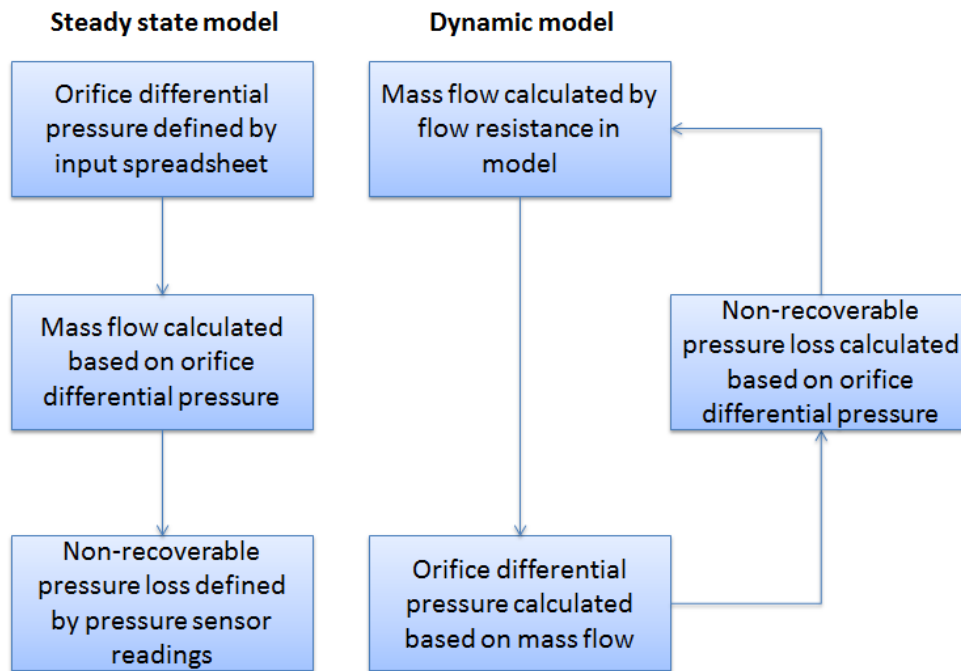


Figure 4-9 - Process flow diagram showing differences in mass flow and pressure drop calculation.

Figure 4-9 shows a simple process flow diagram which visualizes the fundamental difference of mass flow and pressure drop calculations between the steady state model and the dynamic model.

#### Injection module

The injection module is modelled with a mixer. The mixer equalizes the pressures of the inlet and outlet, and is simplified to be without pressure drop. The outlet temperature is calculated by HYSYS as an energy balance in the mixer, assuming thermal equilibrium of the Compressor inlet.

The temperature of the water stream is defined by sensor TT-500.24 (Water temperature). The flow rate of water is used as a boundary condition defined by FT-1.5 (water flow rate). The pressure is not specified in order to obtain the correct degree of freedom.

The SPRDSHT-GMF spreadsheet operator calculates the actual GMF of the compressor inlet stream. The unit is similar to the GMF spreadsheet of the steady state model. The calculated GMF value is exported as a specification to the compressor operator.

#### Compressor

The compressor is modelled with four main operators:

- K-Compressor operator
- SPRDSHT-Motor spreadsheet
- SPRDSHT-Speed Transfer spreadsheets
- IC-VSD controller

The SPRDSHT-Motor spreadsheet is shown in Figure 4-10. The spreadsheet calculates the difference between the available power and the shaft power, and determines a new compressor speed

according to (2-23) and (2-24) of Section 2.6. The new speed is temporarily stored in the SPRDSHT-Speed transfer spreadsheet before it is exported to the compressor operator in the next time step.

The SPRDSHT-Motor spreadsheet is based on an existing model of the NTNU lab facility received from co-supervisor H. Nordhus at Statoil.

The IC-VSD controller is used to adjust the available power such that the compressor speed reaches a desired set point. The current model assumes the compressor block to be adiabatic, but it is possible to insert relations for heat loss to the surroundings. A compressor trip can be activated by setting the value of cell B3 (trip) to zero. The available power will be set to zero, and the calculated compressor speed will be reduced as a function of shaft power and inertia.

	A	B	C	D
1	SYNC MOTOR			
2	On/off	1		
3	Trip	1		
4	Rated power	450.0 kW		
5	VSD Output	19.14		
6	Available power	86.14 kW		
7				
8	Shaft power	86.14 kW	<-- includes losses	78.41 kW
9	Losses	0.0000 kW	3.440 kW	7.733 kW
10	Power balance	-3.782e-004		
11				
12	Inertia	1.175		
13				
14	Gearbox ratio	1.000		w - speed
15	Motor acceleration	-2.708e-003 rpm		dw/dt = P/l/w
16	Motor speed	1.084e+004 rpm		
17	New speed	1.084e+004 rpm		wnew=wold+dw/dt*c
18				
19				
20	Timestep	1.000e-002 seconds		

Figure 4-10- Motor spreadsheet of the dynamic model

The compressor operator is specified in terms of compressor curves. Each curve is labeled with compressor speed and IGV-position. The latter is a number between 0.7 and 1.0 and represents the GMF of the compressor inlet stream. The compressor speed is imported from the SPRDSHT-Speed transfer spreadsheet and the IGV-position is imported from the SPRDSHT-GMF spreadsheet. By evaluating the current inlet and discharge pressure, the suction volumetric flow through the compressor is given by the curves. Figure 4-11 shows the rating tab of the compressor operator. The curves are sorted into curve collections for three different GMF values. Each collection contains curves for different rotational speeds. The compressor operator automatically interpolates between different speed and GMF-values.

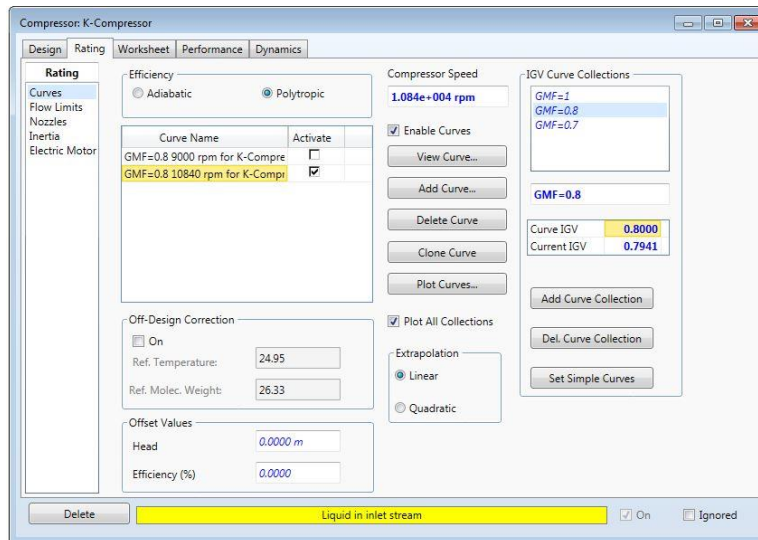


Figure 4-11 - Compressor operator rating tab of the dynamic model

### Discharge valve

The discharge valve is modelled with a valve operator and a flow controller. The flow controller represents the manual adjustment of the discharge valve position performed by the operator in the lab. When the discharge valve position is altered, the mass flow rate will be changed by the pressure-flow relations in the flow sheet. Any change in mass flow will also affect the orifice differential pressure and consequently the non-recoverable pressure loss of the orifice plate.

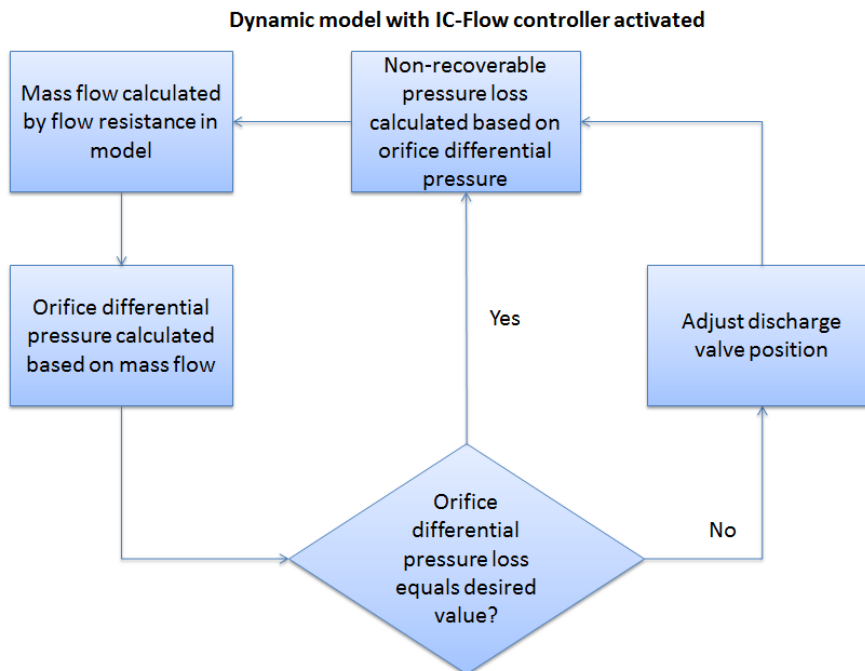


Figure 4-12 - Process flow diagram showing mass flow and pressure drop calculation of the dynamic model

The IC-flow controller is used to achieve a specific differential pressure over the orifice plate. By adjusting the pressure drop in the discharge valve, the mass flow of the dynamic model will be identical to test data. When activated, the IC-Flow controller adjusts the discharge valve position until the calculated orifice differential pressure in the SPRDST-Orifice reaches the set point defined



by the PT-3.1 (dP Orifice) in the SPRDSHT-Input. When the desired operational point is achieved, the flow controller is deactivated. Figure 4-12 indicates the principal calculation procedure of mass flow and pressure drop when the IC-Flow controller is activated.

## 4.4.Compressor characteristics

### Introduction

The dynamic model requires actual compressor characteristics to predict performance. These curves were developed based from testing in the current lab facility. The test results were evaluated with the steady state model. Complete test data is provided in Appendix B.

### Polytropic head

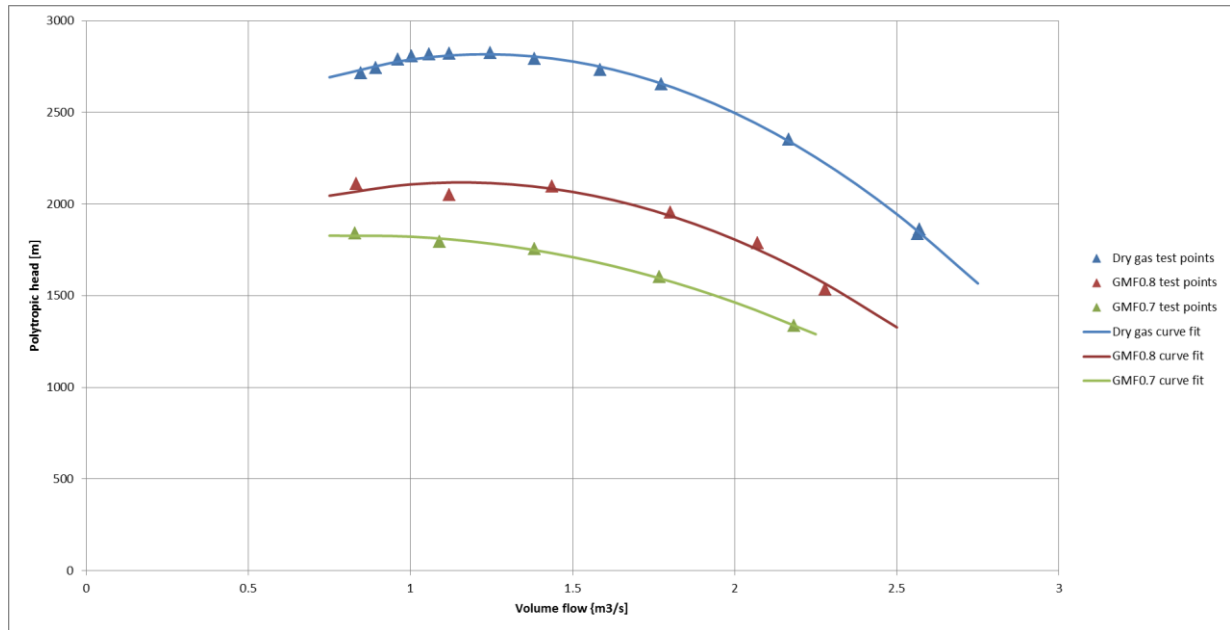


Figure 4-13 - Polytropic head of test points and fitted curve

Figure 4-13 shows the polytropic head for different volume flows and GMF at 11 000 rpm. The triangles represent test points performed in the lab. The solid lines are curve fits of the test points. Appendix B includes the curve-fit polynomials. Affinity laws are assumed to be valid also for wet gas compression, and were used to evaluate performance at other rotational speeds.

Wet gas compressor performance is severely affected by the liquid phase. Evaporative heating and cooling, heat transfer, liquid entrainment and deposition and film formation may significantly alter the compressor performance. Any change in these wet gas effect are not taken into consideration when using affinity laws to predict performance at other rotational speeds.

The accuracy of affinity laws for wet gas compression is not further investigated. Development of compressor characteristics based on lab facility testing at other rotational speeds is recommended as further work.

## Polytropic efficiency

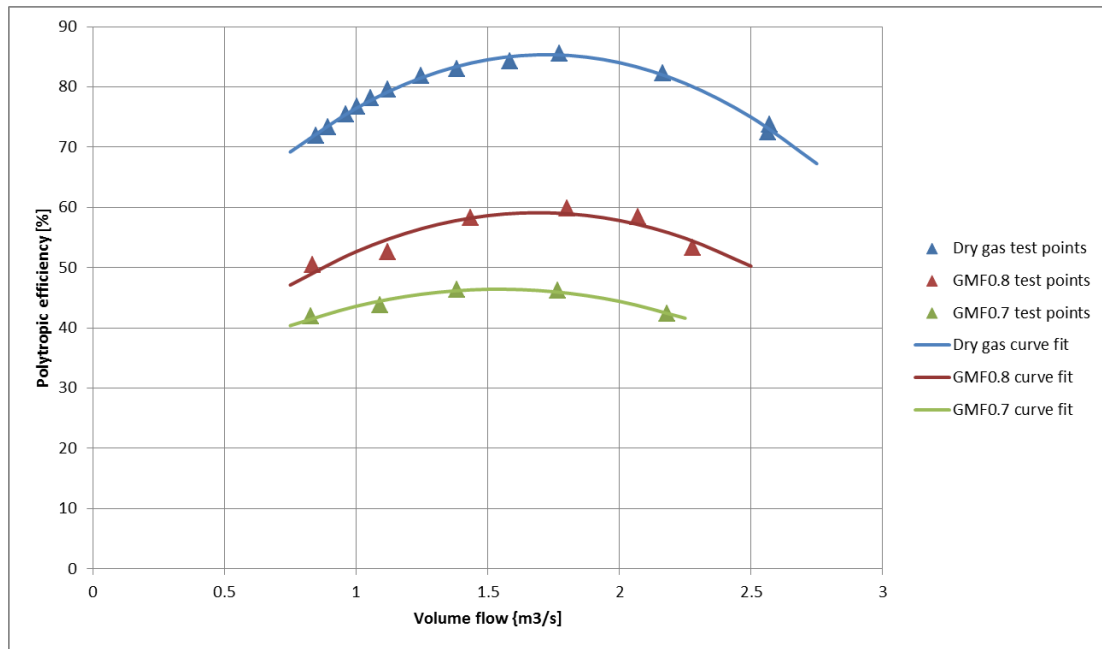


Figure 4-14 - Polytropic efficiency of test points and fitted curve

Figure 4-14 shows the polytropic efficiency for different volume flows and GMF at 11 000 rpm. Affinity laws were used to evaluate performance at other rotational speeds. The triangles represent test points performed in the lab. The solid lines are curve fits of the test points.

### Deviation between test points and fitted curve

The operational points are fitted to a polynomial of second order. The largest deviation of the fitted curves is located at  $1.12\text{m}^3/\text{s}$  and GMF 0.8. The deviation is shown in Table 4-3. The curve fitting will reduce the accuracy of the dynamic model. A deviation up to 3% for the polytropic head is very unfavorable in terms of overall accuracy.

	Test point	Curve fit	Deviation
<b>Volume flow</b>	1.12[m <sup>3</sup> /s]	1.12 [m <sup>3</sup> /s]	-
<b>GMF</b>	0.8 [-]	0.8 [-]	-
<b>Polytropic head</b>	2049.28 [m]	2110.78 [m]	3.0%
<b>Polytropic efficiency</b>	52.57%	54.50%	3.7%

Table 4-3 - Deviation of curve fit at  $1.12\text{m}^3/\text{s}$  and GMF0.8

Still it is preferable to convert the test point to a polynomial of second degree, as experience has shown instability challenges in HYSYS Dynamics when non-smooth curves are introduced into the compressor operator. The curve fitted polynomials are included in Appendix B.

## 4.5. Tuning of orifice non-recoverable pressure loss

### Introduction

The non-recoverable pressure loss over the orifice plate needs to be predicted in order to model the compressor lab in HYSYS Dynamics. A relation was given in Equation (2-17). Early experience revealed this relation to be highly inaccurate for the current lab facility. Further investigation suggested the non-recoverable pressure loss and the differential pressure of the orifice plate to be proportional, as indicated by (2-17). The constant of proportionality could however not be determined from the equation.

An experimental investigation was initiated to determine an appropriate relation non-recoverable pressure loss.

### Experimental data

Six points of operation was investigated, shown in Table 4-4. The orifice differential pressure is the average sensor readings of PT-3.1 (dP Orifice) during steady state compressor operation. The non-recoverable pressure loss is the average difference of sensor PT-3.3 (Orifice inlet pressure) and PT-1.1 (IM-Pressure).

	dp orifice [mbar]	GMF [-]	Non-recoverable pressure loss [mbar]
<b>Dry gas surge</b>	32.2	1.00	27.0
<b>Dry gas BEP</b>	95.2	1.00	69.3
<b>Dry gas open valve</b>	184.1	1.00	130.8
<b>Wet gas surge</b>	40.7	0.7990	30.5
<b>Wet gas BEP</b>	100.2	0.7941	70.9
<b>Wet gas open valve</b>	153.6	0.7958	107.1

Table 4-4 - Test points for development of non-recoverable pressure loss in orifice plate

The differential pressure of the orifice plate and the non-recoverable pressure loss is plotted in Figure 4-15. A curve fit through the test points was performed in Excel. The linear function is defined

$$y = 0.7104x \quad (4-1)$$

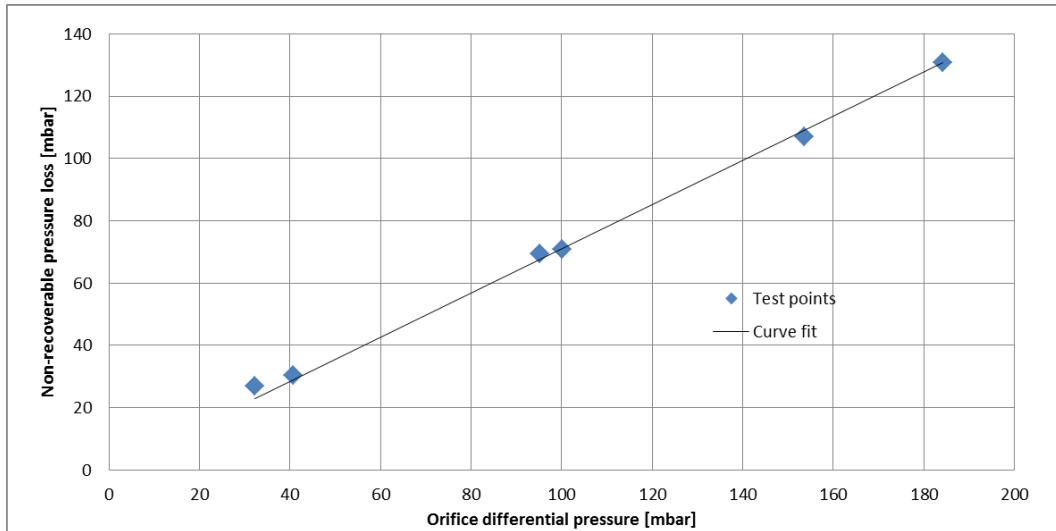


Figure 4-15 - Non-recoverable pressure drop versus orifice differential pressure for a selection of test points

### Conclusion

By using the experimental data, a new pressure loss relation for the orifice plate was determined. The new relation will be used in the orifice spreadsheet operator of the dynamic model to predict the non-recoverable pressure loss in the orifice valve. The relation is given as:

$$\Delta p_{experimental} = 0.7104 \Delta p_{orifice} \quad (4-2)$$

Equation (4-2) replaces Equation (2-17) from Section 2.5.

## 4.6. Instability challenges in HYSYS Dynamics

### Introduction

During development of the dynamic model, severe challenges related to simulation stability in HYSYS Dynamics occurred. It has not succeeded to determine the exact cause and effect of the problems. The experienced instability is however limited to wet gas compression applications.

This section will briefly present two representative scenarios where the system functionality of HYSYS Dynamics was severely challenged by unstable and random behavior.

Great efforts have been made to identify and solve the functionality defects. HYSYS Dynamics is based on an intuitive and graphical interface. The software is easy to use, but user access to calculation procedures is limited. No similar challenges have been found in literature.

### Instable behavior during trip

The main source of instability has proven to be the inclusion of volumes between the compressor unit and discharge valve. The actual compressor lab is equipped with 2420 mm piping of inner diameter 200 mm between the compressor block and the discharge valve. Attempts to include a representative volume into the model failed. All efforts to model piping geometry resulted in similar unstable behavior as indicated in Figure 4-16. Volumes have been tried represented both by pipe segments, gas pipe segments, tank operators and separator operators.

The presence of sufficient small volumes does not seem to affect the calculation stability. As the volume is gradually increased it suddenly reaches a critical size and the simulation starts predicting very large fluctuations in pressure and volume flow. Figure 4-16 shows an example of the operational point oscillating beyond physical behavior during a trip test in the early stage development of the dynamic model. In this example a representative discharge volume is modelled. The red point shows the operating point. Its current location appears to be random, without any link to the previous time step at the bottom of the fluctuating run down characteristic.

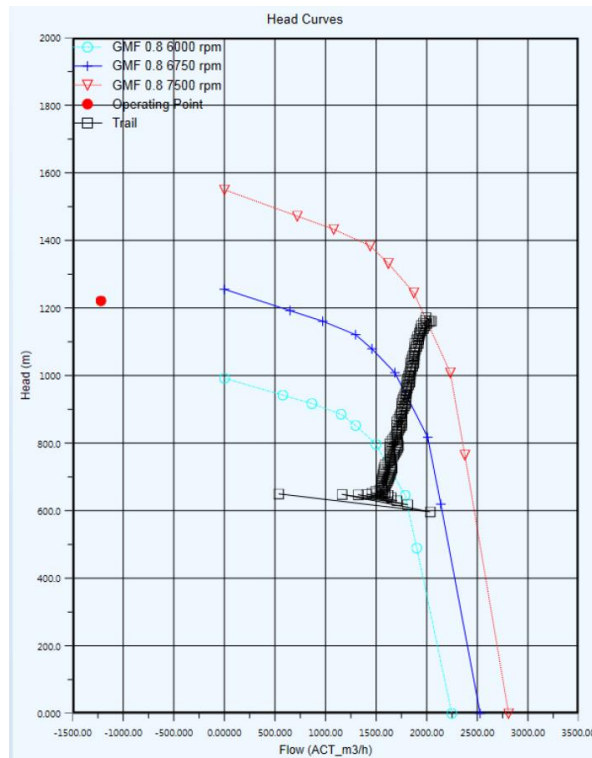


Figure 4-16 - Instable behavior of HYSYS Dynamics during early stage model development

It has failed to identify the cause of the instability. Experience suggests the challenges to increase as the downstream volume is increased and the compressor pressure ratio is reduced. Wet gas compression has proven more problematic compared to dry gas simulation.

Similar unstable behavior has even occurred without any volume included in the model. This will be shown in the open valve wet gas trip simulations in Section 5.4. Regardless of great efforts, the simulation scenario has not been completed as seen in Figure 5-24.

#### Mixing of non-saturated air and water

Air with relative humidity less than 100% are mixed with water in the mixer-unit. Under certain circumstances the mixing led to severe instability in the compressor operator. Despite great effort is has not succeeded to identify the mechanisms which trigger the instability. Figure 4-17 shows such instable operation in a head-volume flow diagram. Note that both the head and volume flow alternates severely for each time step.

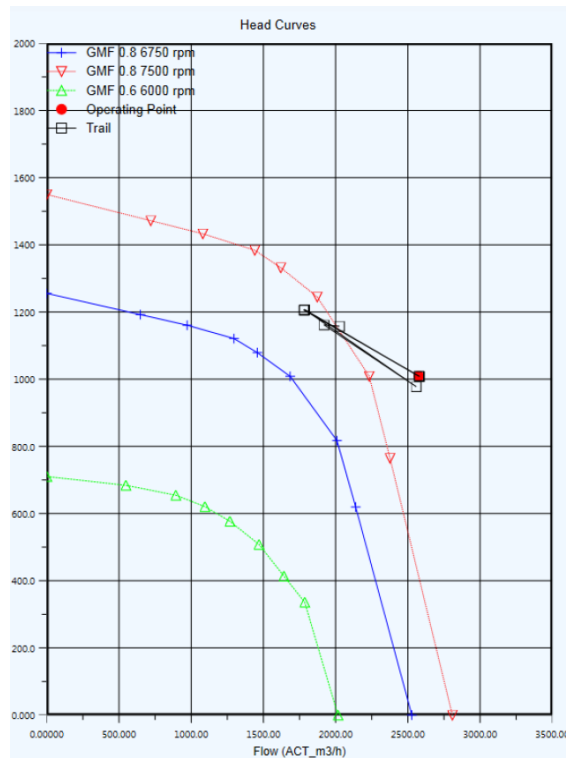


Figure 4-17 - Instability in HYSYS Dynamic during mixing of non-saturated air and water

The dynamic model was not able to validate the wet gas performance at low volume flow. This was due to instabilities related to mixing of non-saturated air and water. As a consequence the current scenario had to be simulated with relative humidity of 100%, shown in Section 5.2. Note that the wet gas trip close to surge was successfully performed. The wet gas low volume flow validation was the only activity related to humidity-related instabilities presented in this work.

### Conclusion

It has been shown that HYSYS Dynamics under certain circumstances predicts very unstable operation. The triggering mechanisms have not been identified. The unstable behavior is considered random and not related to actual behavior of the compression system. The most evident common factor of unstable prediction is associated with wet gas and low pressure ratio compression scenarios.

Dry gas simulation scenarios are not subject for instabilities as described above. All instabilities are eliminated in simulation cases which do not include compressor units.



## 4.7. Shortcomings of HYSYS Dynamics model

### Introduction

A number of simplifications are performed in order to obtain a simple and reliable dynamic model. The general strategy for the model development was to avoid complex modelling of phenomena that cannot be validated against test results for the current lab facility. The shortcomings considered to be most severe are presented in the text below. Model functionality is also addressed in Chapter 5 during discussion of test results.

This following text does only consider the main shortcomings of the current dynamic model. For further reference to the general system functionality of HYSYS dynamic, consult (Owren 2013).

### Piping

The dynamic model does not include any pipe segments or other units which contain physical volume. This is chosen partly due to the instability challenges discussed in Section 4.6, but also to avoid complex system behavior which cannot be investigated with the current lab facility.

Separator or tank unit operators can be used to simulate volumes in the simulation flow sheet. This is advantageous as it allows the effect of compressed gas to be modelled, but eliminates the need to perform complex and time consuming pipe-flow calculations. Experience revealed that these units also induced instable behavior of the system, and were hence omitted too.

The lack of piping or similar equipment implies that some phenomena present in the actual lab facility will not be subject to evaluation in the dynamic model:

### **Pressure loss**

The only units restricting flow in the dynamic model is the orifice plate and the discharge valve. Steady state pressure loss upstream the orifice plate is taken into account as the system boundary is specified in terms of orifice inlet pressure and temperature. Pressure loss in other piping and injection module is however omitted.

For the current lab facility the pressure loss over the injection module is not known due to lack of pressure sensors. The same applies for the piping between the compressor outlet and discharge valve. Any known pressure drop relation could easily be modelled with a valve operator.

### **Heat loss**

The dynamic model is entirely adiabatic. The real heat loss is considered insignificant due to the small temperature differences involved in the low pressure rate compression.

### **Compressor surge**

Section 2.4 documents compressor trip behavior from literature. As seen in Figure 2-11 the compressor response of trip close to surge can strongly be influenced by the upstream and downstream volumes. These effects will unfortunately not be included in the dynamic model, even though they are expected to influence the transient response of the current compressor rig.

### Boundary conditions

The air intake side of the system is specified in terms of orifice inlet pressure and temperature. The composition is set on the basis of the ambient pressure, temperature and relative humidity. All these values are considered constant for each test scenario. Any actual change in inlet conditions during a trip test will not be evaluated in the dynamic model calculations.

Experience from the lab reveals minor change in orifice inlet pressure and temperature during trip. The relative humidity has a tendency to vary quite a bit, especially during dry gas testing. For dry gas BEP trip the highest measured relative humidity was 46.0% while the lowest was 42.1% giving a variation of approximately 9%. These values were measured over a period of less than 18 seconds.

### Expansion factor of orifice calculations

The dynamic model calculates the differential pressure of the orifice plate based on mass flow and the expansion factor  $Y$  as of (2-13) and (2-15). As the expansion factor is a function of the differential pressure, an iteration process is required to accurately determine the expansion factor with every change in differential pressure. This is however not feasible for a dynamic model where an iteration would create an artificial system response. For this reason the expansion factor is fixed to the initial steady state value prior to the trip. As the volume flow is reduced during trip, the actual increased value of the expansion factor is not taken into account in the dynamic model.

### Phase and thermal non-equilibrium

The model uses the single fluid model for calculations. Phase and thermal equilibrium is assumed at all times in the flow sheet. Mixing of non-saturated air and water along with wet gas compression may be considered two area of application where assumption of thermal equilibrium is especially unfortunate. The compressor inlet temperature is strongly affected by the water evaporation rate in the mixer unit. The high heat capacity of the liquid water may create non-thermal equilibrium at the compressor discharge.

The actual sensor configuration of the compressor lab is however not capable of measuring non-equilibrium temperatures. If the model were able to include non-equilibrium in its calculation, the results could still not be validated by the current lab facility.

### Conclusion

The main shortcoming of the dynamic model is the lack of piping representation. Compared to the total system accuracy, the current shortcomings of the dynamic model are expected to be within acceptable limits. Deviation due to lack of model functionality will be addressed at appropriate sections during discussion of test results.





## 5. Results and discussion

### 5.1. Introduction

This chapter will present and discuss the results related to three different testing activities:

- Validation of steady state performance of dynamic model
- Dry and wet gas trip scenarios
- Speed ramp-up tests

The first activity is related to the establishment of a dynamic simulation model as of subtask one in the assignment text.

The second activity validates dry and wet compressor behavior addressing the second subtask of the assignment text. Main challenges related to accurate transient measurements during trip testing are documented in Section 5.5.

The last activity is a representative transient operating scenario related to subtask three of the assignment text.

All testing presented in this chapter are both simulated in the dynamic model and performed in the compressor test facility.

## 5.2.Validation of steady state performance of dynamic model

### Introduction

The dynamic model is designed to predict transient compressor behavior. The model should however calculate similar results as the steady state model during non-transient operation scenarios. A selection of six points from steady state operation in the wet gas test facility was evaluated with both models. The test points are presented in Table 5-1. All points are at 11 000 rpm. Complete results from the testing are provided in Appendix C.

Test point name	dP orifice [mbar]	Water flow rate [l/s]
Dry gas low volume flow	32.16	0.00
Dry gas BEP	95.23	0.00
Dry gas high volume flow	184.11	0.00
Wet gas low volume flow	40.67	0.3185
Wet gas BEP	100.17	0.5024
Wet gas high volume flow	153.64	0.6037

Table 5-1 - List of test points for steady state validation of dynamic model

### Testing procedure

The test points are a selection of the operational points used for compressor curves development in Section 4.4. The wet gas test data consist of steady state sampling at two Hz for five minutes or more. The dry gas test data consist of approximately two minutes of steady state testing sampled at 20 000 Hz. All sensor readings are averaged for each operational point and inserted into the dynamic model. The flow controller is used to adjust the discharge valve such that the calculated orifice differential pressure becomes identical to the measured value in the lab. After steady state occurs, the results are extracted from the calculations spreadsheet.

When analyzing the complete results in Appendix C please refer to Table 4-1. The sensors market «boundary conditions» contain identical values for the steady state and dynamic model. The «not used» values are calculated by HYSYS Dynamics and are subject to comparison between the steady state and dynamic model.

### Dry gas performance

The dry gas steady state performance of the dynamic model is presented in Table 5-2, Table 5-3 and Table 5-4. The boundary conditions of the dynamic model are defined identical to the steady state model implying no deviation in inlet conditions or compressor speed.

	Steady state model	Dynamic model	Deviation [%]
GMF [-]	1.000	1.000	0.00%
Volume flow [m <sup>3</sup> /s]	1.003	1.000	-0.32%
Polytropic head [m]	2807	2788	-0.68%
Polytropic efficiency [%]	76.77	76.47	-0.39%

Table 5-2 - Steady state validation of dry gas low volume flow

	Steady state model	Dynamic model	Deviation [%]
GMF [-]	1.000	1.000	0.00%
Volume flow [m <sup>3</sup> /s]	1.773	1.777	0.19%
Polytropic head [m]	2653	2654	0.03%
Polytropic efficiency [%]	85.59	85.32	-0.31%

Table 5-3 - Steady state validation of dry gas BEP

	Steady state model	Dynamic model	Deviation [%]
GMF [-]	1.000	1.000	0.00%
Volume flow [m <sup>3</sup> /s]	2.565	2.577	0.49%
Polytropic head [m]	1837	1833	-0.19%
Polytropic efficiency [%]	72.48	72.83	0.48%

Table 5-4 - Steady state validation of dry gas high volume flow

### Orifice differential pressure

The dynamic model is able to adjust the discharge valve such that the orifice differential pressure in the dynamic model is equal to the corresponding sensor reading in lab. An equal orifice differential pressure entails identical mass flow given similar inlet conditions, given by (2-13).

### Orifice pressure drop

The dynamic model predicts a slightly lower non-recoverable pressure loss in the orifice plate for the low volume flow. For the BEP the pressure drop is close to identical, while the dynamic model predicts a slightly higher pressure drop for high volume flow. The deviation is due to inaccuracy in the experimentally determined pressure drop relation of Section 4.5.

### Orifice temperature drop

The dynamic model predicts almost no change in temperature over the orifice plate. Lab results suggest the temperature to drop 0.17 to 0.68 degrees over the orifice plate. This may be related to sensor accuracy and calibration.

### Volume flow

The deviation in pressure and temperature change over the orifice plate causes a different gas density at the compressor inlet. The resulting deviation in suction volume flow varies from 0.19% to 0.49%, which can be considered minor.

### Polytropic head and efficiency

The predicted polytropic head depends on current suction volume flow and the shape of the compressor curve. Any deviation in suction volume flow will move the operational point along the compressor curve, affecting the delivered head. The shape of the compressor curve is based on a curve fit from experimental data. Any deviation between the actual head and the fitted curve will cause a deviation between the dynamic and steady state model. The dry gas polytropic head still deviates with 0.68% or less for the dynamic model, which is considered minor.

The polytropic efficiency will be affected similar to the polytropic head. The deviation is less than 0.5 percent.

## Wet gas performance

The wet gas steady state performance of the dynamic model is presented in Table 5-5, Table 5-6 and Table 5-7. The boundary conditions of the dynamic model are defined identical to the steady state model implying no deviation in inlet conditions of compressor speed. The low volume flow test point is simulated with a relative humidity of 100% due to instability challenges described in Section 4.6.

	Steady state model	Dynamic model	Deviation [%]
<b>GMF [-]</b>	0.7990	0.7967	-0.28%
<b>Volume flow [m<sup>3</sup>/s]</b>	1.120	1.128	0.71%
<b>Polytropic head [m]</b>	2049	2034	-0.74%
<b>Polytropic efficiency [%]</b>	52.57	54.50	3.67%

Table 5-5 - Steady state validation of wet gas low volume flow

	Steady state model	Dynamic model	Deviation [%]
<b>GMF [-]</b>	0.7941	0.7941	0.00%
<b>Volume flow [m<sup>3</sup>/s]</b>	1.801	1.805	0.22%
<b>Polytropic head [m]</b>	1954	1906	-2.45%
<b>Polytropic efficiency [%]</b>	59.78	58.18	-2.68%

Table 5-6 - Steady state validation of wet gas BEP

	Steady state model	Dynamic model	Deviation [%]
<b>GMF [-]</b>	0.7958	0.7959	0.01%
<b>Volume flow [m<sup>3</sup>/s]</b>	2.278	2.290	0.52%
<b>Polytropic head [m]</b>	1535	1540	0.37%
<b>Polytropic efficiency [%]</b>	53.30	53.73	0.81%

Table 5-7 - Steady state validation of wet gas high volume flow

### **Orifice differential pressure**

The dynamic model is able to tune the discharge valve such that the orifice differential pressure is close to equal in the two models. Consequently the mass flow of the two models will be equal according to (2-18). This is not the case for the low volume flow test where the composition of the dynamic model deviates due to the saturated intake air.

### **Orifice pressure drop**

The dynamic model predicts a slightly lower non-recoverable pressure loss in the orifice plate for the low volume flow case. The pressure drop is slightly higher for the BEP and high volume flow case. The deviation is due to deviation between the fitted curve and real test data described in Section 4.4.

### **Orifice temperature drop**

The dynamic model predicts almost no change in temperature over the orifice plate. Lab results suggest a temperature drop of 0.20 to 0.47 degrees over the orifice plate. This may be related to sensor accuracy and calibration.

### **Volume flow**

The deviation in pressure and temperature change over the orifice plate causes a different gas



density at the compressor inlet. The resulting deviation in suction volume flow varies from 0.22% to 0.71% which is considered minor.

**GMF**

The dynamic model is not able to predict correct GMF values for the wet gas low volume flow case. This is due to the relative humidity of the inlet air, which is set to 100% for the dynamic model. The actual value was 73.58%. Thus none of the water flow of the dynamic model will evaporate into the air, resulting creating a lower GMF value. The GMF prediction is accurate for the BEP and high volume flow test point.

**Polytropic head and efficiency**

A large deviation of 2.45% is found for the polytropic head at the BEP test point. The deviation is 0.74 or less for the high and low volume flow. The deviation is due to three main reasons:

- Curve fitting
- Linear interpolation
- GMF offset

The compressor curves are developed based on a second degree polynomial curve fit of the test points as described in Section 4.4. This is done to ensure smooth curves in the HYSYS Dynamics compressor operator. Experience reveals the compressor operation may become unstable if the test points are directly imported to the operator. The polynomial is used to calculate compressor curve points which is exported to the compressor unit in the flow sheet. Figure 5-1 shows the test data points in red, the fitted curve in black and the compressor curve points in blue.

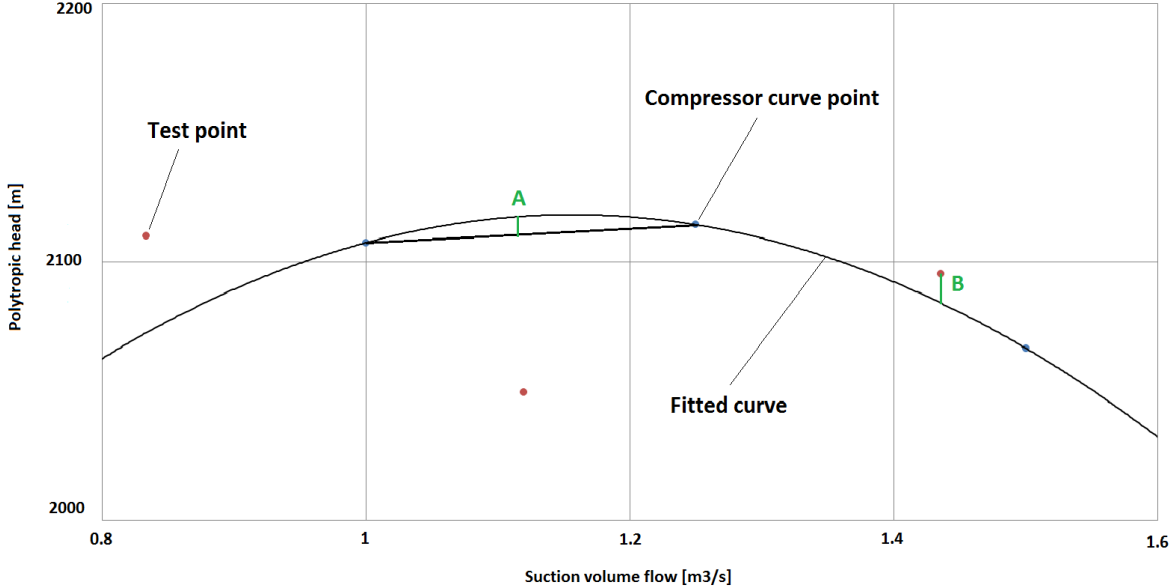


Figure 5-1 - Deviation in polytropic head due to curve fit and linear interpolation

The fitted curve may deviate from the actual test point. An example is indicated with the letter «B» in Figure 5-1. This deviation is addressed in Section 4.4.

The dynamic model performs a linear interpolation between the operational points of the speed curves. It would have been more accurate if the compressor unit used a polynomial to determine the

polytropic properties. This could be approached by specifying the compressor curves with a large number of compressor curve points. The linear interpolation may give small offsets, marked with the letter «A» in Figure 5-1.

During development of wet gas speed curves, each test point was labeled to a GMF value of exactly 0.80 or 0.70. The actual GMF value of the test points typically deviates slightly from the labeled value. As an example the wet gas BEP test point had an actual GMF value of 0.7931. When the same test point is evaluated with the dynamic model, the compressor operator will interpolate the polytropic head from the GMF0.8 and GMF0.7 curves because 0.7931 is in between. This creates a small offset as the real head value is the exact same as the initial test point.

An unfavorable combination of these three effects causes the polytropic head to deviate severely for the BEP test point.

The polytropic efficiency will be affected similar to the polytropic head. A large deviation is observed for the BEP due to challenges as for the polytropic head. The efficiency also deviates for the low volume flow test point, but in this scenario the polytropic head prediction is quite good. An inspection of the compressor curves shows the deviation is most likely addressed to the curve fit, as the experimental data and fitted curve deviates quite heavily for the efficiency curves of GMF 0.8.

For the wet gas low volume flow case the steady state model predicts a compressor inlet temperature of 22.3 degrees. The corresponding relative humidity is 73.58%. The dynamic model calculated the performance with 100% relative humidity of the intake air due to instability challenges. The corresponding compressor inlet temperature is 23.35 degrees. The temperature is higher because no liquid evaporates into the gas.

For compressor performance analysis this error would strongly affect the polytropic performance. If the relative humidity is set to 100% in the steady state model, the polytropic efficiency increases to 74.4%. Because the steady state model calculates the efficiency based on the measured temperature difference over the compressor, any change in inlet temperature will cause great impact of the polytropic efficiency. The dynamic model is however not specified in terms of discharge temperature. Any increase in inlet temperature will be represented by an increased discharge temperature and hence not change the efficiency in the same manner as for the steady state model.

#### Suggestions for model improvement

The accuracy is expected to increase with the number of experimental test point used to specify the compressor characteristics. As a result, the curve fit offset could be eliminated.

Some of the imprecision is due to the orifice valve and orifice spreadsheet in the dynamic model. The prediction of pressure and temperature change over the orifice valve is not without deviation. The orifice relations of Section 4.5 may be individually tuned to each specific test case to obtain a higher accuracy. Heat loss relations or a cooler could be implemented to take into account the temperature drop through the orifice.

## Conclusion

Based on steady state testing of the dynamic model, some numbers regarding accuracy of prediction is given in Table 5-8. The table presents the maximum deviation for the tested cases. Larger deviations may occur at other operational points. For dry gas the dynamic model is able to predict compressor performance quite accurate. For wet gas a deviation of at least 2.45% may be present even before transient calculations are introduced.

	<b>Dry gas</b>	<b>Wet gas</b>
<b>Volume flow [m<sup>3</sup>/s]</b>	0.49%	0.71%
<b>Polytropic head [m]</b>	0.68%	2.45%
<b>Polytropic efficiency [-]</b>	0.48%	3.67%

Table 5-8 - Maximum deviation of dynamic model

### 5.3. Trip test scenarios

#### Introduction

Task two of the assignment text is to validate the dynamic simulation model against dry and wet trip scenarios. Three dry gas and three wet gas trip tests have been performed in the lab. The same scenarios were later simulated in the dynamic model based on actual operating conditions.

This chapter presents and discusses the results from dynamic trip simulations and trip testing in lab. The main objective is to analyze the performance of the dynamic model related to real compressor behavior. Attention will be given to the dynamic models ability to handle wet gas compared to dry gas. The general performance deviation of dry and wet gas compression is not investigated in this section.

#### Testing procedure

Table 5-9 presents the six operational points from where trips were performed. The desired test points were obtained in the lab by adjusting the water pump speed and manually adjusting the discharge valve. The logging system was activated when stable operation was reached, logging all sensor readings at a frequency of 1000 Hz. A trip signal was sent to the compressor control system after one minute of stable operation. The controlled ramp down function of the driver system was deactivated, and the compressor spun freely from 11 000 rpm to 100 rpm where the test was stopped.

Name	dP Orifice [mbar]	Water flow rate [l/s]	Suction volume flow [m <sup>3</sup> /s]	GMF [-]
<b>Dry gas open valve</b>	181.46	[-]	2.522	1
<b>Dry gas BEP</b>	96.65	[-]	1.777	1
<b>Dry gas surge</b>	32.32	[-]	1.005	1
<b>GMF0.8 open valve</b>	158.10	0.637	2.266	0.7930
<b>GMF0.8 BEP</b>	90.00	0.478	1.660	0.7952
<b>GMF0.8 surge</b>	31.97	0.282	0.9669	0.7992

Table 5-9 - Test points for trip scenarios

The gathered data was analyzed with the steady state model using HYSYS Active workbook. In order to save calculation time, the polytropic analysis was performed every 10<sup>th</sup> time step (0.01 seconds interval). As seen in Section 2.4, challenges related to driver trips are expected to appear within the first few seconds. The test data was analyzed from five seconds prior the trip until the compressor reached 7000 rpm. Total length of analyzed data was less than 20 seconds for each case.

The six trip tests were simulated in the dynamic model. The sensor readings from the last five seconds prior to the trip were averaged and exported to the input spreadsheet of the dynamic model. Five seconds of steady state operation was simulated before a compressor trip was activated. The simulation was stopped when the compressor reached 7000 rpm.

## 5.4. Trip test results

### Introduction

This section presents the results from the trip tests and trip simulations for the six scenarios. Each trip is illustrated with four charts:

- Compressor speed versus time
- Polytropic head versus time
- Suction volume flow versus time
- Polytropic head versus suction volume flow

The maximum deviation of the trip test and dynamic simulation is given for compressor speed, polytropic head and suction volume flow. The stated deviation is a maximum average value over five subsequent time steps in order to reduce the effect of fluctuations in the test results.

The results are presented in the following order:

1. Dry gas BEP
2. Wet gas BEP
3. Dry gas surge
4. Wet gas surge
5. Dry gas open valve
6. Wet gas open valve

Wet gas trip tests and dry gas simulations are presented in red color.

Dry gas trip tests and wet gas simulations are presented in blue color.

The results are discussed in Section 5.5.

### Dry gas trip test BEP

Results from dry gas trip test at BEP along with predicted performance of the dynamic model are provided below.

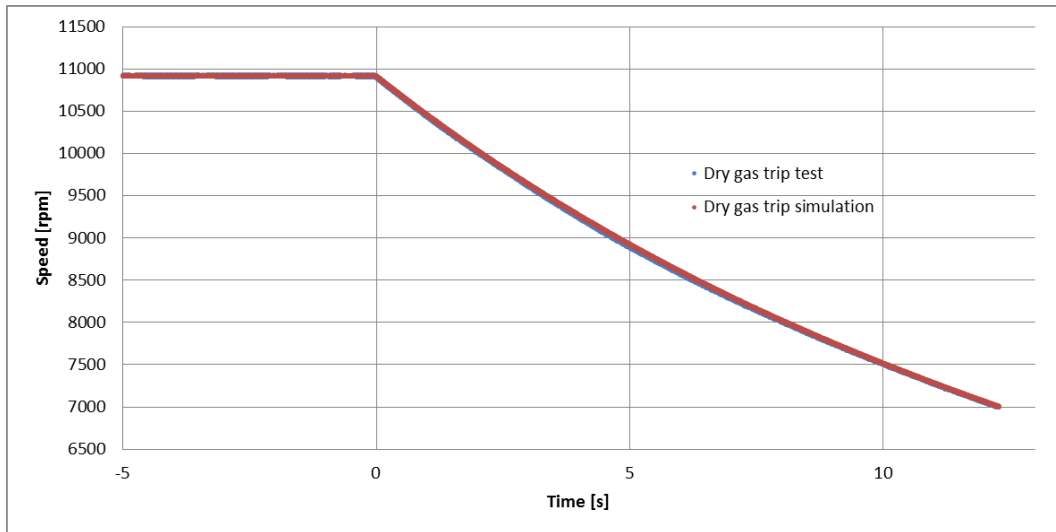


Figure 5-2 - Compressor speed versus time for dry gas BEP trip

Figure 5-2 shows the compressor speed reduction. The speed reaches 7 000 rpm 12.24 seconds after the trip signal. The maximum deviation is 0.41% after approximately five seconds.

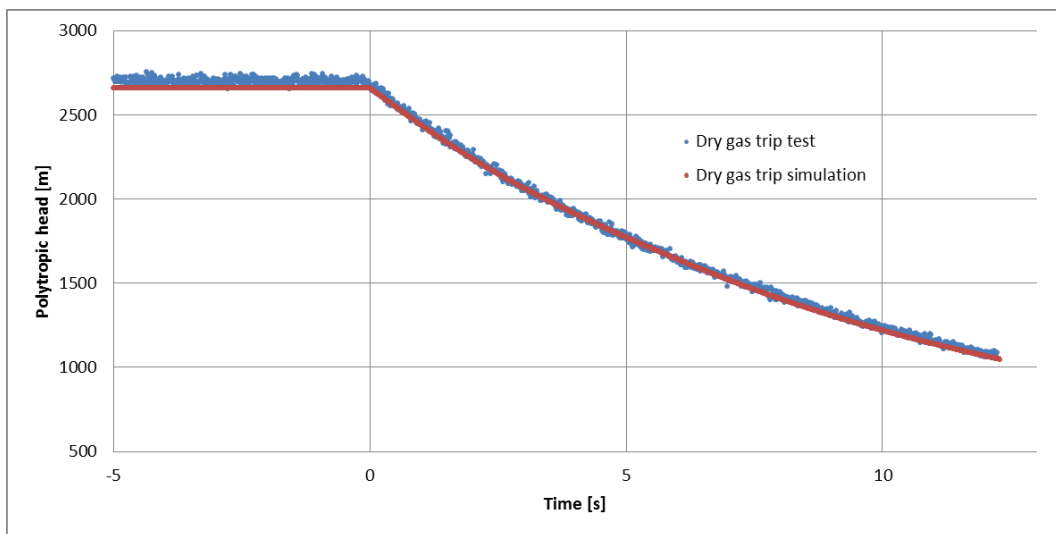


Figure 5-3 - Polytropic head versus time for dry gas BEP trip

Figure 5-3 shows the polytropic head during trip. The maximum deviation is 2.49% both prior to the trip and towards the end.

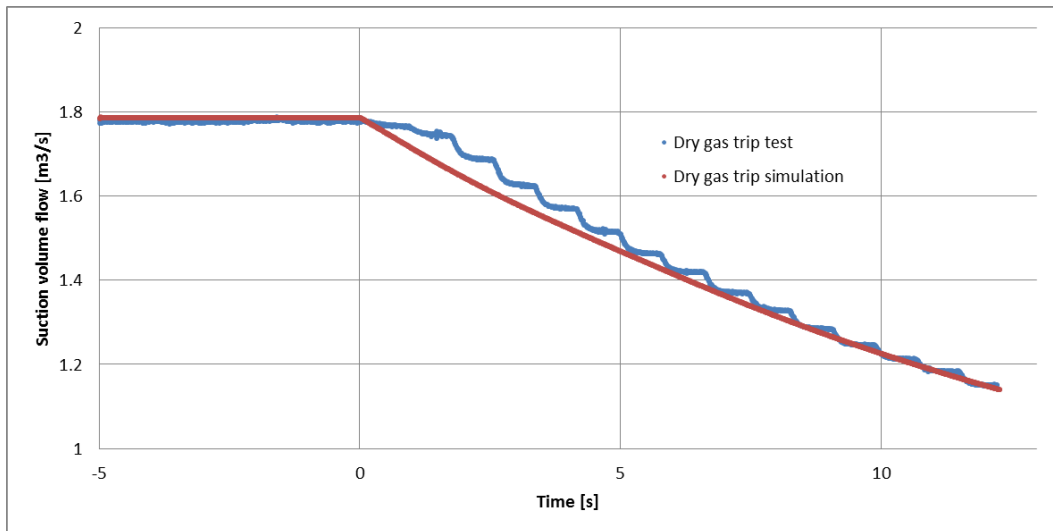


Figure 5-4 - Suction volume flow versus time for dry gas BEP trip

Figure 5-4 shows the compressor suction volume flow. The dynamic model deviates 4.70% the first five second after the trip. After 10 seconds the test data and dynamic model curves coincide.

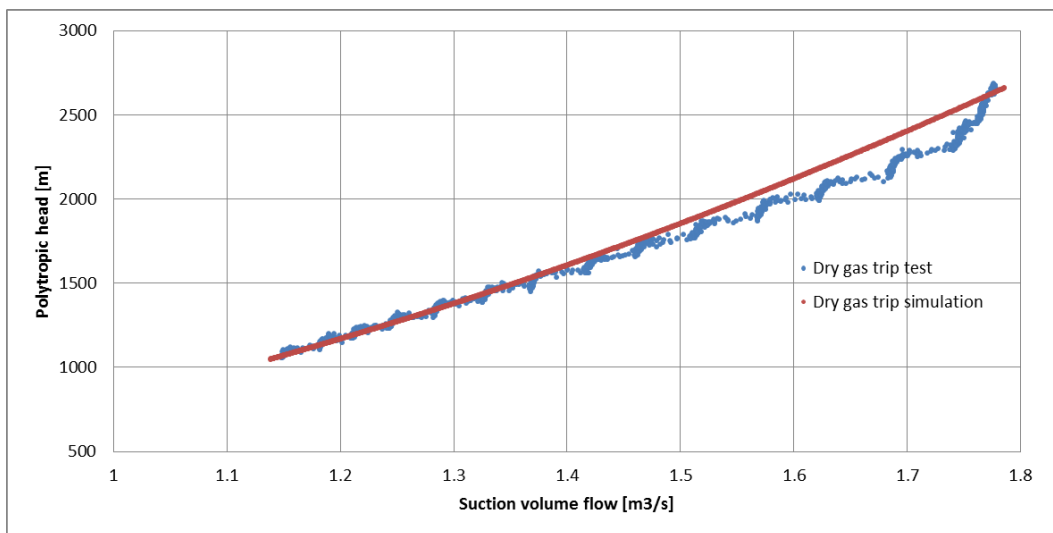


Figure 5-5 - Polytropic head versus suction volume flow for dry gas BEP trip

Figure 5-5 shows the run down characteristics of the system in a polytropic head and volume flow diagram. The initial deviation is due to the inaccurately predicted volume flow during the first seconds of the trip. The curves coincide towards lower volume flow.

### Wet gas trip test BEP

Results from wet gas trip test at BEP along with predicted transient performance of the dynamic model are provided below.

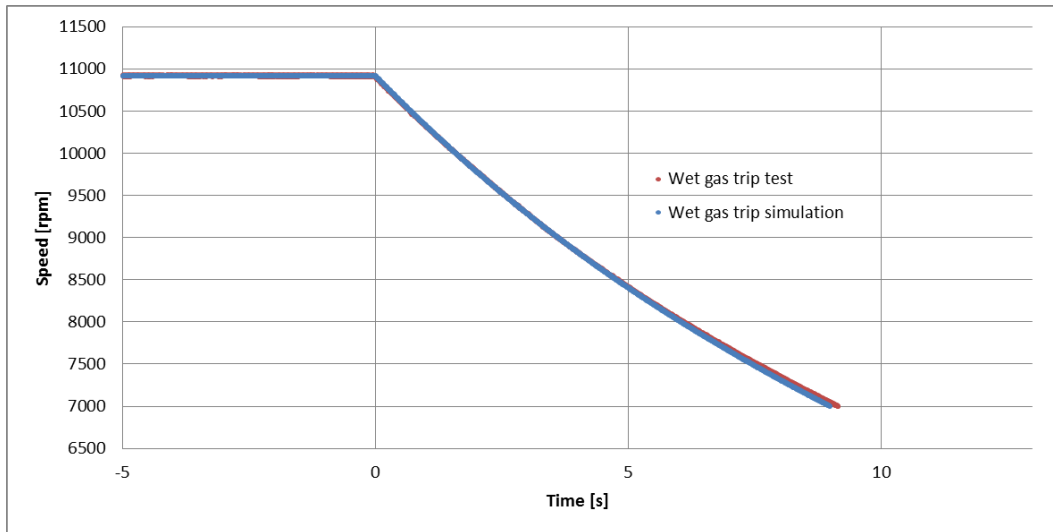


Figure 5-6 - Compressor speed versus time for wet gas BEP trip

Figure 5-6 shows the compressor speed reduction. It takes 9.16 seconds for the compressor to reach 7 000 rpm. The deviation of the dynamic model grows larger with time to a maximum value of 0.70% at 7 000 rpm.

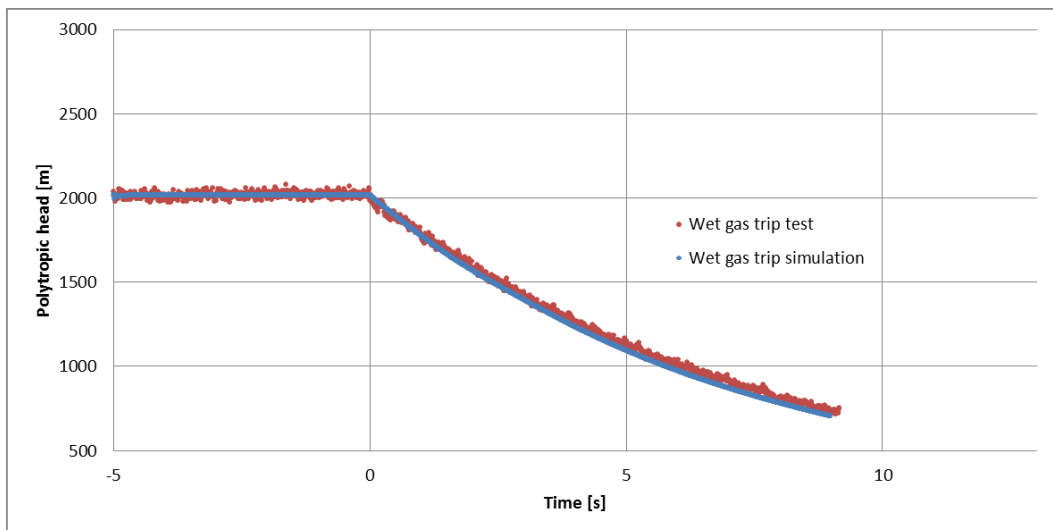


Figure 5-7 - Polytopic head versus time for wet gas BEP trip

Figure 5-7 shows the polytopic head during trip. The deviation grows in time similar to the rotational speed to a maximum deviation of 7.21% approximately 8 seconds after the trip signal.



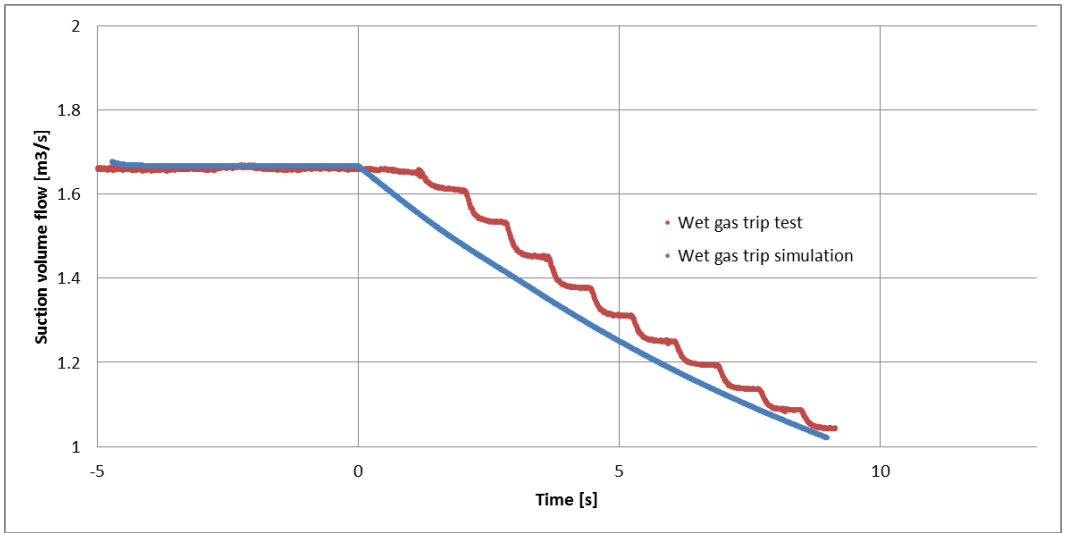


Figure 5-8 - Suction volume flow versus time for wet gas BEP trip

Figure 5-8 shows the compressor suction volume flow during wet gas trip from BEP. The dynamic model deviates up to 8.17% the first five second after the trip. The deviation in volume flow decreases with time, but does not quickly converge to the experimental values as quick as the dry gas scenario.

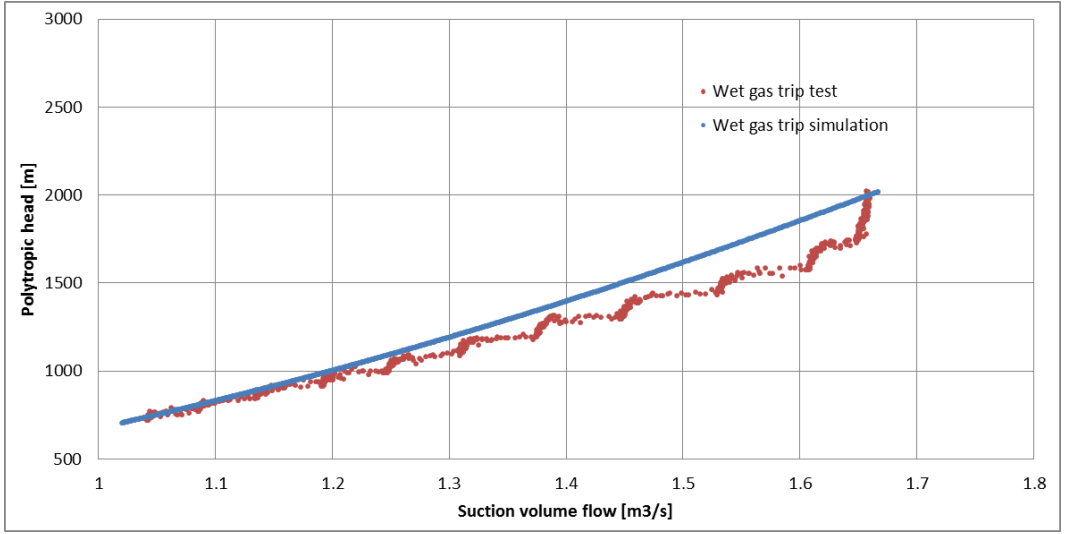


Figure 5-9 - Polytropic head versus suction volume flow for wet gas BEP trip

Figure 5-9 shows the run down characteristics of the system in a polytropic head and volume flow diagram. The dynamic model does in general predict too low polytropic head for a given volume flow. The deviation decreases towards low volume flows.

### Dry gas trip test surge

Results from dry gas trip testing close to surge along with predicted transient performance of the dynamic model are provided below.

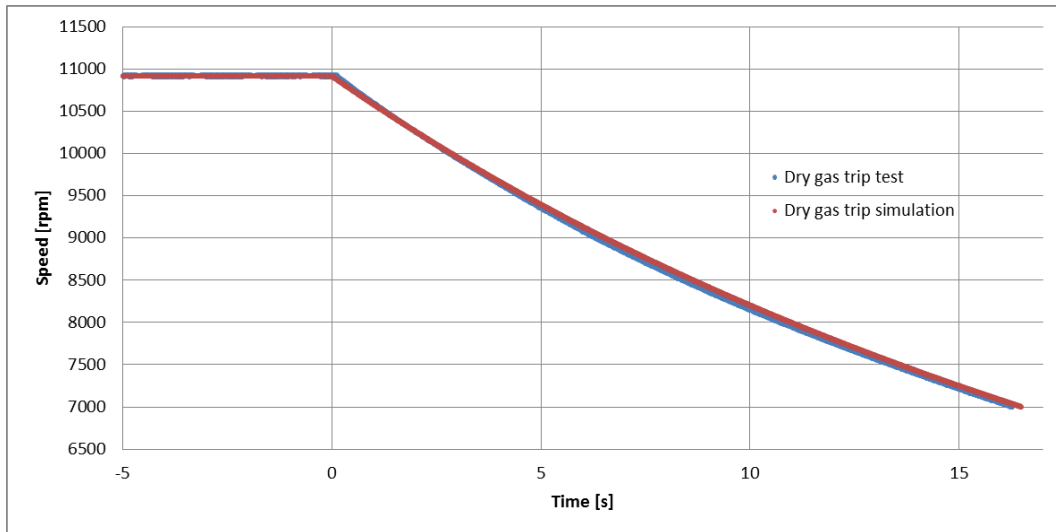


Figure 5-10 - Compressor speed versus time for dry gas surge trip

Figure 5-10 shows the compressor speed reduction. It takes 16.29 seconds for the compressor to reach 7 000 rpm. The dynamic model deviates 0.69% about eight seconds after the trip signal.

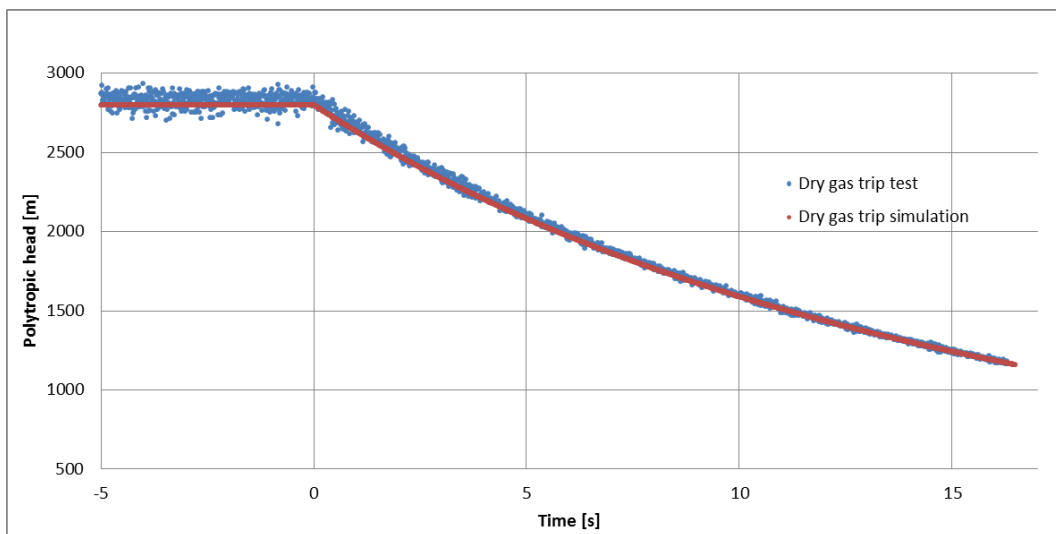


Figure 5-11 - Polytopic head versus time for dry gas surge trip

Figure 5-11 shows the polytopic head during trip. The largest deviation is 3.05% which occur prior to the trip signal. The largest deviation during trip is 2.42%.

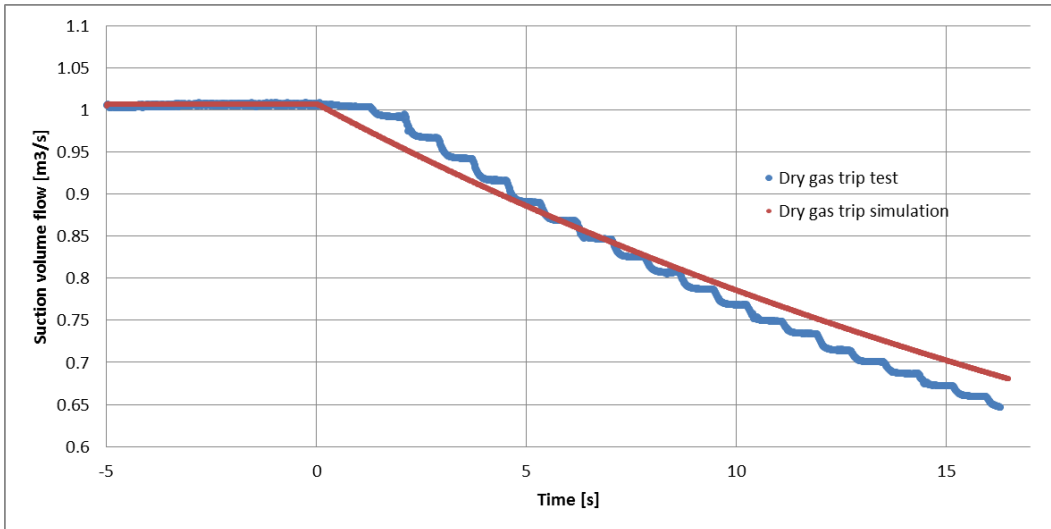


Figure 5-12 - Suction volumetric flow versus time for dry gas surge trip

Figure 5-12 shows the compressor suction volume flow during dry gas trip close to surge. The predicted volume flow is 3.90% too low during the first seconds from trip. The predicted volume flow does not seem to converge toward the test results. At 7000 rpm the dynamic model predicts 5.64% higher volume flow than the test results suggests.

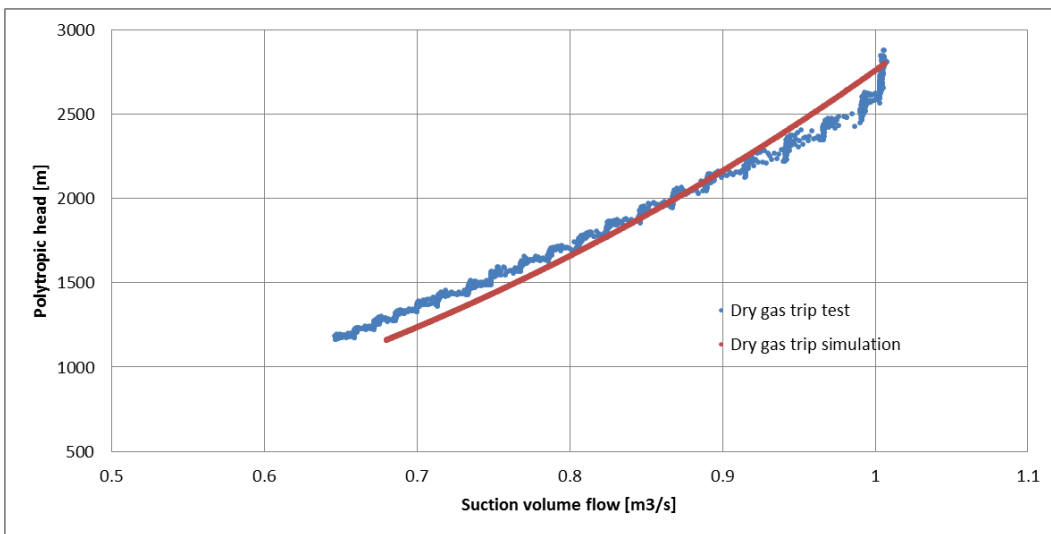


Figure 5-13 - Polytropic head versus suction volume flow for dry gas surge trip

Figure 5-13 shows the run down characteristics of the system in a polytropic head and volume flow diagram. The dynamic model does not predict the actual run down characteristics accurately.

### Wet gas surge trip test

Results from wet gas trip testing close to surge along with predicted transient performance of the dynamic model are provided below. This scenario was simulated with compressor curves for dry gas and GMF0.7. The curves for GMF0.8 were not used in order to avoid instabilities in the dynamic model.

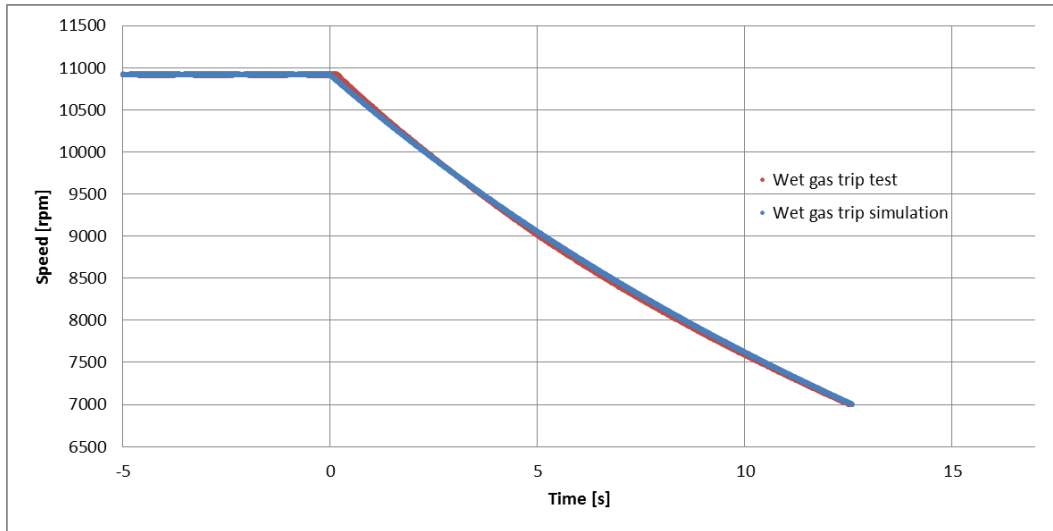


Figure 5-14 - Compressor speed versus time for wet gas surge trip

Figure 5-14 shows the compressor speed reduction. It takes 12.53 seconds for the compressor to reach 7 000 rpm. The maximum deviation of the dynamic model is 0.67% just after the trip signal.

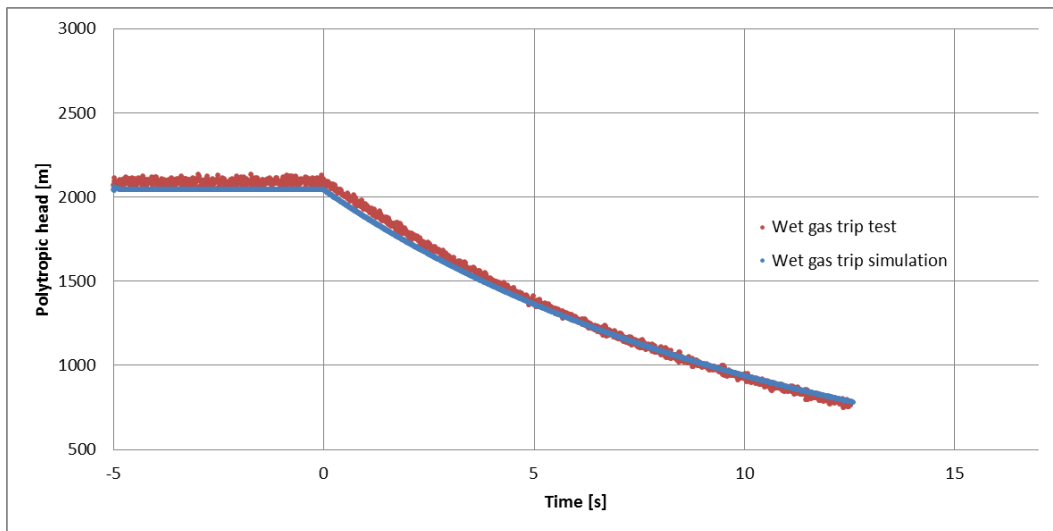


Figure 5-15 - Polytropic head versus time for wet gas surge trip

Figure 5-15 shows the polytropic head during trip. The largest deviation is 3.77% at approximately 7 000 rpm.

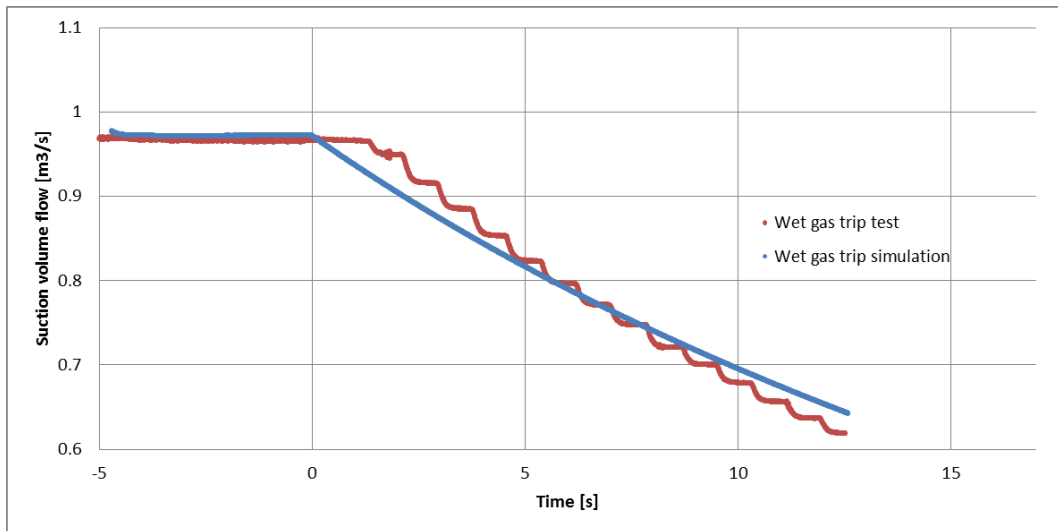


Figure 5-16 - Suction volume flow versus time for wet gas surge trip

Figure 5-16 shows the compressor suction volume flow during wet gas trip from surge. The dynamic model deviates up to 5.05% the first five second after trip. The volume flow prediction does not seem to converge toward test data. At 7000 rpm the volume flow prediction is about 4.79% too high.

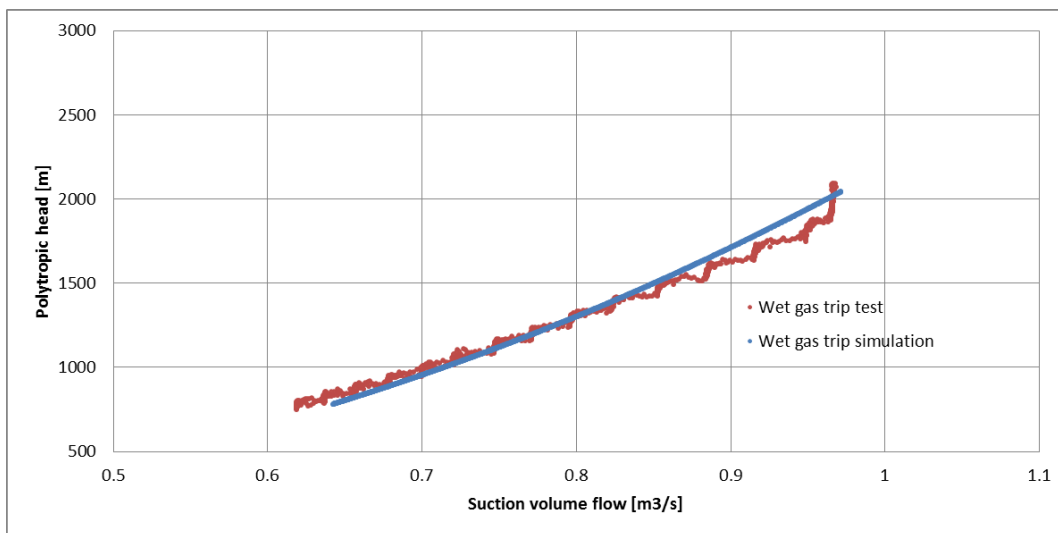


Figure 5-17 - Polytropic head versus suction volume flow for wet gas surge trip

Figure 5-17 shows the run down characteristics of the system in a polytropic head and volume flow diagram. The initial deviation is due to the inaccurately predicted volume flow.

### Dry gas trip test open valve

Results from dry gas trip test at open valve along with predicted transient performance of the dynamic model are provided below.

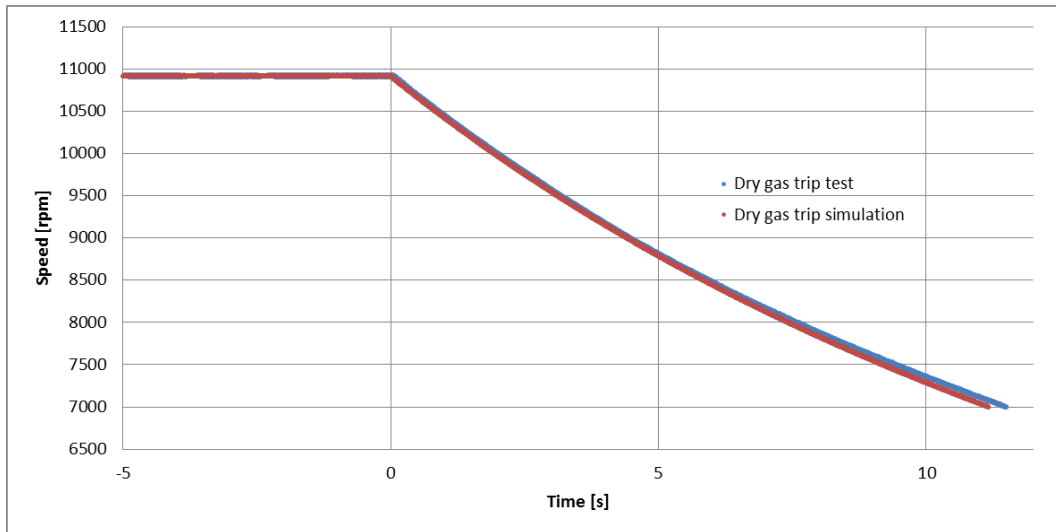


Figure 5-18 - Compressor speed versus time for dry gas open valve trip

Figure 5-18 shows the compressor speed reduction. It takes 11.5 seconds for the compressor to reach 7 000 rpm. The largest deviation is 1.10% at approximately 7 000 rpm.

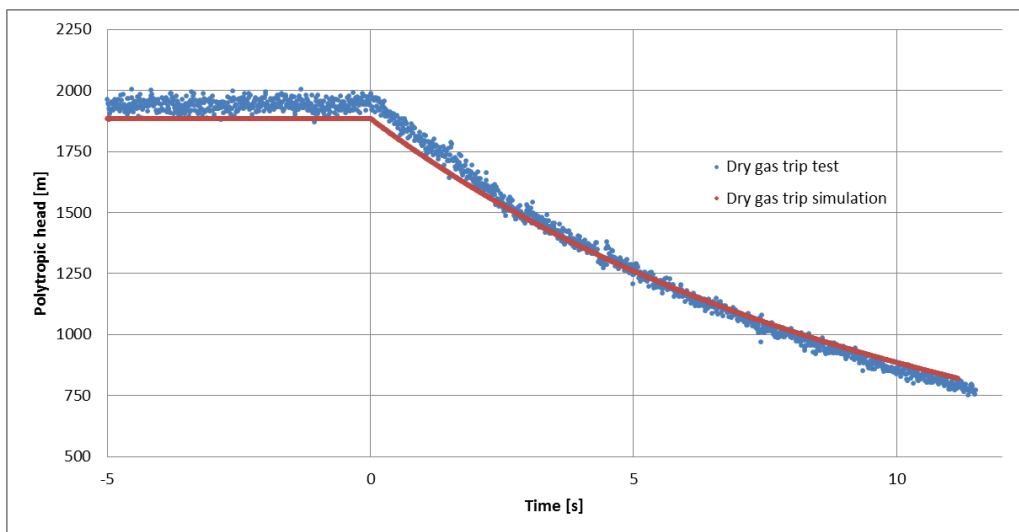


Figure 5-19 - Polytropic head versus time for dry gas open valve trip

Figure 5-19 shows the polytropic head during trip. The dynamic model initially predicts too low polytropic head. The largest deviation is 5.78% 1.5 seconds after the trip signal. During run down the predicted head curve crosses the test data, and a large deviation of 5.68% is found at 7 000 rpm.

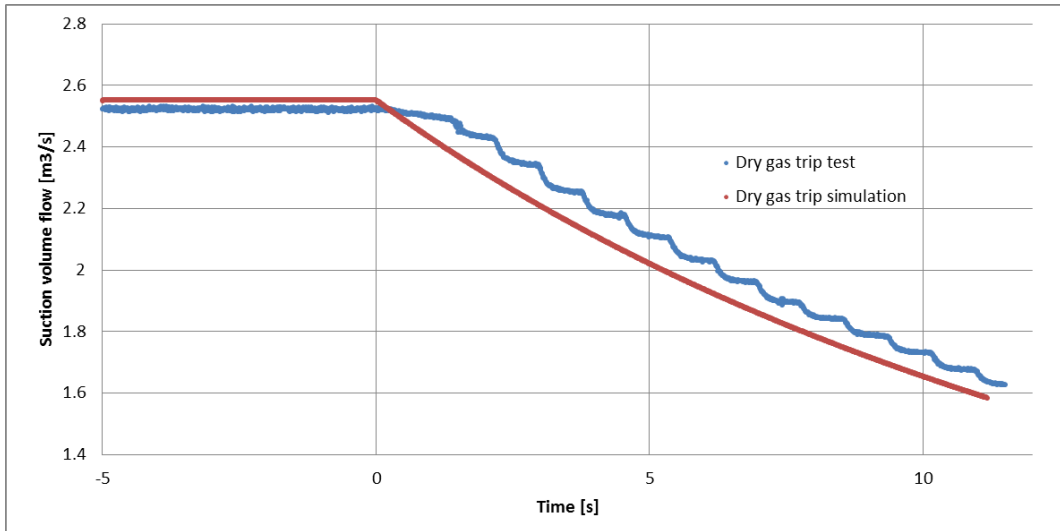


Figure 5-20 - Suction volume flow versus time for dry gas open valve trip

Figure 5-20 shows the compressor suction volume flow during dry gas trip from open valve. The dynamic model deviates up to 5.44%. The deviation is fairly constant.

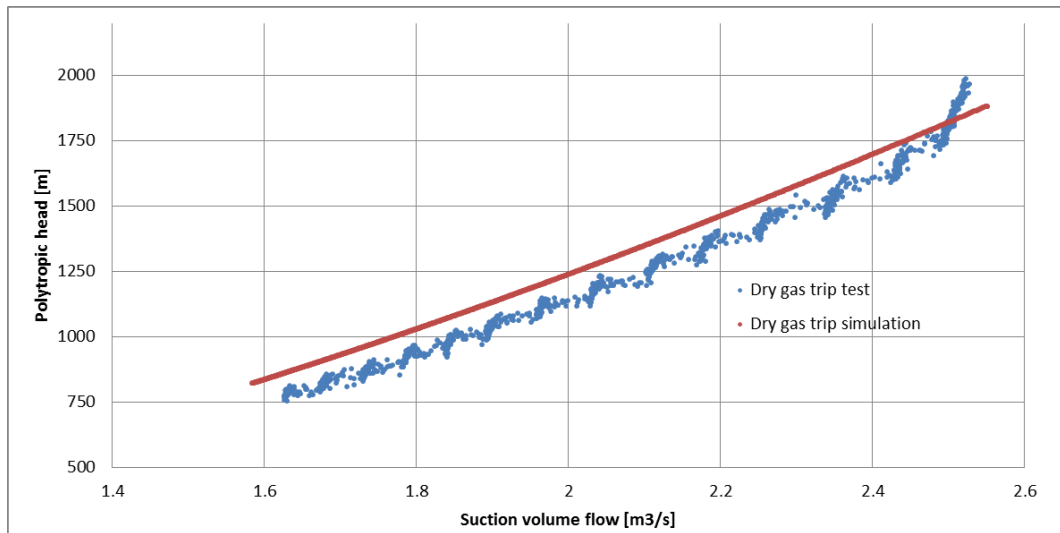


Figure 5-21 - Polytropic head versus suction volume flow for dry gas open valve trip

Figure 5-21 shows the run down characteristics of the system in a polytropic head and volume flow diagram.

### Wet gas trip test open valve

The dynamic model was not able to successfully predict the wet gas trip from an open valve point of operation. Severe stability problems occur as the compressor speed decreases below 8250 rpm.

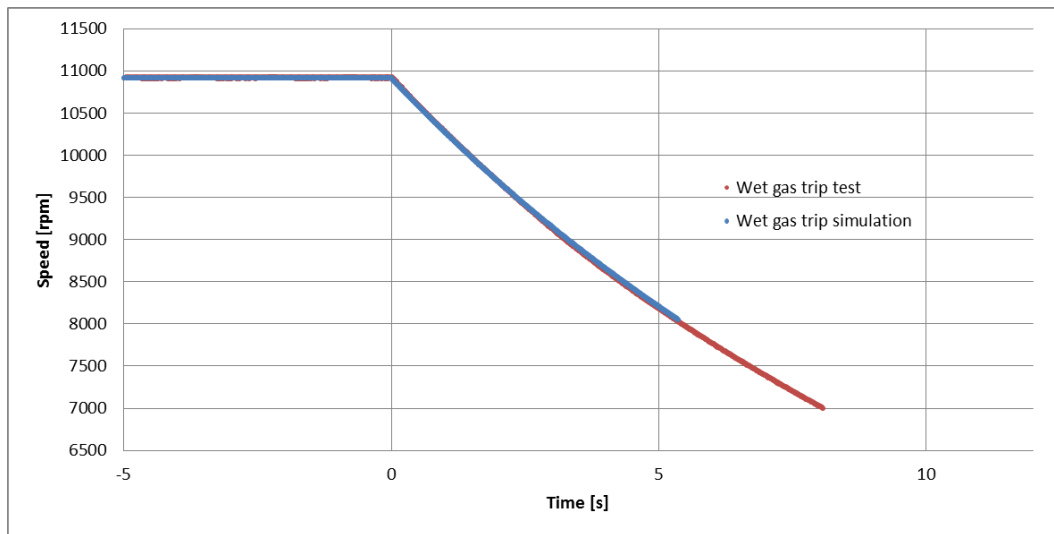


Figure 5-22 - Compressor speed versus time for wet gas open valve trip

Figure 5-22 shows the compressor speed reduction. It takes 8.07 seconds for the compressor to reach 7 000 rpm. The dynamic model is stopped 5.36 seconds after trip where severe instability problems already have occurred. The compressor speed prediction is however rather accurate, with a maximal deviation of 0.32% after about 3 seconds.

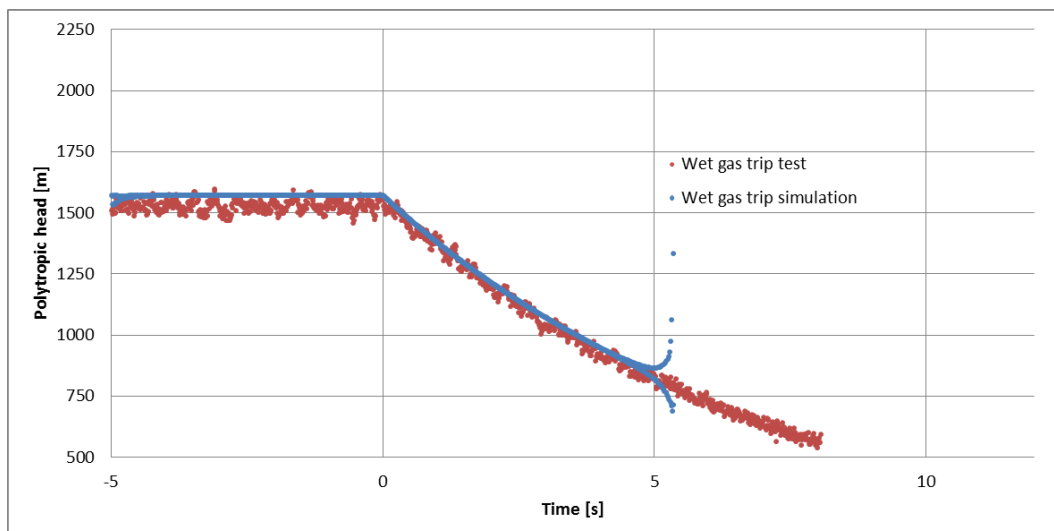


Figure 5-23 - Polytropic head versus time for wet gas open valve trip

Figure 5-23 shows the polytropic head during trip. The maximum deviation during the first 5.28 seconds of run down is 5.98%. After 5.28 seconds the models becomes unstable with very high deviations. HYSYS automatically stops the integrator 5.43 seconds after the trip signal.



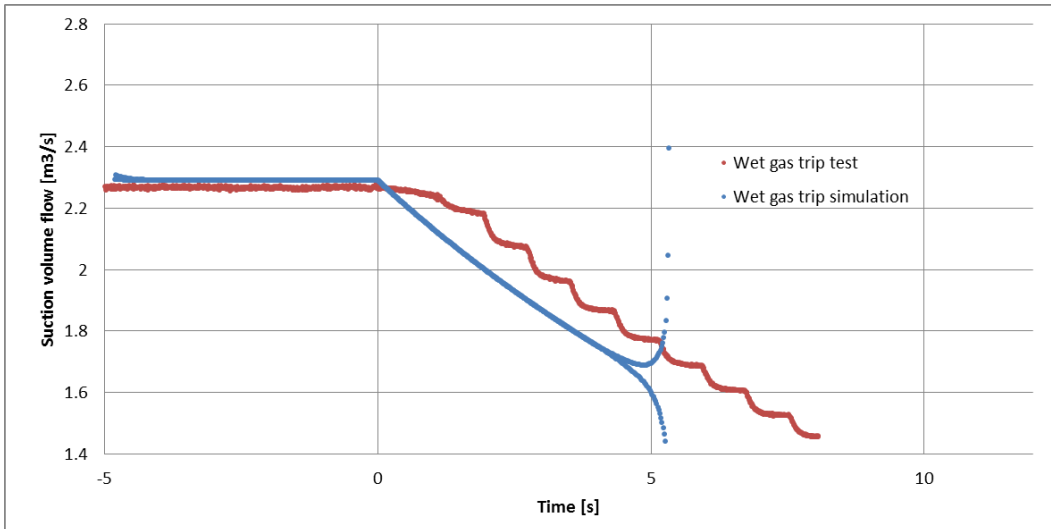


Figure 5-24 - Suction volume flow versus time for wet gas open valve trip test

Figure 5-24 shows the suction volume flow during trip. Maximum deviation during the first 5.28 seconds of run down is 8.68% after about two seconds. After 5.28 seconds the model becomes unstable with very high deviations.

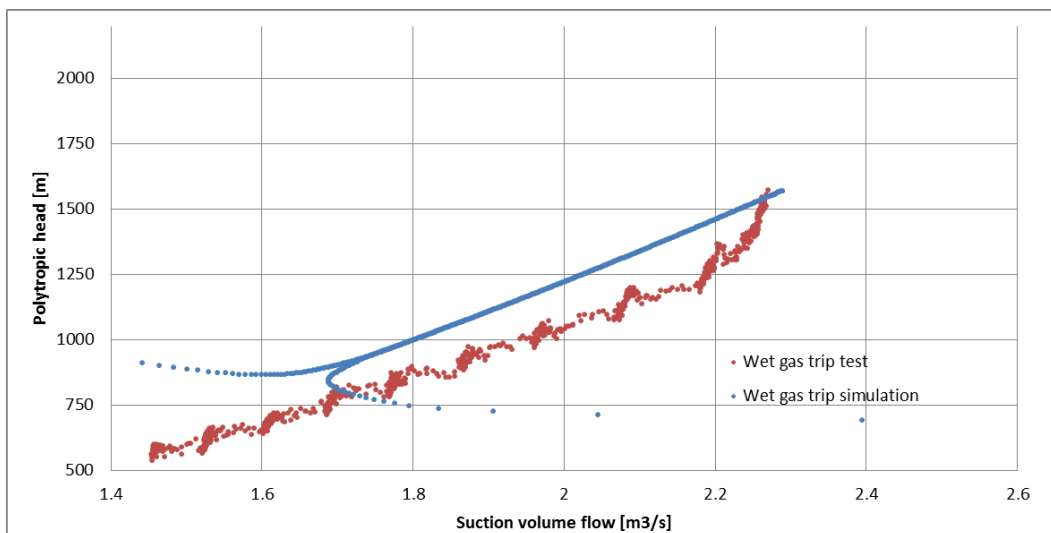


Figure 5-25 - Polytropic head versus suction volume flow for wet gas open valve trip

Figure 5-25 shows the rundown characteristics from the wet gas open valve operational point. Due to inaccuracies in the suction volume flow prediction, the dynamic model predicts too high polytropic head for a given volume flow. The deviation is however rather constant until the simulation becomes unstable at approximately 8250 rpm.

Maximum deviation of trip simulation in dynamic model

Table 5-10 shows the maximum deviation of the predicted performance of the dynamic model.

	<b>Compressor speed [%]</b>	<b>Polytropic head [%]</b>	<b>Suction volume flow [%]</b>
<b>Dry gas BEP</b>	0.41	2.49	4.70
<b>Wet gas BEP</b>	0.70	7.21	8.17
<b>Dry gas surge</b>	0.69	3.05	5.64
<b>Wet gas surge</b>	0.67	3.77	5.05
<b>Dry gas open valve</b>	1.10	5.78	5.44
<b>Wet gas open valve</b>	0.32*	5.98*	8.68*
*During first 5.28 seconds after trip			

Table 5-10 - Maximum deviation of dynamic trip simulation

## 5.5.Challenges related to accurate transient measurements

### Introduction

This section will document the most important challenges related to accurate transient measurements in the lab facility.

### Performance fluctuations

The sensor readings from the compressor lab facility fluctuate severely. For the wet gas open valve test, the polytropic head varies with up to 84 m between two subsequent time steps. In percentage this corresponds to a difference of 15%. This makes distinction of actual deviation from random fluctuations challenging.

In order to reduce the effect of random fluctuations, the maximum deviation between the dynamic model and the test data is averaged over five time steps as described in Section 5.4.

### Temperature readings

The compressor performance prediction is very sensitive to the temperature readings. This is especially true for wet gas compression which has very low temperature rise through the compression process. As documented by (Nøvik 2013), it is not likely that current standards for dry gas performance evaluation is satisfying for wet gas applications.

Experience has revealed the time response of the temperature sensors to be very slow. In general the measured discharge temperature cannot be applied to transient calculations. Through this work evaluation of transient polytropic efficiency is omitted partly due to the expected lack of dynamic accuracy. The dynamic temperature performance could be improved by installing smaller thermal elements. Torque measurements could also be used to determine the compressor power and efficiency.

### Volume flow delay

The flow through the compressor is calculated based on the differential pressure of the orifice plate. The calculated mass flow in the orifice spreadsheet is assumed valid for the compressor inlet at the current time step. The orifice plate is however placed 1.77 meter upstream the compressor block implying the measured value in the orifice plate to be delayed due to the travel time.

At 7 000 rpm the volume flow of the wet gas surge trip is just  $0.619\text{m}^3/\text{s}$ , implying the gas to use 0.14 seconds to flow from orifice plate to compressor inlet, corresponding to 14 time steps. During dry gas open valve testing the corresponding travel time is just 0.034 seconds.

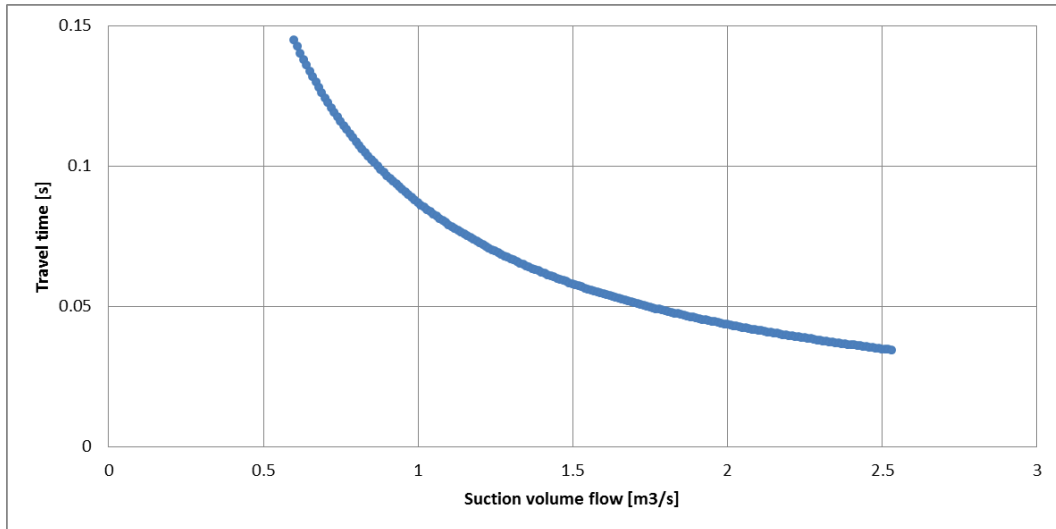


Figure 5-26 - Travel time for different suction volume flow

Figure 5-26 shows the travel time for air from orifice plate to compressor inlet as a function of suction volume flow. The minimum flow value is set to  $0.61 \text{ m}^3/\text{s}$  which corresponds to the wet gas surge trip case at 7 000 rpm. The maximum value is set to  $2.6 \text{ m}^3/\text{s}$  representing the dry gas open valve case prior to trip.

## 5.6. Discussion of trip scenarios

### Introduction

The following section discusses the observed deviation of the dynamic model compared to test data in terms of suction volume flow, polytropic head and compressor speed. Behavior related to surge along with overall accuracy is given special attention.

### Suction volume flow

The poorest performance of the dynamic model is by far the suction volume flow prediction. By inspection of Figure 5-4, Figure 5-8, Figure 5-12, Figure 5-16, Figure 5-20 and Figure 5-24 it is evident that the trip test data deviates from the trip simulation in three ways:

- The reduction in suction volume flow is delayed
- The trip test curve is wavy
- The lines are not parallel

The dynamic model calculates the flow based on affinity laws which suggest the suction volume flow to be proportional to the compressor speed. As a consequence the dry gas speed curves and suction volume flow curves should be identical of shape. The wet gas volume flow curves will deviate slightly due to the shift in compressor characteristics with GMF.

The initial delayed reduction of suction volume flow for the trip test may be addressed to the air traveling distance from orifice to compressor inlet. For the dry gas BEP case the steady state volumetric flow rate is  $1.777\text{m}^3/\text{s}$ . The distance from the orifice plate is 1.77 m, and the pipe diameter is 0.25m. The resulting traveling time equals less than 0.05 seconds and may be disregarded as the main cause of delay at trip. The traveling time may become more significant at lower rotational speeds as discussed in Section 5.5.

It is suggested that the wavy nature of the suction volume flow is most likely related to slow pressure response of the differential pressure meter of the orifice plate.

Detailed investigation of the suction flow pattern is considered to be outside the scope of this work. As no similar behavior is observed for the polytropic head and compressor speed, the phenomenon is suspected to be a result of measurement shortcomings or unfavorable calculation procedures. An evaluation of the above presented measurements representing actual compressor behavior could be a subject for further research.

The compressor characteristics used in the dynamic model is solely based on test data for 11 000 rpm. In Section 5.2 the maximum deviation in volume flow was 0.71%. The large deviations in volume flow at lower rotational speeds (up to 8.68% at 7 000 rpm) may be due to the real compressor behavior. In reality the compressor rig may not follow the affinity laws which the dynamic model is based.

### Polytropic head

The predicted curves for polytropic head are similar of shape to the actual performance. Still some consistent offset is observed between the simulation and test data. This is especially true for the dry gas open valve trip scenario (Figure 5-19). During five seconds prior to the trip the dynamic model

predicts 3.01% lower polytropic head compared to test data. The actual volume flow of this test point is  $2.52\text{m}^3/\text{s}$ .

Table 5-4 of Section 5.2 presents the deviation of the dynamic model for an operational point of  $2.56\text{m}^3/\text{s}$  and 11 000 rpm. The deviation in this test point is just 0.19% for the polytropic head. This value is based on testing related to development of compressor characteristics. It is inconsistent that the dynamic model predicts a deviation of 3.01% at an almost identical operational point during trip testing a month later. The compressor characteristics developed from test data at an early state does not accurately predict performance during later trip testing at a similar operational point. This example suggests individual tuning of the compressor curves for each trip scenario in order to improve accuracy.

### Compressor speed

The compressor speed prediction is very accurate with a maximum deviation of 1.10%. The compressor speed measurements are quite reliable with minimal fluctuations. The overall impression is that the actual compressor lab facility follows the simplified energy equations given in (2-23) of which the dynamic model is based.

### Surging

A central challenge during trip is the tendency for the compressor to enter the surge area. Two trip tests were performed near surge in this work. Figure 5-13 and Figure 5-17 shows the run down characteristics for the two tests. During the first seconds the polytropic head falls quickly at almost constant suction flow rate. This behavior differs significantly from the trip scenarios from Troll-Kollsnes (Figure 2-8, Figure 2-10 and Figure 2-11) where the suction flow rate is quickly reduced at high polytropic head, forcing the operational point into the surge area.

The reason for which the compressor rig at NTNU does not enter surge during driver trip is related to low pressure ratios and small downstream volumes. The dynamic model contains no units which includes physical volumes, such as pipe segments. This is due to instability challenges described in Section 4.6. Consequently the dynamic model cannot predict surging due to evacuation of downstream compressed gas. For the test data at hand however, no such surge behavior is observed. If the dynamic model is to be used for other compressor systems, inclusion of volumes must be assessed to ensure performance reliability.

### Overall accuracy

The compressor speed prediction is very accurate. The polytropic head prediction deviates up to 7.21%, but the shape of the curves are very similar to test data. The accuracy of the polytropic head prediction is expected to be considerably improved by performing some minor tuning of the compressor characteristics to eliminate the consistent offset especially seen in the open valve tests.

The predicted suction volume flow deviates from the values suggested by test data. The difference is most pronounced during the first seconds after trip. This is the most critical phase in terms of surge behavior (Bakken, Bjørge et al. 2002, Tveit, Bakken et al. 2004, Schjøberg, Hyllseth et al. 2008) The predicted curve is not similar of shape as test data, but it is not confirmed if the error is associated with limitations in rig instrumentation or shortcomings of dynamic model.

## Conclusion

The compressor speed prediction is very accurate with a maximum deviation of just 1.10%. The polytropic head prediction is less accurate with a maximum deviation of 7.21%. The polytropic head curves are similar as the measured curves in terms of shape. It is expected that the polytropic head prediction can be tuned to reduce the deviation significantly. The predicted volume flow is worse with 8.68% maximum deviation. The predicted curve does not match the performance calculated by the steady state model. The measured volume flow does not follow the affinity laws during trip.

The polytropic head and the suction volume flow are calculated in the steady state model based on sensor readings. Because the measurements are taken from a transient operating scenario, the calculated values may not represent actual compressor behavior.

## 5.7.Speed ramp-up scenarios

### Introduction

The final task of the assignment text is to establish a representative transient operating scenario and predict deviation between dry and wet compressor behavior. It is desirable to choose a scenario which may be performed in the compressor lab facility in order to validate the prediction. As trip testing was performed in subtask two, a logical advancement is to investigate the compressor behavior during speed ramp-up.

A speed ramp-up test will not only reveal any liquid phase impact, but it may also provide some information regarding the accuracy of the motor representation in the dynamic model.

It should be noted that the scope of this section is to predict deviation between dry and wet compressor behavior. The specific performance of the dynamic model to the actual compressor performance is not emphasized in the same comprehensive manner as for the trip tests.

### Other possible transient scenarios

It would have been interesting to investigate the system response to change in upstream or downstream pressure and temperature. Unfortunately the open-loop nature of the compressor test facility leaves the operator very limited means to control these parameters. Inlet temperature, pressure and relative humidity are dictated by current room conditions.

Another possibility is to explore compressor response to variation in discharge valve position. This option was also disregarded due to the manual operation of the valve which would challenge the prospect of performing repeatable testing. It is difficult to accurately recreate a manual transient valve adjustment in the dynamic simulation tool. The current set up demands an operator to fine-tune the valve position during steady state to obtain a specific operational point.

Liquid surge waves was presented as an operational challenge for subsea compressor in (Owren 2013). The liquid flow rate can be altered through the lab-control system which allows repeatable testing. Challenges are however related to the water pump being positioned a long distance from the injection module, with wandering piping in between. Similarly the water flow meter is positioned a distance upstream of the injection module, with vertical piping in between. For steady state operation, the water entering the compressor will be identical to the flow meter reading, but for transient scenarios the distance to the flow meter and water pump would challenge the accuracy of the water amount actually entering the compressor at a given time.

Compressor speed ramp-up tests enables both repeatable testing in lab, and can be accurately performed with identical conditions in the dynamic model.

### Testing procedure

One dry and one wet BEP ramp-up test from 9 000 rpm to 11 000 rpm were performed in the lab. The operational points were established by adjusting the discharge valve and water pump. When stable operation was obtained, 60 seconds were logged at a frequency of 1000 Hz. Then the speed was changed instantly to 11 000 rpm in the lab control system. The logging was stopped 60 seconds after the ramp-up signal. The two test points are given in Table 5-11.



Name	dP orifice [mbar]	Water flow rate [l/s]	GMF [-]
Dry gas BEP speed ramp-up	62.99	[-]	1
Wet gas BEP speed ramp-up	62.90	0.406	0.795

Table 5-11 - Test points for speed ramp-up test

The test results were analyzed with the steady state model. The analysis started 5 seconds prior to the ramp-up signal and ended 20 seconds after the trip signal. Every 10<sup>th</sup> time step (0.01 seconds interval) was analyzed in order to save calculation time.

Average values of the steady state operation 60 seconds prior to the ramp-up were imported to the dynamic model. The discharge valve was adjusted by the flow controller to obtain correct differential pressure over the orifice plate. Five seconds prior to ramp-up plus 20 seconds after the ramp-up was then simulated in the dynamic model.

## 5.8.Speed ramp-up results

### Introduction

The result section is divided into two parts. First the predicted deviation between dry and wet gas compressor behavior is documented in terms of rotational speed, polytropic head and suction volume flow. The next part documents actual prediction between dry and wet gas in terms of rotational speed, polytropic head and suction volume flow based on experimental test results from the compressor rig.

Deviation between dry and wet gas are addressed in terms of time to reach 95% and 99% of respective steady state values. The time is measured from ramp-up signal until the first time step with values equal or greater than the stated values.

The tests revealed minimal differences between dry and wet gas.

### Prediction of dry and wet gas deviation

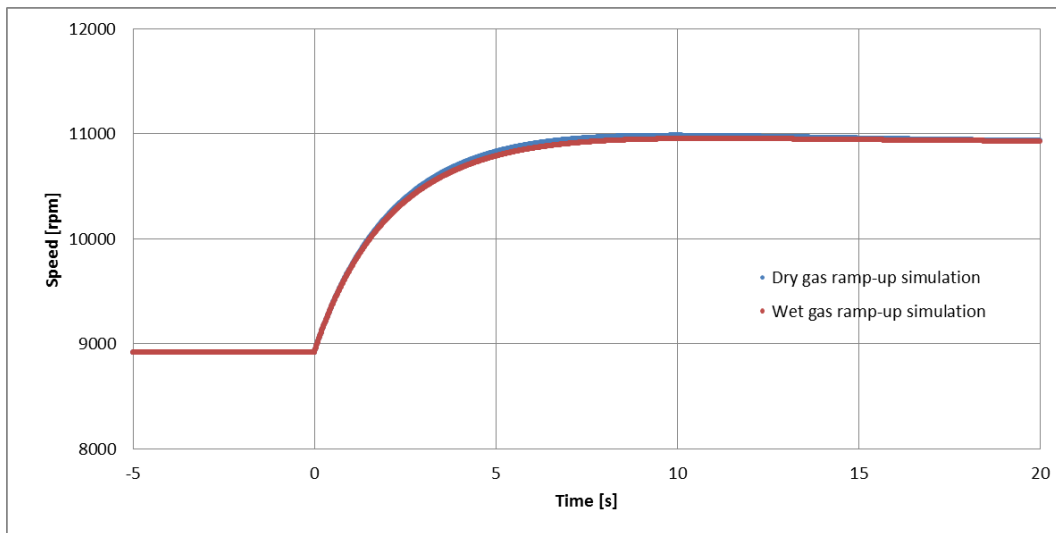


Figure 5-27 - Compressor speed versus time for dry and wet ramp-up simulation

Figure 5-27 shows the predicted speed ramp-up for dry and wet gas. The curves are almost coincided. The maximum deviation is 0.38% after approximately five seconds.

	Steady state speed [rpm]	95% speed [rpm]	99% speed [rpm]	Time to 95% speed [s]	Time to 99% speed [s]
<b>Dry gas ramp-up simulation</b>	10913.86	10368.16	10804.72	2.47	4.79
<b>Wet gas ramp-up simulation</b>	10914.07	10368.37	10804.93	2.57	5.23

Table 5-12 - Time to reach 95% and 99% of steady state speed for ramp-up simulation

Table 5-12 shows the time duration from ramp-up signal for the predicted compressor speed to reach 95% and 99% of the steady state value. The wet gas simulation is the slower.

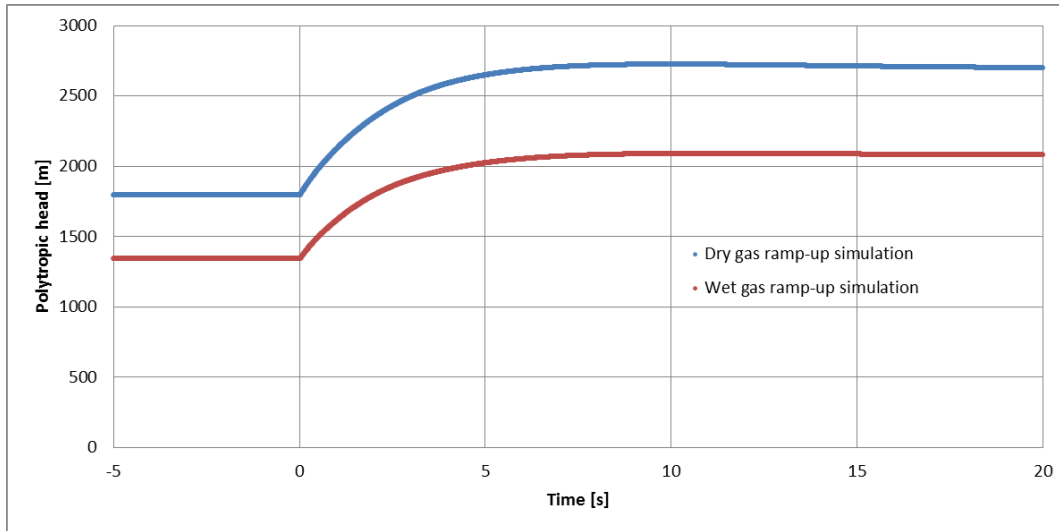


Figure 5-28 - Polytopic head versus speed for dry and wet gas ramp-up simulation

Figure 5-28 shows the predicted polytopic head for dry and wet gas ramp-up. The curves are similar of shape, but the produced head is lower for the wet gas scenario.

	Steady state polytopic head [m]	95% polytopic head [m]	99% polytopic head [m]	Time to 95% polytopic head [s]	Time to 99% polytopic head [s]
<b>Dry gas ramp-up simulation</b>	2689.28	2554.82	2662.39	3.60	5.39
<b>Wet gas ramp-up simulation</b>	2072.85	1969.21	2052.12	3.90	6.08

Table 5-13 - Time to reach 95% and 99% of steady state polytopic head for ramp-up simulation

Table 5-13 shows the time duration from ramp-up signal for the predicted compressor speed to reach 95% and 99% of the steady state values. The wet gas simulation is the slower.

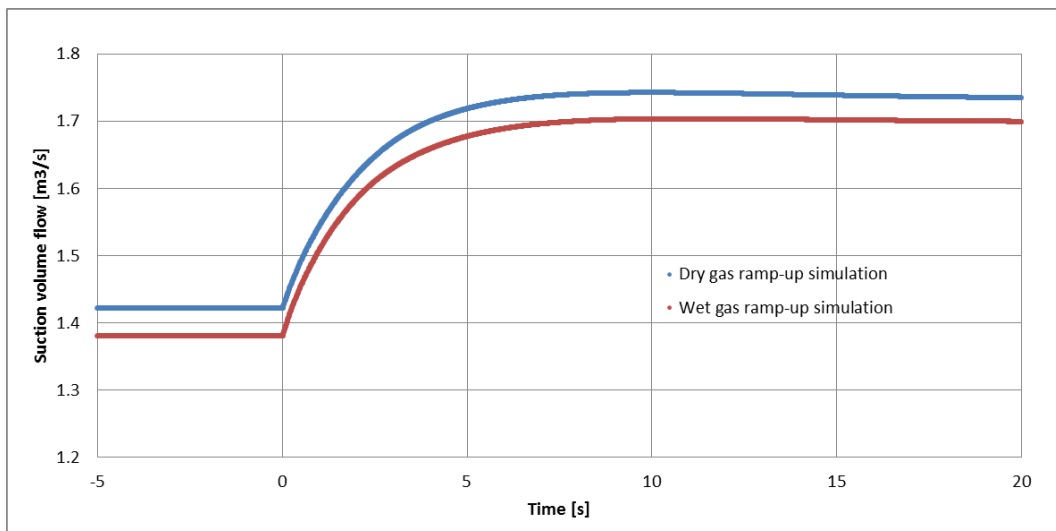


Figure 5-29 - Suction volume flow versus time for dry and wet ramp-up simulation

Figure 5-29 shows the suction volume flow of the dry and wet gas ramp-up simulation. The shapes of the curves are similar, but the wet gas scenario has lower volumetric flow rate.

	Steady state volume flow [m <sup>3</sup> /s]	95% volume flow [m <sup>3</sup> /s]	99% volume flow [m <sup>3</sup> /s]	Time to 95% volume flow [s]	Time to 99% volume flow [s]
<b>Dry gas ramp-up simulation</b>	1.7314	1.6448	1.7141	2.47	4.76
<b>Wet gas ramp-up simulation</b>	1.6969	1.6121	1.6799	2.56	5.24

Table 5-14 - Time to reach 95% and 99% of steady state suction volume flow for ramp-up simulation

Table 5-14 shows the time duration from ramp-up signal for the predicted suction volume flow to reach 95% and 99% of the steady state value. The wet gas simulation use longer time to reach the steady state values.

Actual deviation between dry and wet gas

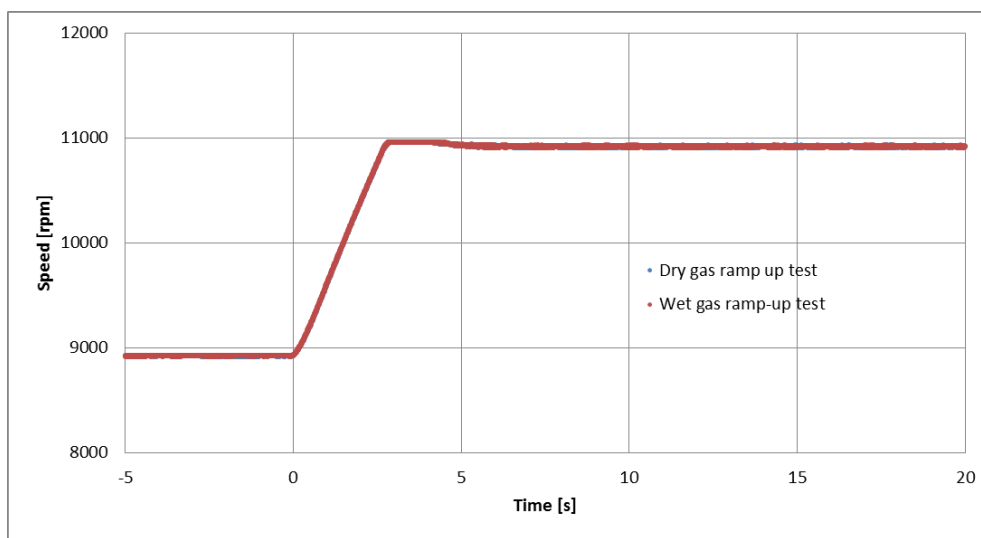


Figure 5-30 - Compressor speed versus time for dry and wet gas ramp-up test

Figure 5-30 shows the test speed ramp-up for dry and wet gas. The curves are almost coincided. The maximum deviation is less than 0.1%

	Steady state speed [rpm]	95% speed [rpm]	99% speed [rpm]	Time to 95% speed [s]	Time to 99% speed [s]
<b>Dry gas ramp-up test</b>	10913.86	10368.16	10804.72	1.99	2.58
<b>Wet gas ramp-up test</b>	10914.07	10368.37	10804.93	1.99	2.58

Table 5-15 - Time to reach 95% and 99% of steady state speed for ramp-up test

Table 5-15 shows the time duration from ramp-up signal for the predicted compressor speed to reach 95% and 99% of the steady state value. No deviation is observed for dry and wet gas.

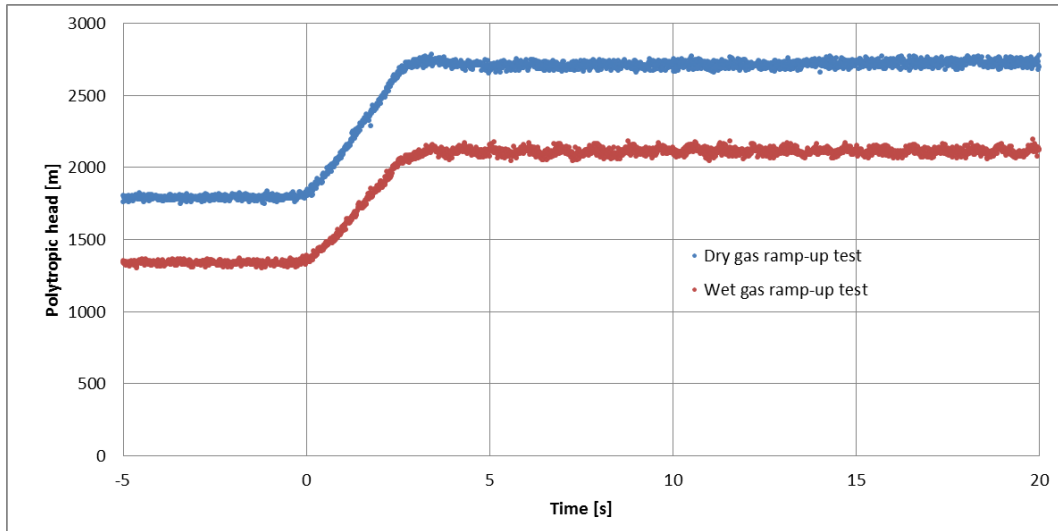


Figure 5-31 - Polytopic head versus time for dry and wet gas ramp-up test

Figure 5-31 shows the predicted polytopic head for dry and wet gas ramp-up test. The curves are similar of shape, but the produced head is lower for the wet gas scenario.

	Steady state polytopic head [m]	95% polytopic head [m]	99% polytopic head [m]	Time to 95% polytopic head [s]	Time to 99% polytopic head [s]
<b>Dry gas ramp-up simulation</b>	2726.966	2590.62	2699.70	2.33	2.70
<b>Wet gas ramp-up simulation</b>	2111.15	2005.59	2090.04	2.46	2.90

Table 5-16 - Time to reach 95% and 99% of steady state polytopic head for ramp-up test

Table 5-16 shows the time duration from ramp-up signal for the polytopic head to reach 95% and 99% of the steady state value. The wet gas test use longer time to reach the steady state polytopic head.

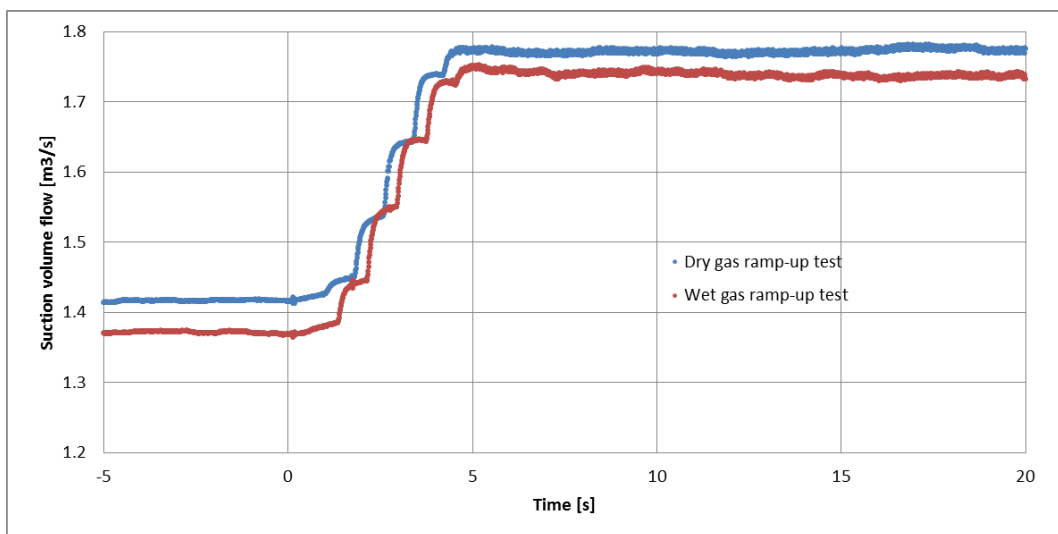


Figure 5-32 - Suction volume flow versus time for dry and wet ramp-up test

Figure 5-32 shows the suction volume flow of the dry and wet gas ramp-up test. The shapes of the curves are similar, but the wet gas scenario has lower volumetric flow rate.

	Steady state volume flow [m <sup>3</sup> /s]	95% volume flow [m <sup>3</sup> /s]	99% volume flow [m <sup>3</sup> /s]	Time to 95% volume flow [s]	Time to 99% volume flow [s]
<b>Dry gas ramp-up test</b>	1.7746	1.6859	1.7569	3.50	4.32
<b>Wet gas ramp-up test</b>	1.7361	1.6493	1.7188	3.78	4.01

Table 5-17 - Time to reach 95% and 99% of steady state suction volume flow for ramp-up test

Table 5-17 shows the time duration from ramp-up signal for the suction volume flow to reach 95% and 99% of the steady state value. In this scenario the wet gas reaches the 99% steady state value before the dry gas.

Polytropic head versus suction volume flow

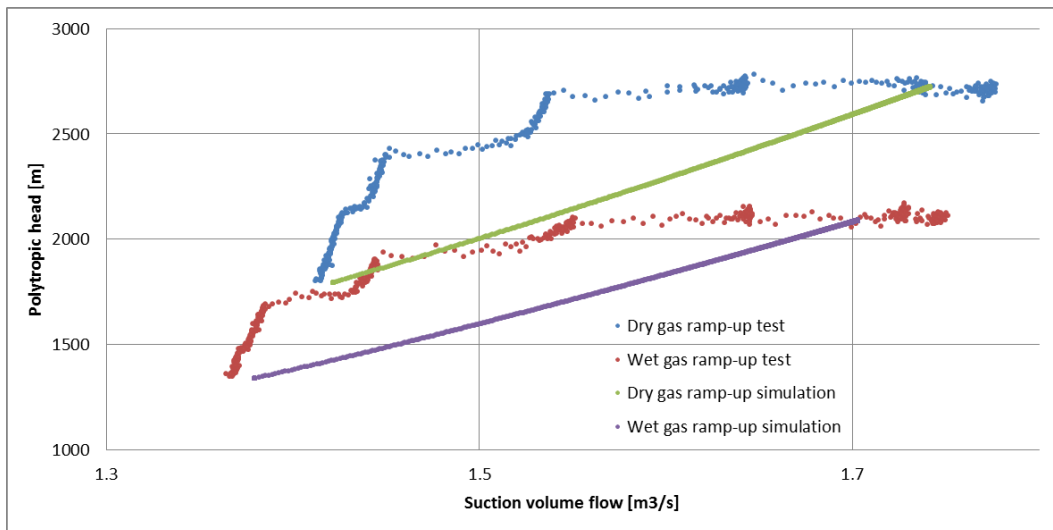


Figure 5-33 - Test and simulation results in a polytropic head versus suction volume flow diagram

Figure 5-33 shows both test data and simulation results in a polytropic head versus suction volume flow diagram. The initial values are down to the left. The final steady state values are at the top right side of the diagram. The initial prediction is quite accurate both for suction volume flow and polytropic head. The final steady state prediction is good for polytropic head, but deviates for suction volume flow.

## 5.9. Discussion of speed ramp-up results

### Introduction

The following section will discuss the speed ramp-up results. The main objective is to address the predicted deviation between dry and wet gas, but the simulation results will also be subject to comparison with test data from compressor lab.

### Rotational speed

The dynamic model predicts the wet gas speed ramp-up to reach 95% of its steady state value 4.05% later compared to dry gas. 99% of its steady state value is reached 9.19% later for the wet gas. The rotational speed is dictated by the VSD-output which is determined by the PI-controller «IC-VSD». It adjusts the delivered power based on the current difference in rotational speed and the set point. As a result, the controller will increase the delivered power similarly for the dry and wet gas case. The wet gas does however have a larger flow in terms of mass due to the liquid phase, and the resulting speed acceleration is slower.

The maximum available power from the VSD is 450kW in the dynamic model. The speed controller never exceeds 38% of maximum delivered power, which implies the compressor behavior to be a function of the control configuration, not limited by motor rating.

The ramp-up test reveals the actual compressor rig to behave different than predicted by the dynamic model. The speed increases virtually linearly, with no deviation between dry and wet gas. The ramp-up time to 95% of steady state value is 24% slower for the dry gas simulation and 29% slower for the wet gas simulation compared to the actual behavior. To 99% of steady state value the simulated results deviates with 86% and 103% respectively for dry and wet gas.

It is evident that the control system of the dynamic model does not represent actual compressor lab behavior in terms of speed control. It is not within the scope of this work to obtain in-detail knowledge of the lab facility control parameters.

### Polytropic head

The predicted polytropic head for the wet gas ramp-up reaches 95% of its steady state value 8.33% slower compared to the dry gas simulation. For the 99% steady state value the deviation is 12.80%. A longer time is required to reach the steady state values for polytropic head relative to rotational speed, for which reason the deviation between dry and wet gas is larger. Because the dynamic model contains no units with physical volume, there is no time delay due to pressure build up. The polytropic head is directly given by the current speed according to affinity laws (2-10). The larger time duration is a result of the polytropic head which has to be increased more relative to its initial value to reach the 95% and 99% steady state values compared to the rotational speed. This is evident by referring to the affinity laws (2-10) which states the polytropic head to be proportional to the speed squared. In theory, the polytropic head will reach its 99% steady state value when the speed reaches 0.995% of its steady state value.

The deviation of the wet gas polytropic head increases less between the 95% and 99% steady state value compared to rotational speed. This is partly due to the increase in GMF as the volumetric flow rate is increased while the water flow rate is held constant. As a consequence the compressor

characteristics for the wet gas ramp-up moves towards dry gas and associated faster system response.

As for the rotational speed the test data reveals ramp-up behavior which is more linearly of nature. An interesting observation is the deviation of dry and wet gas. As opposed to the rotational test results, the polytropic head shows a distinct deviation in the time required to reach the 95% and 99% steady state values. The reason is most likely the wet gas polytropic head which has to be increased more relative to its initial value to reach the 95% and 99% steady state values.

#### Suction volume flows

The dynamic model predicts the wet gas suction volume flow to reach 95% of its steady state value 3.64% slower compared to the dry gas simulation. For the 99% steady state value the deviation is 10.08%. Affinity laws in equation (2-9) states the suction volume flow to be proportional to the rotational speed, which implies the deviation for suction volume flow should be identical to the rotational speed deviation. The deviations are not equal however, which may be explained by rounding errors in the dynamic model. Inspection of Table 5-12 and Table 5-14 reveals time differences of just 0.01 seconds, or one time step. The small nature of the differences in time may suggest the time step being too large. Rounding errors can induce significant inaccuracy when evaluating the time response of the dynamic model.

The ramp-up test results from the lab facility reveal the time duration to reach 95% of steady state value to be slower than predicted by the dynamic model. This is non-consistent with results for rotational speed and polytropic head which states opposite behavior. It is further observed that the 99% steady state value is reached by the wet gas ramp-up quicker compared to the dry gas ramp-up, which is also non-consistent with the initial observed behavior.

The suction volume flows of the ramp-up tests are subject to a similar delay of action as described for the trip tests in Section 5.6. This is the reason why the ramp-up simulations predicts a quicker volume flow build up to 95% of the steady state value.

The latter phenomenon is explained by the curvy behavior of the suction volume flow curve. The 99% steady state value point is by random positioned at the end of a flat segment of the dry gas ramp-up test. For the wet gas ramp-up test, the 99% steady state value point is located at the end of a steep part of the curve. As discussed in Section 5.6, it is not confirmed if the wavy curves represent real compressor lab behavior.

#### Polytropic head versus suction volume flow

The objective of the last subtask was to predict deviation between dry and gas transient behavior. Still Figure 5-33 has been included to illustrate deviation between the dynamic model and test results from the lab facility. The initial prediction for head and suction volume flow is accurate. The final prediction for polytropic head is also quite good. The steady state prediction for suction volume flow is clearly lower than the measured value.

The dynamic model is however not able to predict the path of the operational point during ramp-up. For the test data the polytropic head start to increase before the volume flow. The polytropic head approaches its steady state value while the volume flow still increases. As a result the curves are



bow-shaped. The dynamic model on the other hand predicts the suction volume flow and polytropic head to increase simultaneously. The predicted curve appears linear but is actually slightly curved the opposite way compared to the test data. This is related to the suction volume flow being proportional to the rotational speed while the polytropic head is proportional to the speed squared.

### Conclusion

The predicted deviation between dry and wet gas during compressor speed ramp-up has been discussed. The ramp-up behavior is mainly dictated by the speed controller configuration in the dynamic model. The polytropic head and volume flow prediction is determined in the dynamic model based on affinity laws.

A longer time is required to approach steady state for the wet gas case compared to the dry gas case. This is mainly due to the increased mass flow of the wet gas. Because the liquid flow rate into the compressor is constant, the GMF will be reduced as the speed increases. This causes the wet gas deviation to decrease at higher volume flows.

Ramp-up testing revealed the compressor to behave quite different than predicted by the dynamic model. The deviation is mainly related to the control system configuration.



## 6. Conclusion

A dynamic simulation model for the compressor test facility has been developed in HYSYS Dynamics. The model performance is based on actual equipment specifications. Compressor curves developed from experimental data for the current impeller are used to determine polytropic head and volume flow. The model includes wet gas impact, but does not include any representation of the piping layout or associated pressure drop and heat exchange.

The steady state performance of the dynamic model has been validated against dry and wet test results. The performance is considered good. The non-transient polytropic head and suction volume flow prediction deviates less than 1% for all operational points but one.

Six trip scenarios have been investigated both in the dynamic model and in the lab facility. The trip behavior was analyzed from five seconds prior to the trip signal until the compressor reached 7 000 rpm. The dynamic model predicts the rotational speed accurately with a maximum deviation of 1.10%. The polytropic head predictions follow the test data closely. Some consistent offset is present making the prediction deviate up to 7.21%. It is expected that the predicted head curves can be fitted to eliminate the offset.

The dynamic model is not able to predict similar behavior as suggested by test data in terms of suction volume flow. The predicted volume flow is reduced according to affinity laws. The volume flow calculated from the test results suggest an initial delay of the volume flow reduction along with a different decay rate. It is not known whether the deviation is due to dynamic model performance or related to inaccurate measurement readings in the compressor lab.

Due to instability challenges in HYSYS Dynamics, it did not succeed to simulate the wet gas trip from open valve. The wet gas low volume flow operational point was not completed during validation of steady state performance of the dynamic model. Instability challenges have proven to be a major drawback of HYSYS Dynamics functionality.

A representative operating scenario has been established. Due to limitations in compressor test facility it was chosen to perform dry and wet gas speed ramp-up scenarios. The scenarios were both simulated in the dynamic model and tested in the compressor facility. The results revealed that the ramp-up behavior is dictated by the speed control configuration. The dynamic model predicts a slower system response while operating under wet gas conditions. This is not confirmed by the ramp-up tests which suggest no difference in compressor speed ramp-up.

Ramp-up testing revealed the compressor to behave quite different than predicted by the dynamic model. The deviation is mainly related to the control system configuration.



## **7. Further work**

In order to investigate pressure drop and pressure build-up/relief-effects the dynamic model should be developed further to include lab facility piping. The dynamic model could also include more accurate representation of the motor and speed control system in order to simulate a larger range of transient scenarios.

More steady state testing should be performed in order to develop compressor characteristics at other rotational speeds and hence reduce the use of affinity laws to predict wet gas performance.

## References

- Aguilera, L. C. P. (2013). "Subsea Wet Gas Compressor Dynamics." Master Thesis. NTNU, Trondheim.
- Aspen Engineering (2009). "What's New in V7.0 and V7.1."
- Bakken, L. E., et al. (2002). "VALIDATION OF COMPRESSOR TRANSIENT BEHAVIOUR." Proceedings of ASME Turbo Expo 2002.
- Brenne, L., et al. (2008). "Prospects for Sub Sea Wet Gas Compression." Proceedings of ASME Turbo Expo 2008: Power for Land, Sea and Air.
- Brenne, L., et al. (2005). "Performance Evaluation of a Centrifugal Compressor Operating Under Wet Gas Conditions." Proceedings of the Thirty-fourth Turbomachinery Symposium.
- Crane Co. (2011). FLOW OF FLUIDS.
- Hundseid, Ø. and L. E. Bakken (2006). "Wet Gas Performance Analysis." Proceedings of ASME Turbo Expo 2006: Power for Land, Sea and Air.
- Hundseid, Ø., et al. (2008). "Wet Gas Performance of a Single Stage Contrifugal Compressor." Proceedings of ASME Turbo Expo 2008: Power for Land, Sea and Air.
- Hundseid, Ø., et al. (2006). "A Revised Compressor Polytropic Performance Analysis." Proceedings of ASME Turbo Expo 2006: Power for Land, Sea and Air.
- Huntington, R. A. (1985). "Evaluation of Polytropic Calculation Methods for Turbomachinery Performance." Journal of Engineering for Gas Turbines and Power.
- Ministry of Petroleum and Energy (2014). "Facts 2014."
- Nøvik, H. (2013). "Validering av våtgassytelse." Master Thesis. NTNU, Trondheim.
- Owren, B. B. (2013). "Subsea Compressor Operation." Project Thesis. NTNU, Trondheim.
- Patel, V., et al. (2007). "Application of Dynamic Simulation in the Design, Operation, and Troubleshooting of Compressor Systems." Proceedings of the Thirty-sixth Turbomachinery Symposium.
- Saravanamutto, H., et al. (2009). "Gas Turbine Theory sixth edition."
- Schjøllberg, I., et al. (2008). "DYNAMIC ANALYSIS OF COMPRESSOR TRIPS IN THE SNØHVIT LNG REFRIGERANT CIRCUITS." Proceedings of ASME Turbo Expo 2008.
- Schultz, J. M. (1962). "The Polytropic Analysis of Centrifugal Compressors." Journal of Engineering for Power.
- Tveit, G. B., et al. (2004). "COMPRESSOR TRANSIENT BEHAVIOUR." Proceedings of ASME Turbo Expo 2004.
- Tveit, G. B., et al. (2005). "IMPACT OF COMPRESSOR PROTECTION SYSTEM ON RUNDOWN CHARACTERISTICS." Proceedings of ASME Turbo Expo 2005.

Urner, G. (1997). "Pressure loss of orifice plates according to ISO 5167-1." Flow Meas. Instrum. Vol 8. No. 1.



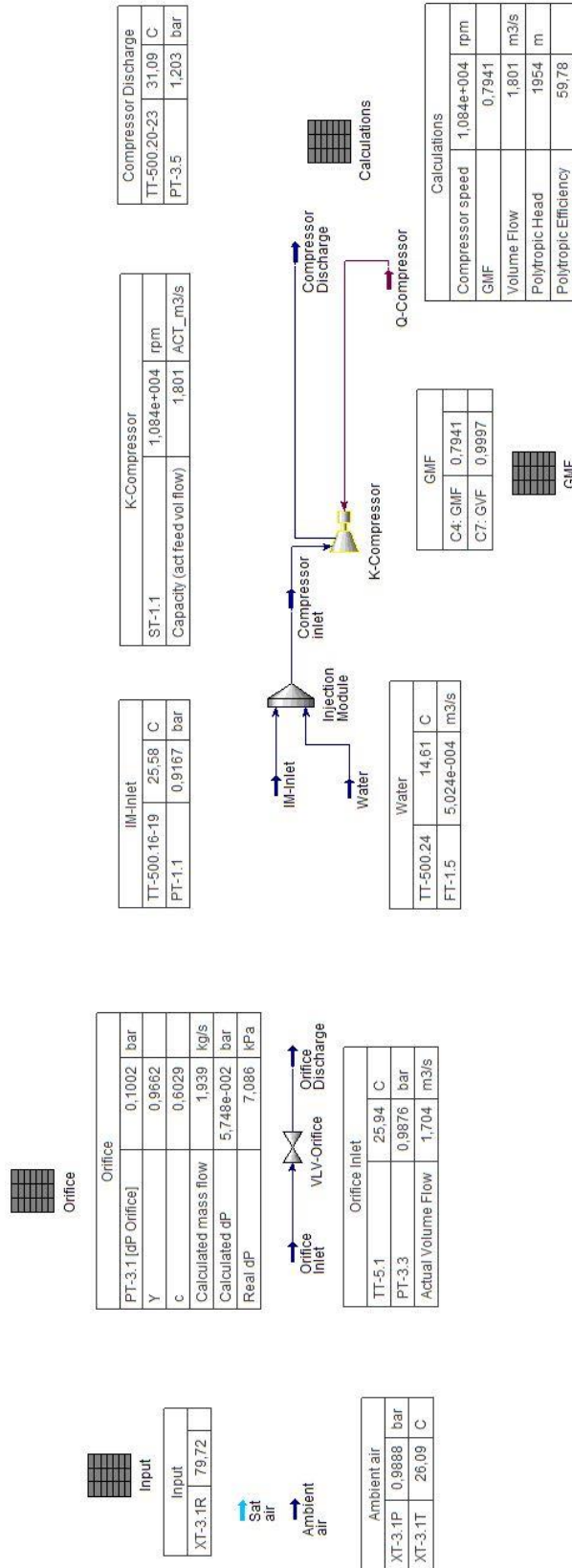


## Appendices

A	Steady state model layout	ii
B	Test data for development of compressor curves	iii
C	Steady state validation of dynamic model	v

## A. Steady state model layout

The architecture of the steady state model is shown below.



## B. Test data for development of compressor curves

All test points are for rotational speed 11 000 rpm. The polytropic head and efficiency are calculated with the HYSYS Steady state model

### Dry gas test points

Volume flow [m <sup>3</sup> /s]	Polytropic Head [m]	Polytropic efficiency [%]
0.85	2713.08	71.91
0.89	2741.42	73.34
0.96	2789.76	75.53
1.00	2806.64	76.77
1.06	2817.25	78.20
1.12	2821.76	79.55
1.25	2825.11	81.83
1.38	2792.67	82.98
1.59	2733.19	84.33
1.77	2652.95	85.59
2.17	2352.83	82.23
2.56	1836.53	72.48
2.57	1861.91	73.71

### Dry gas curve fit

$$H_p = -542.062889830395*Q^2+1334.76841964278*Q+1995.81373687385$$

$$\eta_p = -17.1107725532974*Q^2+58.9190479041182*Q+34.6500127344494$$

### GMFO.8 test points

Volume flow [m <sup>3</sup> /s]	Polytropic Head [m]	Polytropic efficiency [%]
0.83	2110.05	50.41
1.12	2049.28	52.57
1.44	2095.29	58.31
1.80	1953.60	59.78
2.07	1787.22	58.36
2.28	1534.50	53.30

### GMFO.8 curve fit

$$H_p = -437.928239744768*Q^2+1012.86043469647*Q+1532.55634918422$$

$$\eta_p = -13.5616445747628*Q^2+45.8623595629536*Q+20.3606355742364$$

GMFO.7 test points

Volume flow [m <sup>3</sup> /s]	Polytropic Head [m]	Polytropic efficiency [%]
0.83	1838.93	41.88
1.09	1793.35	43.83
1.38	1756.57	46.34
1.77	1601.17	46.23
2.18	1337.76	42.36

GMFO.7 curve fit

$$H_p = -269.794013918072 * Q^2 + 451.068988831204 * Q + 1641.19186753439$$

$$\eta_p = -9.60874213966929 * Q^2 + 29.6474996948213 * Q + 23.5610671110359$$

### C. Steady state validation of dynamic model

Steady state validation of dry gas performance, low volume flow

Sensor	Name	Unit	Steady state model	Dynamic model	Deviation
ST-1.1	Compressor speed	rpm	10899	10899	0.00%
PT-3.1	dP Orifice	mbar	32.16	32.16	0.00%
PT-1.1	IM Pressure	mbar	984	987	0.38%
TT-5.1	Orifice inlet temperature	C	27.70	27.70	0.00%
PT-3.3	Orifice inlet pressure	mbar	1011	1011	0.00%
PT-3.5	Discharge pressure	mbar	1328	1330	0.16%
FT-1.5	Water flow rate	l/s	0.00	0.00	
XT-3.1P	Ambient pressure	Pa	100180	100180	0.00%
XT-3.1T	Ambient temperature	C	27.74	27.74	0.00%
XT-3.1R	Relative humidity	%	27.60	27.60	0.00%
TT-500.16-19	Inlet temperature	C	27.53	27.70	0.60%
TT-500.20-23	Discharge temperature	C	63.39	63.45	0.10%
TT-500.24	Water temperature	C	20.20	20.20	0.00%
	Compressor speed	rpm	10899	10899	0.00%
	GMF	-	1.00	1.00	0.00%
	Volume flow	m <sup>3</sup> /s	1.00	1.00	-0.32%
	Polytropic head	m	2807	2788	-0.68%
	Polytropic efficiency	-	76.77	76.47	-0.39%

Steady state validation of dry gas performance, BEP

Sensor	Name	Unit	Steady state model	Dynamic model	Deviation
ST-1.1	Compressor speed	rpm	10898	10898	0.00%
PT-3.1	dP Orifice	mbar	95.23	95.23	0.00%
PT-1.1	IM Pressure	mbar	936	936	0.03%
TT-5.1	Orifice inlet temperature	C	29.08	29.08	0.00%
PT-3.3	Orifice inlet pressure	mbar	1005	1005	0.00%
PT-3.5	Discharge pressure	mbar	1245	1244	-0.02%
FT-1.5	Water flow rate	l/s	0.00	0.00	
XT-3.1P	Ambient pressure	Pa	100171	100171	0.00%
XT-3.1T	Ambient temperature	C	28.30	28.30	0.00%
XT-3.1R	Relative humidity	%	33.44	33.44	0.00%
TT-500.16-19	Inlet temperature	C	28.39	29.06	2.35%
TT-500.20-23	Discharge temperature	C	58.77	59.54	1.31%
TT-500.24	Water temperature	C	19.96	19.96	0.00%
	Compressor speed	rpm	10898	10898	0.00%
	GMF	-	1.00	1.00	0.00%
	Volume flow	m <sup>3</sup> /s	1.77	1.78	0.19%
	Polytropic head	m	2653	2654	0.03%
	Polytropic efficiency	-	85.59	85.32	-0.31%

Steady state validation of dry gas performance, high volume flow

Sensor	Name	Unit	Steady state model	Dynamic model	Deviation
ST-1.1	Compressor speed	rpm	10898	10898	0.00%
PT-3.1	dP Orifice	mbar	184.11	184.11	0.00%
PT-1.1	IM Pressure	mbar	869	867	-0.29%
TT-5.1	Orifice inlet temperature	C	28.65	28.65	0.00%
PT-3.3	Orifice inlet pressure	mbar	1000	1000	0.00%
PT-3.5	Discharge pressure	mbar	1061	1057	-0.36%
FT-1.5	Water flow rate	l/s	0.00	0.00	
XT-3.1P	Ambient pressure	Pa	100180	100180	0.00%
XT-3.1T	Ambient temperature	C	27.94	27.94	0.00%
XT-3.1R	Relative humidity	%	33.31	33.31	0.00%
TT-500.16-19	Inlet temperature	C	28.03	28.62	2.09%
TT-500.20-23	Discharge temperature	C	52.87	53.29	0.79%
TT-500.24	Water temperature	C	19.93	19.93	0.00%
	Compressor speed	rpm	10898	10898	0.00%
	GMF	-	1.00	1.00	0.00%
	Volume flow	m <sup>3</sup> /s	2.56	2.58	0.49%
	Polytropic head	m	1837	1833	-0.19%
	Polytropic efficiency	-	72.48	72.83	0.48%

Steady state validation of wet gas, low volume flow:

Sensor	Name	Unit	Steady state model	Dynamic model	Deviation
ST-1.1	Compressor speed	rpm	10839	10839	0.00%
PT-3.1	dP Orifice	mbar	40.67	40.67	0.01%
PT-1.1	IM Pressure	mbar	961	962	0.11%
TT-5.1	Orifice inlet temperature	C	25.92	25.92	0.00%
PT-3.3	Orifice inlet pressure	mbar	992	992	0.00%
PT-3.5	Discharge pressure	mbar	1274	1270	-0.35%
FT-1.5	Water flow rate	l/s	0.32	0.32	0.00%
XT-3.1P	Ambient pressure	Pa	98860	98860	0.00%
XT-3.1T	Ambient temperature	C	26.04	26.04	0.00%
XT-3.1R	Relative humidity	%	73.58	100.00	35.91%
TT-500.16-19	Inlet temperature	C	25.72	25.92	0.76%
TT-500.20-23	Discharge temperature	C	32.68	34.76	6.37%
TT-500.24	Water temperature	C	15.06	15.06	0.00%
	Compressor speed	rpm	10839	10839	0.00%
	GMF	-	0.80	0.80	-0.28%
	Volume flow	m <sup>3</sup> /s	1.12	1.13	0.71%
	Polytropic head	m	2049	2034	-0.74%
	Polytropic efficiency	-	52.57	54.50	3.67%



Steady state validation of wet gas, BEP

Sensor	Name	Unit	Steady state model	Dynamic model	Deviation
ST-1.1	Compressor speed	rpm	10840.70	10840.70	0.00%
PT-3.1	dP Orifice	mbar	100.17	100.18	0.00%
PT-1.1	IM Pressure	mbar	916.75	915.08	-0.18%
TT-5.1	Orifice inlet temperature	C	25.94	25.94	0.00%
PT-3.3	Orifice inlet pressure	mbar	987.61	987.61	0.00%
PT-3.5	Discharge pressure	mbar	1202.74	1192.52	-0.85%
FT-1.5	Water flow rate	l/s	0.50	0.50	0.00%
XT-3.1P	Ambient pressure	Pa	98875.37	98875.37	0.00%
XT-3.1T	Ambient temperature	C	26.09	26.09	0.00%
XT-3.1R	Relative humidity	%	79.72	79.72	0.00%
TT-500.16-19	Inlet temperature	C	25.58	25.93	1.35%
TT-500.20-23	Discharge temperature	C	31.09	31.08	-0.04%
TT-500.24	Water temperature	C	14.61	14.61	0.00%
	Compressor speed	rpm	10840.70	10840.70	0.00%
	GMF	-	0.79	0.79	0.01%
	Volume flow	m <sup>3</sup> /s	1.80	1.81	0.22%
	Polytropic head	m	1953.60	1905.75	-2.45%
	Polytropic efficiency	-	59.78	58.18	-2.68%

Steady state validation of wet gas, high volume flow

Sensor	Name	Unit	Steady state model	Dynamic model	Deviation
ST-1.1	Compressor speed	rpm	10841	10841	0.00%
PT-3.1	dP Orifice	mbar	153.64	153.64	0.00%
PT-1.1	IM Pressure	mbar	878	874	-0.47%
TT-5.1	Orifice inlet temperature	C	25.55	25.55	0.00%
PT-3.3	Orifice inlet pressure	mbar	985	985	0.00%
PT-3.5	Discharge pressure	mbar	1088	1083	-0.40%
FT-1.5	Water flow rate	l/s	0.60	0.60	0.00%
XT-3.1P	Ambient pressure	Pa	98886	98886	0.00%
XT-3.1T	Ambient temperature	C	25.83	25.83	0.00%
XT-3.1R	Relative humidity	%	80.63	80.63	0.00%
TT-500.16-19	Inlet temperature	C	25.05	25.52	1.87%
TT-500.20-23	Discharge temperature	C	28.87	28.88	0.05%
TT-500.24	Water temperature	C	13.86	13.86	0.00%
	Compressor speed	rpm	10841	10841	0.00%
	GMF	-	0.80	0.80	0.01%
	Volume flow	m <sup>3</sup> /s	2.28	2.29	0.52%
	Polytropic head	m	1535	1540	0.37%
	Polytropic efficiency	-	53.30	53.73	0.81%